NUCLEAR STRUCTURE IN BUDDING YEAST: IMPACTS OF CHROMATIN
ORGANIZATION AND GENE EXPRESSION

By

Laura Titus Burns

Dissertation

Submitted to the Faculty of the

Graduate School of Vanderbilt University

in partial fulfillment of the requirements

for the degree of

DOCTOR OF PHILOSOPHY

In

Cell and Developmental Biology

December, 2013

Nashville, Tennessee

Approved:

Dr. Susan Wente (Advisor)

Dr. William Tansey (Chair)

Dr. P. Anthony Weil

Dr. Todd Graham

Dr. Melanie Ohi

NUCLEAR STRUCTURE IN BUDDING YEAST:

IMPACTS OF CHROMATIN ORGANIZATION AND GENE EXPRESSION

LAURA CALLIE BURNS

Dissertation under the direction of Professor Susan Wente

The genome of a eukaryotic cell tightly packed within the nucleus with a high degree of structural organization. Two mechanisms accounting for nuclear structure and the dynamics of subnucler organization in *S. cerevisiae* are presented within. First, two powerful genetic screens identify requirements for the RSC chromatin-remodeling complex in maintaining nuclear morphology. The major NE-malformations observed in *rsc* mutants likely result from aberrant transcription and lipid homeostasis. Second, nuclear organization of transcriptional events in response to osmotic stress in *S. cerevisiae* involves the relocalization of the Hot1 transcription factor to foci that overlap with corresponding target genes. Casein Kinase II negatively regulates Hot1 localization to foci, and also leads to a reduced transcriptional response. These results suggest that the nuclear organization of transcription events impact the stochastic activity of environmentally induced genes. In conclusion, both chromatin organization and transcription events result in dynamic alterations in nuclear structure impacting the output of the genome.

To my loving husband and family

ACKNOWLEGEMENTS

TABLE OF CONTENTS

LIST OF TABLES

LIST OF FIGURES

LIST OF ABBREVIATIONS

3C	chromatin conformation capture
4C	chromosome conformation capture-on-chip
5C	chromosome conformation capture carbon copy
BA	benzyl alcohol
ChIP	chromatin immunoprecipitation
CK2	casein kinase II
DNA	deoxyribonucleic acid
Dox	doxycycline
ENCODE	encylopedia of DNA elements
FISH	fluorescence in situ hybridization
GFP	green fluorescence protein
GPI	glycosylphosphatidyl inositol
GRS	gene recruitment sequence
HDAC	histone deacetylase
HLBs	histone locus bodies
hnRNP	heterogenous nuclear ribonucleoproteins
HOG	high osmolarity glycerol
HSP	heat shock protein
HU	hydroxyurea
INM	inner nuclear membrane
kb-Mb	kilobase, megabase
kDa-MDa	kilodalton, megadalton
LAD	lamin associated domain
MAPK	mitogen-activated protein kinase
mRNA	messanger RNA
MRS	memory recruitment sequence
NAD	nucleolar-associated domain
NAR	nucleoporin-associated region
ncRNA non-coding RNA	
NE	nuclear envelope
NPC	nuclear pore complex
nSB	nuclear stress body
NUP	nucleoporin
Orf	open reading frame
PALM	photoactivated light microscopy
Pom	pore membrane protein
rDNA/RNA	ribosomal DNA/RNA
RNA	ribonucleic acid
RNAPI/II/III	RNA polymerase I/II/III
RNP	ribonucleoprotein
RSC	remodels the structure of chromatin
snRNP	small nuclear ribonucleic particles
SPB	spindle pole body
TAD	topologically associated domain
TBZ	thiabendazole
TEM	transmission electron microscopy
tRNA	transfer RNA
UTR	untranslated region

CHAPTER 1

INTRODUCTION TO THE SPATIAL ORGANIZATION OF THE GENOME

Features of the Functional Genome

From the first initial glimpses into the cell with the invention of the microscope in the 1600s, much attention has been given to understanding the visible features of the nucleus and the functionality of the DNA it contains. Pioneering work of molecular biologists uncovered the composition and structure of DNA, as well as the mechanistic processes of DNA replication, repair and transcription. Hand-in-hand with these molecular discoveries were advances in microscopy and a growing interest in the organization of proteins and DNA into subnuclear domains, presumably compartmentalizing and coordinating regions of the genome for specified functions. Our knowledge is increasingly expanding, although 12 years after the sequencing of the human genome, a challenging and yet exciting frontier in modern day cell biology is uncovering the relationship between nuclear organization and the functionality of the genome.

Nuclear Architecture

In eukaryotes, the nuclear envelope (NE) provides a physical barrier dividing the cytoplasm and nucleus. Within the NE are membrane pores that are embedded with nuclear pore complexes (NPCs). These NPCs are macromolecular assemblies of multiple nucleoporin (Nups) proteins ranging in size from 66MDa in *yeast* (Rout and Blobel, 1993) to 125MDa in humans (Reichelt et al., 1990) and function with transport receptors

for selective import and export of proteins and RNPs (Hetzer, 2010; Tetenbaum-Novatt and Rout, 2010). Thus the NE and the NPCs provide key structural features distinguishing the nuclear composition from the cytoplasm.

Beyond serving as a physical barrier with selective transport channels, the NE harbors multiple critical cellular activities. The NE provides a scaffold for the organization of chromatin into selective zones of heterochromatin and euchromatin, and serves as a platform for genomic transcription and repair (Strambio-De-Castillia et al., 2010; Van de Vosse et al., 2011). In metazoans, the nuclear lamina and associated proteins act as a platform to bridge chromatin interactions. In *S. cerevisiae* and other organisms lacking nuclear lamins, inner nuclear membrane proteins perform these key functions. The NE also harbors protein complexes that communicate between the nuclear and cytoplasmic compartments. The microtubule organization center, or the spindle pole body (SPB) in *S. cerevisiae*, is embedded into the NE and links cytoskeletal microtubules to chromatin throughout the cell cycle. Furthermore, conserved SUN/KASH-domain containing proteins bridge cytoskeletal communications to the chromatin for signaling events (Razafsky and Hodzic, 2009).

Apart from the NE and associated protein-complexes, the nucleus is further divided into architectural subdomains known as nuclear bodies (Mao et al., 2011b). The most apparent of the nuclear bodies conserved from yeast to mammals is the nucleolus, which occupies a third of the nuclear volume. Confined to the nucleolus are the rDNA and protein machinery necessary for ribosome biogenesis. Additionally, the nucleolus adds further to the compartmentalization of nuclear proteins by sequestering proteins that contain nucleolar localization signals (Sirri et al., 2008). Thus nuclear bodies are

subcompartments of the nucleus that are enriched with components necessary for specialized functions. One remaining nuclear body conserved across eukaryotes is the DNA repair focus, which results from phosphorylation and localization of DNA repair proteins to sites of DNA damage (Misteli and Soutoglou, 2009). Further nuclear architecture has significantly diverged among eukaryotes, potentially arising from the requirements for additional organization with the increasing complexity and size of metazoan nuclei. Future sections are dedicated for a more complete description of the metazoan and *S. cerevisiae* nuclear structure.

Chromatin Structure

A major component influencing the three-dimensional organization of DNA in the nucleus is chromatin structure, which occurs through several orders of compaction. The basic unit of chromatin is the nucleosome where DNA is wrapped in an octamer of histone proteins. Nucleosomes are spaced on average 200bp apart, resembling beads on a string, and are compacted into a chromatin fiber with a 30nm diameter. During interphase, these chromatin fibers are ordered into domains that exhibit frequent topological interactions, reflecting both intrachromosomal interactions based on proximity to neighboring regions on the same chromosome, and interchromosomal respective to the 3D positioning within the nucleus. Insulator elements and insulator-binding proteins are thought to establish long-range DNA interactions isolating co-regulated genes into distinct chromatin domains (Vogelmann et al., 2011). These tethers may promote clusters of gene rich regions and gene poor regions. Finally chromatin domains are further organized into chromosome territories easily visualized with

fluorescence microscopy and clever chromosome paints that selectively hybridize to each chromosome (Cremer and Cremer, 2010; Cremer et al., 1988).

At each level of chromatin structure the DNA can be more or less compact resulting in differential access to enzymes responsible for DNA repair, transcription and replication. Additionally enzymes are enriched at nuclear bodies between chromosome territories promoting the expression, repair and replication of chromatin localized to this interchromosomal space (Geyer et al., 2011). Analysis of chromatin positioning with fluorescent microscopy, DamID and genome-wide chromosome conformation capture (3C) techniques have highlighted that chromatin structure is not static, but varies significantly across different cell types, disease states and even between mother and daughter cells (Kind et al., 2013; Kubben et al., 2012; Kuroda et al., 2004; Parada et al., 2003). Chromatin structure will continue to be a rich field for discovery, as we are just beginning to scratch the surface of a mechanistic understanding for the events that regulate each level of compaction.

Epigenetic Influences

Epigenetics is the study of events that act independent from the primary DNA sequence to influence the on and off modes of gene regulation and cellular phenotype. These events include variations of nucleosome compaction, composition and post-translational modifications (also referred to as epigenetic modifications), methylation of the DNA base pairs themselves, the expression of regulatory RNAs, and can extend to heritable protein states known as prions.

Epigenetics account for the phenotypic differences between identical twins and across different cell types within an individual organism. These can be influenced by signaling inputs from the environment and are considerably altered in disease. A striking example of epigenetic regulation is the X-chromosome inactivation in mammals (Jeon et al., 2012). This process arises from a sequence of events where the long non-coding RNAs *Xist* and *Tsix* initiate the random choice to inactivate one of the X-chromosomes. These molecular events result in a compact chromosome territory known as a Barr body that harbors a unique composition of *Xist* RNA, enriched macroH2A variant histone and repressive histone modifications, along with the association of repressive polycomb (PcG) group proteins (Wutz, 2011). Thus small-scale epigenetic events initiated at select regions of the genome can result in dramatic changes in nuclear architecture and the activity of the genome.

The positioning, composition and modifications of nucleosomes are each regulated by distinct classes of enzymes. In *S. cerevisiae*, RSC, SWI/SNF, INO80, SWR1, and ISWI chromatin-remodeling enzymes are key mediators of nucleosome positioning and composition (Clapier and Cairns, 2009). RSC and SWI/SNF chromatin-remodeling complexes remodel nucleosomes to allow RNA polymerases (RNAPs) accessibility to promoter regions for efficient transcription. SWR1 exchanges the histone variant H2AZ for H2A and signifies regions more permissive to activation. INO80 catalyzes the reverse reaction. Classes of chromatin modifying enzymes are also responsible for covalently linking acetyl, methyl, ubiquitin, sumo, and phosphate groups onto histones (Zentner and Henikoff, 2013). These covalent marks serve as docking sites for proteins, for example RSC components contain multiple bromodomains that

recognize acetylated histones (Kasten et al., 2004). Therefore, the combination of events including chromatin modifications and recruitment of remodeling complexes largely influence the functionality and access of select regions of the genome for DNA transcription, repair and replication.

Non-uniform and Stochastic Events in Nuclear Structure and Function

There is a considerable amount of non-uniformity in nuclear structure. That is two genetic loci, chromosome territories, or nuclear bodies may not position identically within a uniform population of cells. There are some cases where large nuclear structures are constantly observed with appreciable variations. Inactive heterochromatin is preferentially positioned towards the nuclear periphery and nucleoli. In the case of the inactivated heterochromatic X-chromosome, it is consistently localized to the nuclear periphery. Remarkably, population-based methods such as 3C and DamID have provided useful tools in resolving regions of the genome that interact more frequently. For example, 3C techniques have provided a link between neighboring chromosomes and frequently observed translocations in human cancers. DamID has defined heterochromatin regions of the genome that are enriched at the nuclear lamina. However, more stochastic changes in chromatin positioning tend to occur across a population of cells. For example, when a gene transitions from a silenced to transcriptionally activated state, it is repositioned to more permissive region of the nucleus. The same gene may however position to different compartments in different cells, and in some cells the positioning may not even change. In part, observing snapshots of a population may not accurately capture these structural rearrangements that are dynamic and malleable. Our

6

best approaches to identify the mechanisms that influence the stochastic nature of nuclear structure in the future will be quantitative measurements at the single cell level.

The Metazoan Nucleus

The diameter of a *S. cerevisiae* nucleus is on average 1.5μm and contains 12Mb of DNA, whereas single mammalian chromosomes occupy 2-4μm and vary from 50-250Mb in size. The average nuclear volume of a human nucleus is approximately 250-times larger than a *S. cerevisiae* nucleus, corresponding to the 250-fold difference in genome size from 12Mb in *S. cerevisiae* to 3Gb in humans. As it is clear that with a larger genome comes increasing complexity of the genetic elements, metazoan nuclei have multiple higher-order chromatin domains and a variety of nuclear bodies providing additional modes for regulating their complex genomes through nuclear architecture (Figure 1.1).

Chromatin domains

Several approaches have provided means to classify the functional elements of the genome and have contributed to our understanding of chromatin domain organization. The Model Organism Encyclopedia of DNA Elements (modENCODE) and Encyclopedia of DNA Elements (ENCODE) projects have provided comprehensive view of histone modifications, DNA methylation, DNA-binding proteins, DNase I hypersensitive sites, active transcription units, and ncRNAs across the genomes of *Drosophila melanogaster, Caenorhabditis elegans* and *Homo sapiens* (Dunham et al., 2012; Gerstein et al., 2010; Kharchenko et al., 2011; Roy et al., 2010). These integrative studies have classified

The Metazoan Nucleus

Nuclear Pore Complex

Nuclear bodies
- Transcription factories
- Polycomb bodies
- GLFG bodies
- Speckles
- DNA-Repair Foci
- Cajal bodies
- PML bodies
- Nuclear stress bodies
- Histone locus bodies
- Clastosome
- Paraspeckles
- Insulator bodies

Nucleoli

Heat shock-specific

Tissue-specific

Chromatin Domains
- 'LADs' Lamin-associated domains
- 'TADs' Topologically associating domains
- 'NARs' Nucleoporin-associated regions
- 'NADs' Nucleolar-associated domains

Chromosome Territories

Relative size of yeast nucleus

Figure 1.1 Structural features of the metazoan nucleus. Multiple compartments with defined composition form and function in specific nuclear functions. The chromatin domains are defined by their preferential enrichment to specific nuclear compartments. Chromosome terrietories are localized regions that each chromosome occupies in an interphase cell. These structural features composition and dynamics vary among cellular contexts including cell fate and environmental stress.

different types of active and inactive chromatin and have provided evidence for a functional organization of the genome. How these functional elements relate to nuclear architecture still remains elusive. Emerging techniques to map chromatin domains have begun to provide three-dimensional maps of higher-order chromatin organization based on spatial positioning and the frequency of chromatin-chromatin associations. Briefly, the chromatin domains identified and descriptions of the corresponding techniques are further summarized below.

TADs

The development of chromatin conformation capture (3C) technology by Job Dekker has provided a breakthrough in mapping chromatin-chromatin associations (Dekker et al., 2002). This technique is able to resolve regions of the genome that interact via chromatin loops, through first crosslinking the chromatin, followed by restriction enzyme digestion and ligation of those regions flanking the looped chromatin. The re-ligated products can then be detected on a candidate approach with qPCR (3C), or coupled to a microarray or sequencing for a genome-wide anlaysis (5C, HiC) (Hakim and Misteli, 2012). As these technologies began to be applied to entire genome analyses, two megabase-pair chromatin compartments were identified: compartments A and B. Compartment A was associated with more open and accessible chromatin, where compartment B encompassed more silent and gene poor regions (Lieberman-Aiden et al., 2009). Subsequent studies in mouse and human cells obtained higher resolution and identified 100kb-1Mb domains classified as topologically associated domains (TADs) (Dixon et al., 2012; Nora et al., 2012). These TADs contain co-regulated genes and are

consistent across different cell types, including mouse and human cells (Dixon et al., 2012), and correlate with units of DNA replication. The major insulator-binding protein CTCF is proposed to demarcate the TADs (Dixon et al., 2012; Nora et al., 2012), though this correlation must be further validated for whether CTCF-binding sites are necessary and sufficient for TAD assembly. Similarly in Drosophila, 10-500kb TADs have also been resolved and tend to partition distinct chromatin states (Hou et al., 2012; Sexton et al., 2012). The borders between TADs are enriched in actively transcribing genes suggesting a causal role of transcription in forming TAD boundaries (Hou et al., 2012). Future studies will be aimed towards identifying the factors that define TADs and will continue to provide the links between domains identified with microscopy and the additional approaches described below.

LADs

The DamID genome-wide mapping strategy developed by Bas Van Steensel has provided a high-resolution view of genomic regions termed lamina-associated domains (LADs) (Pickersgill et al., 2006). These LADS typically span 0.1-10Mb in size, show preferential positioning to the nuclear periphery, and are enriched in transcriptionally inactive chromatin (Gerstein et al., 2010; Guelen et al., 2008; Pickersgill et al., 2006). In humans, LADs are enriched for GAGA motifs and localization is dependent on HDAC3 and the cKrox transcriptional repressor (Zullo et al., 2012). LADs are dynamic and vary between cell types throughout differentiation, though subsets are constitutive (cLADs) and enriched in A/T rich DNA (Meuleman et al., 2013; Peric-Hupkes et al., 2010).

NADs

Recent biochemical approaches coupled with DNA sequencing and microarray technologies identified chromatin domains enriched within nucleoli, termed nucleolar-associated domains (NADs). As expected NADs were enriched in satellite repeats and RNAPI and RNAPIII transcribed genes (rDNA, tRNA and 5S RNA). NADs and LADs exhibit shared features and correlate with repressive histone modifications, inactive regions of the genome, and also span a similar size distribution of 0.1-10Mb (Nemeth et al., 2010; van Koningsbruggen et al., 2010). Though chromatin organization after mitosis is not faithfully transmitted to daughter cells, there is evidence for loci exchanging positioning between nucleoli and the nuclear periphery (Thomson et al., 2004). Therefore, it remains to be determined whether the heterochromatic composition of LADs and NADs may be sufficient for targeting to either subnuclear compartment.

NARs

'Gene-gating' is a long-standing hypothesis in the field of nuclear cell biology first proposed by Gunter Blobel in 1985. Here it was envisioned that NPCs facilitated transcription by gating genes and directing transcripts to the cytoplasm for translation. In the years following, multiple studies have provided convincing evidence for enriched interactions between chromatin regions and nucleoporins. In *D. melanogaster*, ChIP-chip experiments mapped domains spanning 5-500kb that interact with nuclear basket nucleoporins Nup153 and Megator (Vaquerizas et al., 2010). These nucleoporin-associated regions (NARs) are enriched across the male X chromosome, which requires high levels of transcription for dosage compensation. The NARs within the X-

11

chromosome are positioned to the periphery and show decreased expression and peripheral localization upon depletion of Nup153. Though other NARs do not preferentially position to the periphery, the expression also decreased upon Nup153 depletion. Additional studies in *D. melanogaster* observe the dynamic association of Nup50, Nup62, Sec13, Nup98, and Nup88 with both developmental and stress-induced genes (Capelson et al., 2010; Kalverda et al., 2010). This association occurs in both the nucleoplasm and at the nuclear periphery. Similarly, ChIP-seq experiments with the GLFG-domain containing Nup98 in human cells enrich for genes positioned to the nuclear interior and periphery (Liang et al., 2013). Considering these recent results, the 'gene-gating' hypothesis in metazoans can be updated to include NARs and the concept that nucleoporins dynamically associate and regulate chromatin function throughout the nucleus irrespective of their predominant positioning at the nuclear periphery.

Chromosome territories

Historically, chromosomes were proposed to adopt a territorial arrangement throughout interphase similar to the separation observed in mitosis. Early studies by the Cremer brothers, one a physicist and the other a biologist, started to provide the first evidence for chromosome territories (Cremer et al., 1988). With continuing developments of chromosomal paints and 3D imaging techniques, chromosome territories have been observed in a number of organisms (Cremer and Cremer, 2010), and supporting data using 3C technologies has indicated that interchromosomal contacts are far more frequent then intrachromosomal contacts (Lieberman-Aiden et al., 2009; Nora et al., 2012). In general, gene-dense chromosomes show favored positioning to the nuclear

interior and heterochromatic chromosomes to the periphery or nucleolus. However, the

positioning is heterogeneous and varies considerably across cell types (Parada et al.,

2004). These cell specific arrangements are predicted to contribute to the likelihood of

two genetic loci to undergo chromosomal translocations (Brianna Caddle et al., 2007;

Parada et al., 2002; Zhang et al., 2012). It is unclear whether factors regulate the

positioning of chromosome territories, or whether mechanisms exist for positioning

chromatin within the chromosome territory. With the observed variations in positioning,

single-cell microscopy approaches will be irreplaceable for continued discoveries in the

functionality of chromosome territories.

Nuclear bodies

The spatial arrangement of chromatin into domains and chromosome territories

describes only the DNA component of nuclear architecture. Another striking level of

organization occurs through the localization of proteins and RNAs to subnuclear

compartments referred to as nuclear bodies. These nuclear bodies have distinct

compositions of proteins and are sites for several nuclear events including rDNA

processing, snRNP assembly, splicing, proteolysis, DNA repair and transcription (Mao et

al., 2011b). Nucleoli and histone locus bodies are nuclear bodies that stably form and

cluster select regions of the genome. Many additional nuclear bodies are dynamic and

assemble and disassemble in different cell types, stages of the cell cycle and in response

to specific environmental inputs. These dynamic forms of nuclear bodies are also

predicted to localize to regions of the genome to coordinate and increase the efficiency of

nuclear processes. Three models have been proposed for the assembly of nuclear bodies,

one following an ordered assembly, another stochastic, and the last a seeding model (Dundr and Misteli, 2010). The ordered assembly model suggests that components of nuclear bodies are recruited in a hierarchical sequence of events, and the absence of any one component would prevent assembly. In the stochastic model, any grouping of components occurring through random interactions is sufficient for nuclear body assembly. Lastly, the seeding model provides a mechanism for regulating the dynamic assembly of nuclear bodies, whereby nascent RNA or a modified state or levels of a protein provide a signal to initiate *de novo* assembly. Support for stochastic assembly comes from experiments where both RNPs and protein components of Cajal bodies are tethered to chromatin. In these studies, almost any Cajal body component is able to induce the stochastic assembly of Cajal bodies (Kaiser et al., 2008). Additional evidence supports a seeding model where RNAs are sufficient to seed HLBs, Cajal bodies, nuclear speckles, nuclear stress bodies and paraspeckles (Mao et al., 2011a; Shevtsov and Dundr, 2011). Though these models are currently under debate, each provides a possibility for regulated assembly in response to cellular cues thus increasing or decreasing the efficiency of nuclear events required for different cellular phenotypes. Two highly dynamic nuclear bodies regulating transcription in response to different cellular contexts are the focus of the following sections.

Transcription Factories

For decades, studies dissected the molecular components required for events of transcription initiation, elongation, and termination. With developing antibodies and imaging techniques, cell biologists began to classify these molecular components and

their distribution within the nucleus. Strikingly, early localization studies in fixed cells for both nascent transcripts and active forms of RNAPII observed that these components are enriched in distinct foci termed transcription factories (Iborra et al., 1996; Jackson et al., 1993; Wansink et al., 1993).

Much like an industrial factory, nuclear foci enriched in transcriptional machinery and active genes are predicted to be more efficient sites for RNAPII transcription. Evidence for grouping of active genes arose from multiple reports of overlapping co-regulated genes using microscopy-based methods (Mitchell and Fraser, 2008; Osborne et al., 2004). Furthermore, the Fraser group used a biochemical 4C approach for an unbiased detection of chromatin-associations with the globin genes in mouse erythroid cells (Schoenfelder et al., 2010). These 4C experiments find that hundreds of genes from different chromosomes interact in trans with the globin genes, several of which localize to the same transcription factory. The co-clustering genes show a significant enrichment for Klf-transcription factor binding sites in their promoters. Klf1 is required for the clustering into specialized Klf1-transcription factories. Therefore transcription factors are likely a major determinant for the assembly of transcription factories and the clustering of co-regulated genes for cell-specific regulation of gene expression.

Until advances made in recent months, transcription factories were only observed in fixed cells using antibodies to distinguish initiating and elongating forms of RNAPII. The Grosveld group found that transcription factories could be observed through the localization of the Cdk9 kinase that phosphorylates Ser5 on the RNAPII C-terminal domain during events of transcriptional initiation (Ghamari et al., 2013). The real-time localization of Cdk9 indicates the formation of stable transcription factories and also,

convincingly, a separation of transcription factories between initiating and elongating RNAPII. A second study from the Darzacq and Dahan groups employed photoactivated light microscopy (PALM) to monitor individual RNAPII molecules with spatiotemporal resolution (Cisse et al., 2013). This resolution allows measurements of dwell times for transcription factories in cells with normal and activated transcription rates and found that transcription factories are 10x more stable under conditions of activation. Furthermore, transcription elongation inhibitors do not alter the dynamics of transcription factories in agreement with their formation during the rate limiting events of transcriptional initiation.

Our current understanding of transcription factories is that they represent dynamic and specialized sites for transcription of co-regulated genes. Specifically, the dynamic nature of transcription factories suggests that they may form upon requirements for transcription of co-regulated genes tailored to a specific cellular response. In a tissue-specific context, it remains to be determined whether specialized transcription factors such as Klf1 organize co-regulated genes in other cell types in the body. Similarly, the transcription factor assembly in response to cellular stresses likely involves the expression or modification of stress-responsive transcription factors. If the assembly of transcription factories contributes to rate-limiting steps for recruitment of transcription initiation machinery, then one would predict that genes within the transcription factory to be 'on', where genes outside may remain 'off'. Continued studies are needed to identify such transcription factors and resolve whether stochastic gene activity corresponds to the gene's positioning within respect to transcription factories.

Nuclear Stress Bodies

Cells rapidly respond to increasing temperatures by dramatically influencing nuclear events of gene expression including transcription, splicing, and mRNA export. A unique nuclear body known as the nuclear stress body (nSB), forms within a short period after heat shock. Several factors accumulate to nSBs including the heat-shock transcription factor HSF1, splicing factors HSF2/ASF, SRp30, 9G8, the hnRNP HAP1 proteins and SatIII RNAs. The SatIII RNAs are 100-fold induced after heat shock and are transcribed from the human chromosome IX 9q12 band and require the activity of HSF1 (Eymery et al., 2010). This chromosome coordinate is required for the formation and recruitment of nSBs (Denegri et al., 2002). In addition to heat shock, nSBs can also form under osmotic stress, although the TonEBP/NFAT5 osmoresponsive transcription factor assumes the role of HSF1(Valgardsdottir et al., 2008). The function for nSBs remains unresolved, however the enriched transcription and histone acetylation patterns are suggestive of nSBs representing a unique subset of transcription factories. Alternatively, nSBs may represent zones to sequester global transcription factors or RNA-binding proteins as a means to block non-stress related transcription, splicing and mRNA export. With each of these functions being possibilities, future work will be required to resolve the role for nSBs in stress-induced gene expression programs.

Gene positioning in development and disease

Nuclear architecture is highly dynamic, but converging evidence suggests that these dynamics are non-random and correlate with important cell-fate decisions. In *C. elegans*, both gut (*pha-4*)- and muscle (*myo-3*)-specific promoters are sequestered at the

nuclear periphery throughout early development and subsequently migrate to the nuclear interior in fully differentiated cells (Meister et al., 2010). Similarly, in human cell culture models of myogenesis, the MyoD gene remains at the nuclear periphery until a cell transitions into a myotube upon which MyoD shifts to the interior and colocalizes with the TAF3 TFIID subunit necessary for full expression (Yao et al., 2011). The nuclear positioning of several other developmentally regulated genes also shifts from peripheral to nucleoplasmic including the Mash1 locus during neurogenesis, the GFAB locus during astrocyte differentiation, and the β-globin locus during erythroid maturation (Ragoczy et al., 2006; Takizawa et al., 2008; Williams et al., 2006). From these results, an arising model suggests that the peripheral sequestration of cell-fate determining genes may limit their expression until the cell reaches the correct stages of development, upon which the gene is repositioned to a transcriptionally active compartment of the nuclear interior.

Not only is gene positioning regulated throughout development, but it also can be altered in disease states. In a *C. elegans* disease model for Emery-Dreifus Muscular Dystrophy, the nuclear interior migration of *myo-3* no longer occurs upon differentiation, and this loss of nuclear organization specifically links to the muscular defects seen in the diseased animals (Mattout et al., 2011). Similarly, analysis of human cells from individuals with Hutchinson Gilford Progeria Syndrome showed loss of methylation and lamin interactions with chromatin which correlated with HiC results suggesting loss of chromatin A and B subcompartments (McCord et al., 2013). These studies highlight the dysfunctional nuclear-lamina that is observed in these laminopathies, and suggests an active role for the nuclear lamina and inner nuclear membrane proteins in maintaining global chromatin arrangements and nuclear architecture.

<p style="text-align: center;">**The *S. cerevisiae* Nucleus**</p>

Overall Structure

The simplicity of the *S. cerevisiae* genome has made it an attractive organism for the first full genome sequencing (Goffeau et al., 1996) and also for pioneering experiments dissecting principles of 3D genome organization. The *S. cerevisiae* haploid genome is ~12Mb with ~6000 genes spaced across 16 chromosomes and is organized by sequence-specific features such as the centromere, telomeres and rDNA. Chromatin positioning is also influenced by the activity of select genes and their positioning into gene territories, as well as chromosome configurations folding and occupying distinct chromosome territories within the nucleus. Additionally, the nuclear periphery provides a platform for both anchoring of centromeres and telomeres and a permissive region for efficient transcription and repair. These nuclear features are the primary factors influencing *S. cerevisiae* nuclear architecture and described in more detail in the following sections (Figure 1.2).

Rabl-like organization of chromosomes

S. cerevisiae chromosomes adopt a Rabl-like conformation where the centromere and telomeres are positioned towards opposite poles of the nucleus (Yang et al., 1989; Zimmer and Fabre, 2011). The centromeres maintain rosette pairing and are tethered to the SPB, which is embedded in the NE throughout interphase and mitosis (Jin et al., 2000). From the centromere, chromosome arms extend towards the opposite pole of the nucleus where telomere ends are anchored to the NE through two independent anchoring mechanisms, involving the yKu70/80 telomeric and Sir4/Mps3 subtelomeric pathways

<p style="text-align: center;">19</p>

The Yeast Nucleus

Nuclear Bodies
  DNA Repair Foci

Gene Territories
  'GRS' recruitment to periphery
  'MRS' memory of recruitment

Chromosome Territories
  Rabl-like conformation

Nuclear Pore Complex

Inducible genes

Nucleolus

Spindle Pole Body
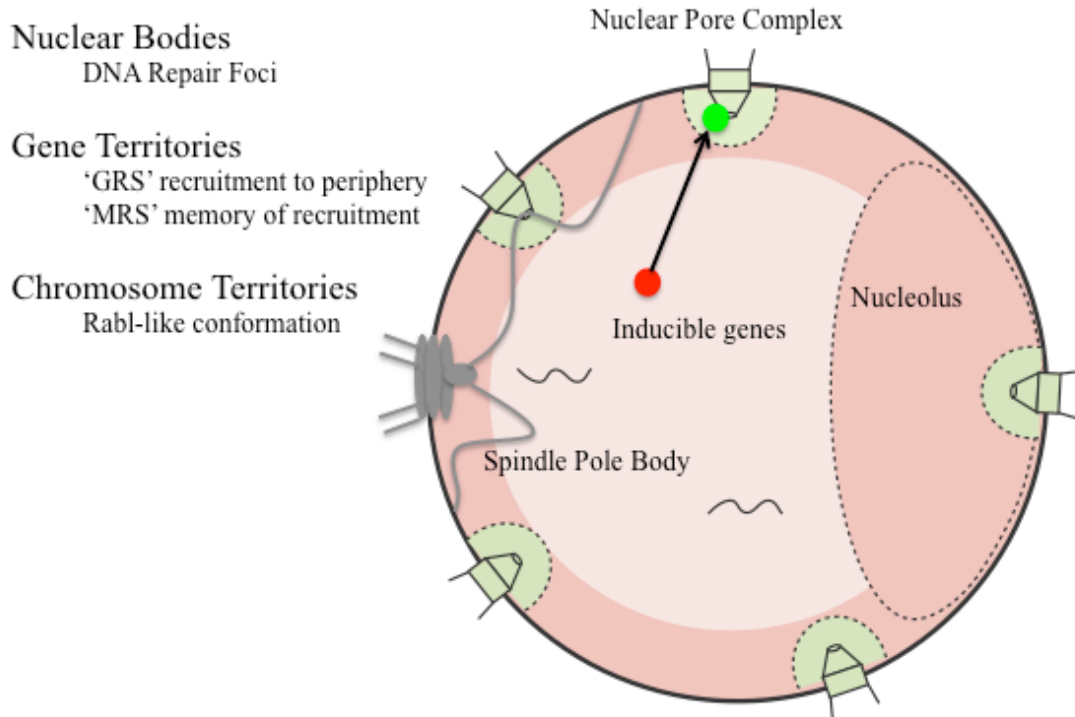
Figure 1.2. Structural features of the *S. cerevisiae* nucleus. The nuclear bodies identified in *S. cerevisiae* are DNA repair foci and the nucleolus. Further structural organization is apparent in the repositioning of genes to distinct gene territories under conditions of induction. The gene recruitment and memory recruitment sequences (GRS and MRS) are cis elements within the promoter of inducible genes that confer peripheral positioning. Though gene positioning is fairly dynamic the chromosomes occupy chromosome territories confined by lengths of the chromosome arms and anchoring to the spindle pole body at the centromere and nuclear envelope at the telomeres.

(Hediger et al., 2002; Schober et al., 2009). The lengths of the chromosome arms impact whether telomeres will cluster to shared regions of the NE, and on average 5-8 telomere clusters are observed per nucleus (Therizols et al., 2010). The *S. cerevisiae* Rabl-like conformation is distinct from the chromosome territory organization of mammalian and Arabidopsis cells, but is shared among other higher eukaryotes such as Drosophila, salamander, and some plant cells.

rDNA and tRNA genes clusters reside in the nucleolus

The nucleolus is the subnuclear compartment where ribosome biosynthesis occurs (Sirri et al., 2008). The 1-2Mb of rDNA are located on the right arm of chromosome XII, encoding 100-200 repeats of the 35S and 5S precursors transcribed by RNAPI and RNAPIII, respectively. This region of chromosome XII occupies one quarter of the nuclear volume clustering to a crescent-shaped compartment directly opposing the SPB, confirmed by both imaging and 3C interaction-based methodologies (Duan et al., 2010; Yang et al., 1989). Approximately ~180 proteins are known to localize to this compartment (Huh et al., 2003), where certain proteins are sequestered in the nucleolus for regulatory purposes. Thus, not only is the nucleolus a compartment of rDNA, but also promotes distinct compositions of proteins between subnuclear domains.

As homologous recombination in *S. cerevisiae* is very robust, chromatin-silencing and NE-tethering mechanisms are required to ensure stability of rDNA repeats. Chromatin silencing occurs through Sir2-dependent mechanisms and requires the Cohibin and the RENT complexes to restrict recombination events and provide stability to the rDNA copies. Futhermore, tethering of the Sir2-silenced rDNA repeats at the

21

nuclear envelope through the Nur1 and Heh1 inner nuclear membrane proteins provides additional stability (Mekhail et al., 2008). Thus positioning of rDNA repeats at the NE provides example for genome organization at the nuclear periphery and a functional requirement in genomic stability.

In addition to the rDNA repeats, the 274 tRNA genes also show preferential positioning within the nucleus. Though these genes are scattered across the genome they are clustered within the nucleolus, presumably facilitating the coordination of RNAPIII transcription (Thompson et al., 2003). More recently, 3C approaches have observed the clustering of tRNA genes to centromeric regions (Duan et al., 2010). These two compartments may function in tRNA-associated silencing and prevent recombination between clustered tRNA genes.

Gene Territories

Not only do the rRNA and tRNA genes position non-randomly within the nucleus, but individual genes also occupy distinct gene territories (Berger et al., 2008). The positioning of these territories is under regulation by DNA transcription and repair events. Recruitment to the nuclear periphery under activating conditions is a paradigm observed among several environmentally influenced genes. This localization requires components of the NPC, variant histones, chromatin-modifying enzymes and mRNA export factors, and is predicted to functionally couple transcription to events of mRNA export (Brickner et al., 2007; Cabal et al., 2006; Taddei et al., 2006). Similarly, persistent DNA lesions are recruited to the nuclear periphery where association with NPC components promotes efficient repair (Khadaroo et al., 2009; Nagai et al., 2008;

Therizols et al., 2006). Therefore functionally, the NPC environment of the NE

represents a more permissive environment for DNA transcription and repair.

Chromosome Territories

Several findings have hinted towards the arrangement of chromosomes into

chromosome territories in *S. cerevisiae*. The Rabl-like conformation of *S. cerevisiae*

chromosomes exhibits territorial organization where centromeres occupy one pole and

telomeres pair at the opposite pole (Bystricky et al., 2005). In a mosaic genome study

labeling with species-specific chromosome paints, chromosomes of *S. cerevisiae* and *S.*

paradoxus were found to occupy distinct zones suggestive of mechanisms for isolating

chromosomes to a defined nuclear space *(*Lorenz et al., 2002). Consistent observations

with 3C measurements of chromatin interactions across the *S. cerevisiae* genome found

an enrichment of intrachromosomal interactions suggestive of chromosome territory

conformations (Dekker et al., 2002). Additionally, a computational approach used to

predict nuclear architecture in *S. cerevisiae* could sufficiently recapitulate these

intrachromosomal interactions with only a few parameters including restraints for the

tethering of centromeres, rDNA and telomeres to their respective nuclear compartments

and the flexible polymer chain conformation of chromatin (Tjong et al., 2012). Much is

anticipated for expanding our view to a more fully resolved 3D organization of the *S.*

cerevisiae genome as technical barriers and limits to computational processing are

overcome.

Functional Roles for Nuclear Architecture in Transcription

The *S. cerevisiae* nucleus has three distinct subcompartments for gene transcription: the nucleoplasm, the nuclear periphery, and the nucleolus (Figure 1.2). The nucleolus is the subcompartment where the majority of RNAPI and RNAPIII transcription occurs. The nuclear periphery is broken down into distinct repressive and active zones for RNAPII gene expression. Centromere and telomere anchoring zones of the periphery generally contact silenced regions of the genome. The intervening zones are occupied by NPCs and provide a permissive environment for active RNAPII gene expression. Several inducible genes including *GAL1, GAL2, HXK1, INO1, TSA2, HSP104* and *MFA2*, move from the nucleoplasm where they are inactive, to the periphery for proper expression (Brickner et al., 2007; Brickner and Walter, 2004; Cabal et al., 2006; Dieppois et al., 2006; Taddei et al., 2006).

The peripheral positioning of *GAL1*, *INO1*, *TSA2* and *HSP104* requires DNA elements within the promoter that mediate gene recruitment to the periphery (Ahmed et al., 2010; Brickner and Walter, 2004). The gene recruitment sequences (GRSs) are necessary and also sufficient for NE positioning when placed in an ectopic *URA3* locus (Ahmed et al., 2010). Most surprisingly, identical GRSs found within the *INO2* and *TSA2* gene loci position to the same site at the nuclear periphery, thus occupying the same gene territory (Brickner et al., 2012). Furthermore, the transcription factor that binds the GRS is required for the gene clustering potentially facilitating interchromosomal interactions between these loci to ensure co-regulated and efficient gene expression (Brickner et al., 2012). In addition to GRS elements, memory recruitment sequences (MRSs) maintain positioning at the periphery for several hours

after the gene is inactivated and this peripheral positioning allows the gene to be reactivated with faster kinetics (Light et al., 2010). Also, a region in the 3'UTR of *HXK1* is required for peripheral recruitment (Taddei et al., 2006). The identification of DNA sequence elements that confer 3D nuclear positioning has provided evidence for the functional organization of the genome.

Components of the NPC, mRNA export factors, the H2AZ variant histone and the Snf1p-dependent Spt-Ada-Gcn5-acetyltransferase (SAGA) complex are each required for peripheral localization of inducible genes suggesting that Gunter Blobel's 'gene-gating' hypothesis accurately describes the mechanisms for coordinating transcription and mRNA export in *S. cerevisiae* (Brickner et al., 2007; Cabal et al., 2006; Dieppois et al., 2006). Multiple cellular inputs are likely contributing to the dynamics of peripheral recruitment and release. The positioning of the *INO1* and *GAL1* loci are released from the periphery in S-phase, in a mechanism involving Cdk1 phosphorylation of Nup2 (Brickner and Brickner, 2010). It is currently unclear how environmental cues signal and result in a change in the 3D organization of the genome. Many of the gene-positioning studies have also only examined one or two gene loci at a time. Future experiments utilizing 3C techniques will help to resolve whether specific gene expression programs alter global nuclear architecture or coordinate expression of hubs of clustering genes.

Not only are genes repositioned within the nucleus, but signaling though mitogen-activated protein kinase (MAPK) pathways alter the subnuclear localization of a multiple nuclear proteins. In the mating pheromone MAPK signaling pathway, transcriptional repressor Dig1 prevents the Ste12 transcription factor from localizing to subnuclear foci (McCullagh et al., 2010). Preventing Ste12-foci formation inhibits intrachromosomal

interactions and the inappropriate activation of pheromone-responsive genes. The

pheromone MAPK and Hog1 MAPK pathways receive input from the same upstream

signaling components. Therefore, these pathways have multiple mechanisms to prevent

cross talk and isolate the two distinct transcriptional responses. Under hyperosmotic

signaling, the transcription factors and nuclear kinases downstream of the pheromone

MAPK pathway are sequestered in subnuclear foci (Vidal et al., 2013). These foci are

predicted to prevent inappropriate activation of pheromone responsive genes under Hog1

MAPK signaling. Additionally, the hnRNP protein Nab2 is localized to subnuclear foci

upon heat shock and is also phosphorylated by Slt2, the MAPK of the cell wall integrity

pathway (Carmody et al., 2010). Nab2 subnuclear foci co-localize with Mlpl and may

contribute to the retention of normal polyA mRNAs under heat shock. These few

examples highlight the dynamics of nuclear proteins, and suggest that MAPK pathways

exploit nuclear architecture for the coordination and isolation of events in gene

expression.

Concluding Remarks

  Past and current studies have unraveled a new field of nuclear cell biology with

the purpose of understanding features of higher order nuclear structure and the impacts

on the functional output of the genome. Major questions remain, as we are just beginning

to understand the pathways that control chromatin organization and nuclear architecture.

We have little knowledge of the components that are required to assemble chromatin

domains, chromatin territories and the overall positioning of chromatin within the

nucleus. Once we begin to identify these components, we can ask what processes

influence the rearrangements that occur during development to produce cell-type specific

chromatin arrangements. Furthermore, it is unclear what cellular cues influence the

assembly or disassembly of nuclear bodies and the dynamic movements of genes between

nuclear compartments. These events are stochastic in nature, but whether these stochastic

events influence the efficiency of gene expression remains undetermined.

Though evolution has led to dramatic differences in genome sequence and size,

budding yeast and mammalian nuclei still exhibit conserved properties of nuclear

organization. Using the budding yeast system, I will expand our understanding for the

relationships between chromatin organization and nuclear structure. Also, I will describe

alterations in nuclear architecture that occur upon *S. cerevisiae* MAPK signaling and will

identify the cellular cue that impacts both the subnuclear localization of a transcription

factor and the stochastic activation of gene expression.

CHAPTER 2

MEMBERS OF THE RSC CHROMATIN-REMODELING COMPLEX ARE REQUIRED FOR MAINTAINING PROPER NUCLEAR ENVELOPE STRUCTURE AND PORE COMPLEX LOCALIZATION

Introduction

The nuclear envelope (NE) double lipid bilayer is a defining feature of the eukaryotic cell, imparting spatial separation between the nuclear chromatin and the cytoplasm. As such, knowing how communication across the NE is mediated will be critical to resolving regulation of gene expression and nucleocytoplasmic signaling. Nuclear pore complexes (NPCs) constitute the site of exchange for all macromolecules between the nucleus and cytoplasm. Each NPC spans a NE pore, and consists of a central channel, cytoplasmic and nuclear ring structures, cytoplasmic fibrils, and a nucleoplasmic basket-like structure (Beck et al., 2004). The composition of the metazoan and budding yeast NPC has been analyzed by a number of groups, and overall both are built from a similar complexity of ~30 total conserved proteins, referred to as nucleoporins (Nups) and pore membrane proteins (Poms) (Cronshaw et al., 2002; Rout et al., 2000; Tran and Wente, 2006). Some Nups are present exclusively on one face of the NPC and others, on both faces (Fahrenkrog and Aebi, 2003; Rout et al., 2000). Recent studies have revealed connections between nuclear face Nups and chromatin (Capelson and Hetzer, 2009), and between NE dynamics and NPCs (Scarcelli et al., 2007). Understanding the structural organization and biogenesis of the NE and NPCs is required to more fully define functional events at the nuclear periphery.

In higher eukaryotes, NPCs assemble at the end of an open mitosis as the NE reforms (Hetzer et al., 2005). Importantly, NPCs also are generated *de novo* in the existing NE during interphase with the number of NPCs nearly doubling (Maul et al., 1971). In organisms with a closed mitosis, such as the budding yeast *S. cerevisiae*, an intact NE is maintained throughout the entire cell cycle and all NPC biogenesis requires *de novo* insertion into this pre-existing NE (Winey et al., 1997). Therefore the NE must be plastic and dynamic for these *de novo* events of NPC assembly, while simultaneously functioning to preserve the structural integrity of the nucleus. Remarkably the NE in *S. cerevisiae* lacks the structural support provided by the nuclear lamins in metazoans, and still retains a spherical nuclear shape with a nonrandom distribution of NPCs (Winey et al., 1997).

Recent evidence suggests that several factors converge to control NE dynamics at sites of de novo NPC assembly. Such new NPCs arise by insertion and not by the duplication and division of existing NPCs (D'Angelo et al., 2006). Thus, first, reorganization and fusion of the NE to form a pore is likely initiated from both sides of the double membrane by the Poms: Pom34, Pom152, and Ndc1 in *S. cerevisiae*, and Pom121, gp210, and Ndc1 in higher eukaryotes (Aitchison et al., 1995; Antonin et al., 2005; Campbell et al., 2006; Dawson et al., 2009; Madrid et al., 2006; Mansfeld et al., 2006; Miao et al., 2006; Onischenko et al., 2009; Stavru et al., 2006). Second, several Nups with predicted COPII/coatomer-like domains are implicated in stabilizing these pore membranes, including the yeast Nup84 (metazoan Nup107-160) subcomplex (Brohawn et al., 2008; D'Angelo et al., 2006; Debler et al., 2008; Devos et al., 2006; Drin et al., 2007; Harel et al., 2003; Hsia et al., 2007; Siniossoglou et al., 1996; Walther et al.,

29

2003), yeast Nup53-Nup59 (metazoan Nup32) (Hawryluk-Gara et al., 2008; Marelli et al., 2001; Onischenko et al., 2009), and yeast Nup170-Nup157 (Flemming et al., 2009; Makio et al., 2009). Notably, Nup53-Nup59 and Nup170-Nup157 also have discrete connections to the Poms. Nup53-Nup59 interact physically with Ndc1 (Mansfeld et al., 2006; Onischenko et al., 2009) and genetically with Pom34 (Miao et al., 2006); whereas Nup170-Nup157 exhibits both genetic and physical interactions with Pom34 and Pom152 (Aitchison et al., 1995; Flemming et al., 2009; Makio et al., 2009; Miao et al., 2006; Tcheperegine et al., 1999). Known to maintain ER tubules (De Craene et al., 2006; Hu et al., 2008; Voeltz et al., 2006)s, yeast *RTN1* and *YOP1* also have genetic linkages to both the *POM*s and genes encoding the yeast Nup84 subcomplex (Dawson et al., 2009). Moreover, loss of Rtn1 and Yop1 results in dramatic alterations of NPC morphology and localization and reduced pore formation in vitro. These discoveries underscore the importance of controlling NE dynamics for NPC assembly.

Several ER/NE integral membrane proteins that affect NE composition or fluidity also impact NPC structure. NPCs are mislocalized into NE herniations in *brr6* and *apq12* mutants (de Bruyn Kops and Guthrie, 2001; Scarcelli et al., 2007), and the membrane fluidizing agent benzyl alcohol rescued the *apq12* phenotype (Scarcelli et al., 2007). Interestingly, flares of NE containing NPCs develop in yeast strains lacking the Spo7/Nem1 holoenzyme, a negative regulator of phospholipid synthesis (Campbell et al., 2006; Siniossoglou et al., 1998). These NE/NPC flares expand directly from the NE region nearest the nucleolus, suggesting that both phospholipid composition and chromatin interactions impact NE and NPC dynamics.

For post-mitotic NE and NPC assembly, recent studies have suggested that the chromatin-associated factor MEL-28/ELYS is required for Nup107-160 complex targeting (Franz et al., 2007; Gillespie et al., 2007; Liu et al., 2009; Rasala et al., 2006). The AT-rich hook of MEL-28/ELYS binds to AT-rich chromatin, and Nup107-160 binding facilitates recruitment of vesicles containing Pom121 and Ndc1 (Rasala et al., 2008). This might reflect the recruitment of Nups to condensed chromatin and formation of a "pre-pore" structure. Moreover, such "pre-pores" could trigger nuclear pore formation coincident with post-mitotic NE re-formation (Anderson and Hetzer, 2008). A similar requirement for Nup-chromatin interactions in biogenesis during *de novo* NPC insertion into intact NEs has not been reported.

Here, we used a combination of innovative genetic approaches in *S. cerevisiae* to comprehensively assess the role of essential factors in NPC localization, structure and, potentially, assembly into the NE. The genes identified encode factors involved in nuclear transport, chromatin remodeling, secretion, lipid anchoring, protein degradation and lipid biosynthesis. Strikingly, multiple components of the RSC chromatin remodeling complex were identified including the essential ATPase catalytic subunit Sth1 (Andrulis et al., 1998). In *S. cerevisiae*, the RSC complex is composed of 15 subunits, several of which are essential for cell viability (Cairns et al., 1996; Martens and Winston, 2003; Saha et al., 2006). Although RSC was first identified for its roles in chromatin remodeling and has been linked to transcriptional activation and inhibition (Angus-Hill et al., 2001; Cairns et al., 1996; Damelin et al., 2002; Kasten et al., 2004; Ng et al., 2002; Soutourina et al., 2006), RSC has also been linked to a wide range of chromatin-based functions such as kinetochore function and cohesin association (Baetz et

al., 2004; Hsu et al., 2003; Huang et al., 2004), and double strand break repair with the

DNA damage response (Chai et al., 2005; Liang et al., 2007; Shim et al., 2007; Shim et

al., 2005). Several reports suggest connections between NPCs and RSC. A *nup84Δ rsc7Δ*

double mutant is synthetically lethal (Wilson et al., 2006), and a *rsc9* mutant has altered

Kap121-GFP localization (Damelin et al., 2002). In this report, we present evidence for

the role of the RSC complex in maintaining proper NE and NPC structure.

Results

Genome-wide genetic screen for essential regulators of GFP-Nup localization

To identify essential factors required for NPC localization, structure and/or

assembly, we designed a genetic screening approach in the budding yeast *S. cerevisiae*.

The rationale for the screen was based on extensive genetic evidence showing that

mutants with defects in NPC assembly or stability have GFP-Nup mislocalization (Bucci

and Wente, 1998; Madrid et al., 2006; Miao et al., 2006; Ryan et al., 2003; Ryan and

Wente, 2002b; Ryan et al., 2007). This can be due to the inability of the GFP-Nup to

incorporate into newly forming NPCs or the disassembly of existing NPCs. We

hypothesized that the genes encoding regulators of the essential NPC structure would

themselves be essential for viability. A collection of yeast strains has been generated

wherein 813 of the 1,105 reported essential genes in *S. cerevisiae* were individually

placed under the control of a doxycycline-regulated promoter (*TetO₇*) (Mnaimneh et al.,

2004). The *TetO₇*-promoter allows regulated transcription of the respective gene (open

reading frame, *orf*) with specific repression in the presence of doxycycline. The

availability of this collection enabled the design of a direct genome-wide strategy to

analyze the effective null or hypomorph phenotype of known essential genes for defects in NPC structure/assembly.

To conduct the screen, a GFP-tagged allele of the essential nucleoporin *NIC96* (*GFP-nic96*) was systematically incorporated into individual doxycycline-sensitive strains of the yeast *TetO$_7$-orf* strain collection (see Materials and Methods). Specifically, the screen used only the *TetO$_7$-orf* strains with a reported slow growth phenotype in the presence of doxycycline (Mnaimneh et al., 2004). Perturbations in growth rate indicated that the essential gene was indeed downregulated. We speculated that if the gene played a role in NPC structure/assembly, then the GFP-Nic96 localization should be perturbed when the given *TetO$_7$-orf* strain was grown in doxycycline. The resulting *GFP-nic96 TetO$_7$-orf* strains were individually examined for GFP-Nic96 localization based on direct fluorescence microscopy of live cells. Strains were cultured in the presence of doxycycline for five hours or overnight. In total, GFP-Nic96 localization was evaluated in 531 strains and compared to that in a parental control strain without a *TetO$_7$-orf*. GFP-Nic96 localization was scored as wild type if the fluorescent signal was detected at the nuclear rim, and as mislocalized if all or a portion of the fluorescent signal was not at the nuclear rim. Mislocalization phenotypes were further ranked as weak, moderate, or severe. In addition, some strains were scored as having speckles (small foci of fluorescent signal in the cytoplasm) or as having foci/clusters of fluorescent signal at the nuclear rim.

We identified 44 *TetO$_7$-orf* strains with mislocalized GFP-Nic96 and/or distorted nuclear rim structure (Figure 2.1A, Table 2.1). Based on functional analysis in published studies, these genes were classified into eight major categories. This included genes
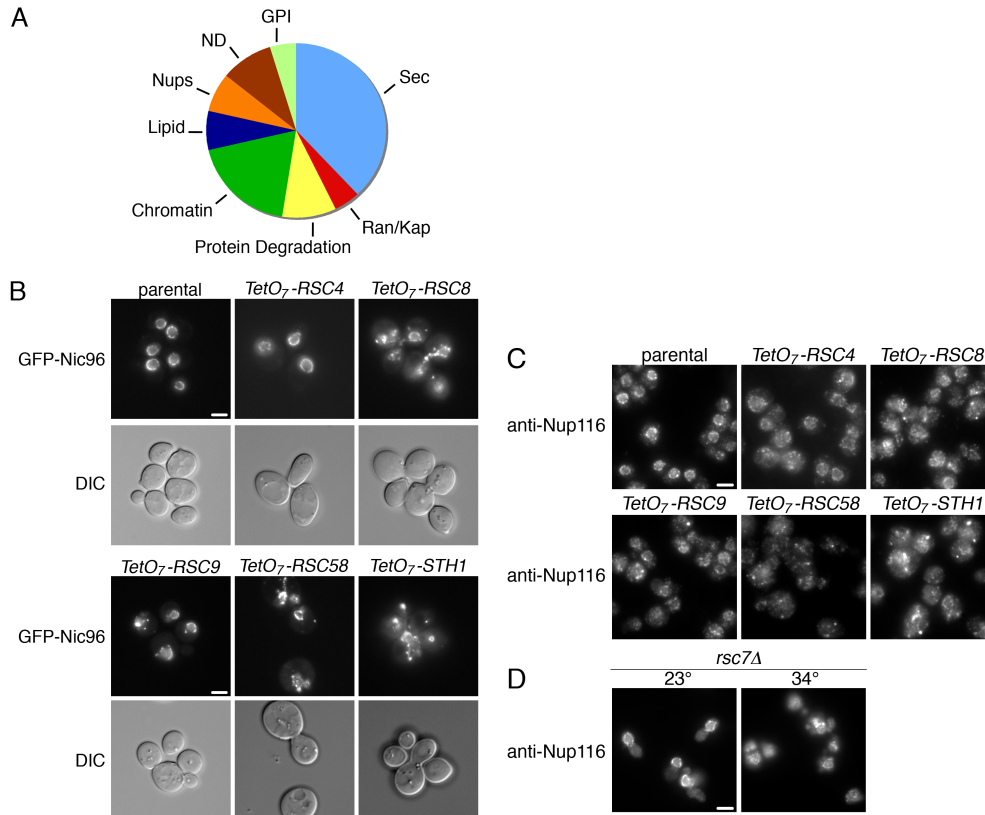
Figure 2.1. GFP-Nic96 mislocalizes in *TetO₇-orf* strains. (A) Pie chart representing the distribution between different classes of *TetO₇-orf* isolates with GFP-Nic96 perturbations. Genes linked to vesicular trafficking (Sec; blue), Ran/Kap (red), protein degradation (yellow), chromatin associated/chromatin remodeling (Chromatin; dark green), lipid biosynthesis (Lipid; purple), Nups (orange), others of defined function but unrelated to preceding (ND; brown), GPI anchoring (GPI; light green). (B) Direct fluorescence microscopy of GFP-Nic96 localization in strains from the *GFP-Nic96 TetO₇-orf* collection is shown after growth in the presence of 10 mg/ml doxycycline for approximately 14 hours. Differential interference contrast (DIC) images reveal cell morphology. (C, D) Indirect immunofluorescence microscopy for Nup116 localization of (C) *TetO₇-orf* strains after culturing in doxycycline (as in (B)), and (D) the *rsc7D* strain at 23°C and after shifting to 34°C for 5 hours. Size bars, 5 mm.

encoding known Nups as well as factors required for nuclear transport (Ran/Kap),

chromatin remodeling, secretion, protein degradation, glycosylphosphatidyl inositol

(GPI) anchoring and lipid biosynthesis. Previous studies have also documented NPC and

NE perturbations in mutants with defective Nups/Poms (Aitchison et al., 1995; Bogerd et

al., 1994; Doye et al., 1994; Heath et al., 1995; Kosova et al., 1999; Madrid et al., 2006;

Miao et al., 2006; Siniossoglou et al., 1996; Wente and Blobel, 1993, 1994), secretion

factors (Nanduri et al., 1999; Nanduri and Tartakoff, 2001; Ryan and Wente, 2002b),

lipid biosynthetic enzymes (Schneiter et al., 1996), the RanGTPase cycle (Ryan et al.,

2003), and Kap95 (Ryan et al., 2007). A small subset of the components known to affect

NPC structure or assembly were not identified by our screen, including the Nups *NDC1*,

NUP1, *NUP159*, and *NUP192*, as well as the RAN cycle members *NTF2* and *RNA1*.

KAP95 and *KAP121* were unresponsive to doxycycline treatment, while *PRP20* and

GSP1 were absent from the collection, and therefore these candidates were not included

in the screen dataset.

Interestingly, the screen here identified genes encoding several essential

components of the RSC chromatin remodeling complex: *STH1*, *RSC8*, *RSC58,* and

ARP9. *RSC4*, *RSC9* and *ARP7* were also identified after direct testing. Each of these

strains showed GFP-Nic96 mislocalization to varying extents (Figure 2.1B, Table 2.1),

which generally correlated with the growth defect of the strain in doxycycline-containing

media. The level of growth in the presence of doxycycline is thought to reflect the level

of transcriptional repression for the respective *TetO$_7$-orf* (Mnaimneh et al., 2004).

Mislocalization and growth defects were severe in the *TetO$_7$-RSC58, TetO$_7$-RSC8*, and

TetO$_7$-STH1 strains. Mislocalization of GFP-Nups in *TetO$_7$-STH1* cells was first

Table 2.1. Results of *TetO₇-orf* strain phenotypes for GFP-Nic96 mislocalzation

Gene	GFP-Nic96 defect[1]	Growth defect[2]	Protein description
Chromatin linked			
STH1	Moderate ML	Severe	RSC complex ATPase
RSC4	Weak ML	Weak	RSC complex
RSC8	Severe ML	Severe	RSC complex
RSC9	Weak ML	Moderate	RSC complex DNA binding protein
RSC58	Moderate ML	Severe	RSC complex
ARP7/RSC11	Weak rim clusters	Severe	RSC and SWI/SNF complexes
ARP9/RSC12	Weak ML	CSG	RSC and SWI/SNF complexes
SPT16	Weak rim clusters	Severe	Remodeling and PolII elongation
TAF6	Weak speckles	Severe	Chromatin modification
DNA2	Severe distorted rim	Severe	DNA repair
Protein degradation			
UFD1	Moderate speckles	Severe	protein degradation
CDC48	Moderate ML	Severe	ATPase involved in protein degradation
PRE6	Weak speckles	Severe	20S proteosome subunit
RPN5	Moderate ML	Severe	26S proteosome regulatory subunit
Lipid synthesis			
LCB2	Weak speckles	Severe	Sphingolipid biosynthesis
FAS2	Moderate speckles	Severe	Fatty acid synthase complex
CDS1	Weak speckles	Severe	Phospholipid biosynthesis
Secretory pathway			
COP1	Moderate speckles	Severe	COPI coat
RET3	Weak speckles	Severe	COPI coat
SAR1	Moderate speckles	Severe	COPII coat
SEC10	Moderate speckles	Severe	Exocyst complex
SEC13	Weak speckles	Severe	COPII complex; Nup84 complex
SEC14	Moderate speckles	Severe	Golgi plasma membane transport
SEC15	Moderate speckles	Severe	Exocyst complex
SEC17	Weak speckles	Severe	ER-Golgi transport, cis-SNARE complex
SEC21	Weak speckles	Severe	COPI coat, ER-Golgi transport
SEC26	Weak speckles	Severe	COPI coat, ER-Golgi transport
SEC27	Weak speckles	Severe	COPI coat, ER-Golgi/Golgi-ER transport
COG4/SEC38	Moderate speckles	Severe	Fusion of transport vesicles to Golgi
YIP1	Moderate speckles	Moderate	COPII transport vesicle biogenesis
SED5	Weak speckles	Severe	t-SNARE syntaxin, ER-Golgi transport
TIP20	Weak speckles	Severe	COPI vesicle fusion with ER
BET1	Weak speckles	Severe	v-SNARE, ER-Golgi transport
Nucleoporins			
NUP145	Severe ML	Severe	Nup84 complex
NUP1	Severe distorted rim	CSG	Nuclear face, FG Nup
NUP49	Weak ML	Moderate	Nic96/Nsp1 complex, FG Nup
Nuclear transport			
RNA1	Severe clusters	Severe	Ran GTPase activating protein
PDS1	Weak ML	Severe	Karyopherin, protein import
GPI anchoring			
CDC91/GAB1	Weak speckles	Severe	Attachment of GPI anchor to proteins
YNL158W/PGA1	Weak speckles	Severe	Mannosyltransferase complex, GPI anchoring
Other			
RIB7	Weak speckles	Severe	Riboflavin biosynthesis
YNL149C/PGA2	Moderate speckles	Severe	Mitochondrion organization/biogenesis
STT4	Weak ML	Severe	PI4 kinase, vacuole morphology
TUB4	Weak speckles	Severe	Spindle organization and biogenesis

[1]GFP fluorescence in the presence of doxycycline ranked as weak, moderate or severe in regard to mislocalization from rim (ML, lack of strong nuclear rim), speckles (small foci away from the nuclear rim), clusters (dots on the nuclear rim), or generally distorted nuclear rims that were still evenly stained with GFP-Nic96.
[2]Growth defect in the presence of doxycycline as observed in this study or as reported in Hughes et al, 2000.
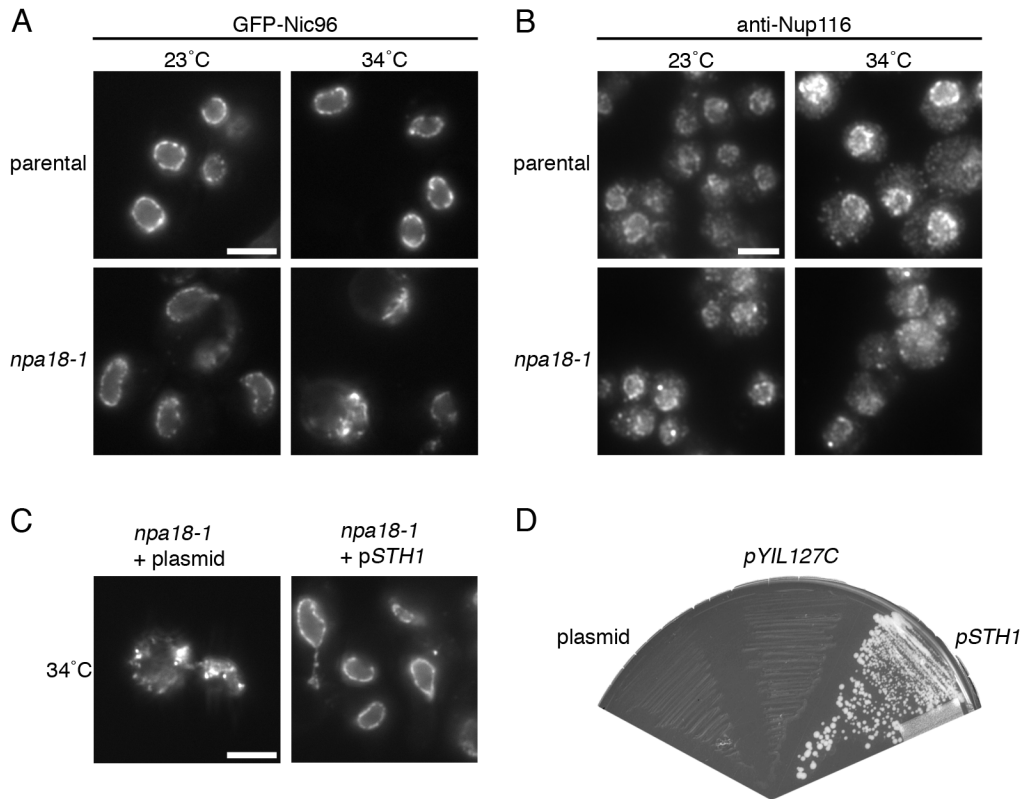
Figure 2.2. Nups mislocalize in the *sth1-F793S* temperature sensitive strain. (A) Direct fluorescence microscopy of GFP-Nic96 and Nup170-GFP of logarithmically growing parental or *sth1-F793S* cells after growth at 23°C or after shifting to growth at 34°C for five hours. Parental cells, SWY2089; *sth1-F793S GFP-nic96 nup170-GFP* cells, SWY3201. (B) Indirect immunofluorescence microscopy of *sth1-F793S* cells for Nup116 localization under the same growth conditions as in (A). Parental cells, SWY518; *sth1-F793S*, SWY3249. (C) *STH1* expression rescues the GFP-Nic96 and Nup170-GFP mislocalization in the *sth1-F793S* mutant. Direct fluorescence microscopy was conducted with the *sth1-F793S GFP-nic96 nup170-GFP* strain (SWY3202) transformed with empty plasmid (pRS315) or the *STH1* plasmid (pSW3051). Size bars (A-C), 5 mm. (D) *STH1* expression rescues the *npa18-1* growth defect at 34°C. The *sth1-F793S* mutant strain (SWY3203) was transformed with empty plasmid (pRS315), plasmid harboring the *STH1* ORF and its 5' promoter region (pSW3051), or the *YIL127C* ORF and its 5' promoter region (pSW3049). The resulting strains were streaked for growth on SM –Leu plates.

apparent after six hours of culturing in the presence of doxycycline. This mislocalization

became more extensive after 12 hours and was detected in over ninety-percent of the

cells. At this time point, the viability assays confirmed that mislocalization was not an

indirect effect of doxycycline toxicity or cell death (data not shown).

To further analyze the localization of NPC proteins in the *TetO7-orf* strains for the

RSC complex, the respective strains were processed for indirect immunofluorescence

microscopy for Nup116 (Figure 2.1C). The *TetO7-RSC8, TetO7-RSC58*, and *TetO7-STH1*

strains showed severe mislocalization of Nup116 when grown in the presence of

doxycycline. The *TetO7-RSC4* and *TetO7-RSC9* strains were again less markedly altered.

Defects in NPC structure/assembly have not been previously documented in RSC

complex mutants. *STH1* encodes the essential ATPase catalytic subunit of the RSC

complex, whereas *RSC4*, *RSC8*, *RSC9*, and *RSC58* encode core or accessory RSC

complex complements (Saha et al., 2006). Overall, this genome-wide screening strategy

identified several essential RSC components that were required for normal Nup

localization.

**Isolation of a temperature sensitive *sth1-F793S (npa18-1*) mutant in a forward
genetic screen for NPC structure defects**

In an independent approach for identifying factors required for NPC

structure/assembly, we previously conducted a visual screen for temperature sensitive

strains with defective GFP-Nic96 and Nup170-GFP localization (Ryan et al., 2003; Ryan

and Wente, 2002b; Ryan et al., 2007). This screen isolated 121 NPC assembly (*npa*)

mutant strains in numerous complementation groups, including those with defects in

secretion factors, Ran-cycle factors, and Kap95. Here we selected one unidentified *npa*

complementation group, *npa18*, to further characterize. The *npa18-1* mutant showed

some GFP-Nic96/Nup170-GFP mislocalization at 23°C, and had severe mislocalization

at the nonpermissive temperature (34˚C) (Figure 2.2A). The GFP-Nic96/Nup170-GFP

signal was no longer localized around the nuclear rim, and instead the fluorescent signal

was detected in large, nonuniform foci throughout the cytoplasm and surrounding the

nucleus. This mislocalization was first observed after three hours at 34˚C in

approximately forty percent of cells (data not shown), and was maximal by five hours.

Cell viability assays found that mislocalization was not due to cell death. Indirect

immunofluorescence detection of Nup116, Nup159 and Pom152 also showed similar

mislocalization (Figure 2.2B and Figure 2.3). Thus, multiple distinct Nup subcomplexes

were perturbed in the *npa18-1* mutant.

Backcrossing the *npa18-1* mutant with the parental strain revealed 2:2 linked

segregation of temperature sensitivity and GFP-Nup mislocalization. This indicated that

the defects were due to the mutation of a single gene. To identify the mutated gene, a

yeast *CEN* genomic library was used to select for complementation of the recessive

temperature sensitive phenotype. The inserts from two unique plasmids that rescued the

temperature sensitive growth defect were isolated from yeast and sequenced. Both

contained nucleotide sequence corresponding to a portion of chromosome IX that

contained the complete ORF for *STH1* and a putative ORF *YIL127C*. Expression of

YIL127C alone did not complement the growth defect (Figure 2.2D). However, an

expression plasmid with *STH1* alone was necessary and sufficient for restoration of

growth (Figure 2.2C).   Furthermore, *STH1* expression also restored nuclear rim

localization of GFP-Nic96 and Nup170-GFP at 34˚C (Figure 2.2C). Sequencing the
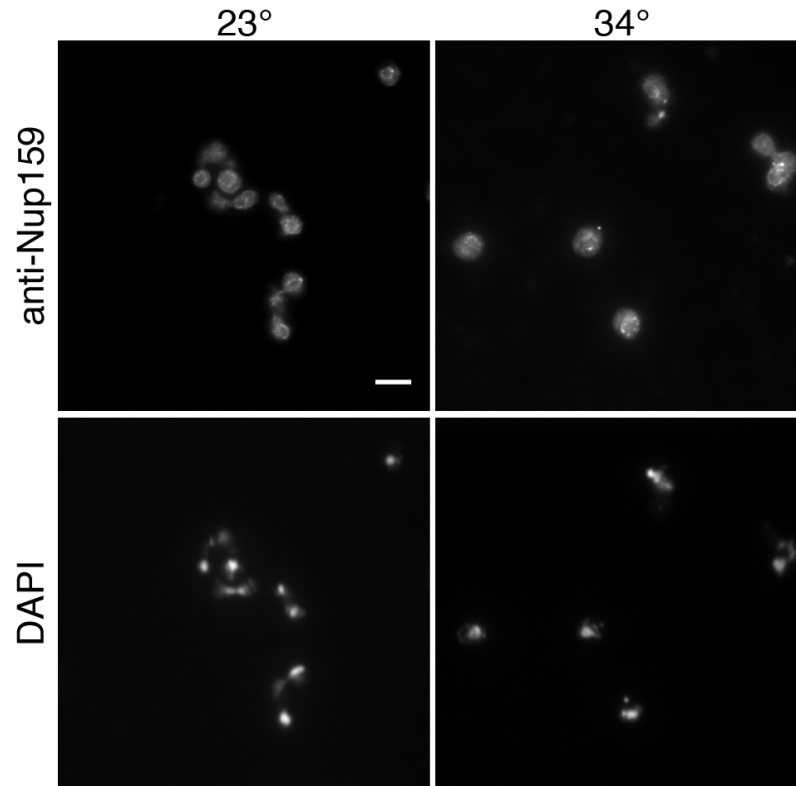
Figure 2.3. Nup159 mislocalizes in the *sth1-F793S* (SWY4143) mutant strain. Indirect immunofluorescence microscopy for Nup159 localization at the 23°C or after shifting to 34°C for five hours. Size bars, 5 **µ**m.

chromosomal DNA from the *npa18-1* mutant strain revealed a single point mutation in the *STH1* nucleotide sequence, which resulted in a single amino acid substitution, F793S, in the ATPase domain. Thus, we designated this *npa18-1* mutant as *sth1-F793S,* and refer to it as such henceforth. Complementation analysis amongst the remaining unidentified *npa* mutant strains identified *sth1-F793S* as the only allele representing this *npa18* complementation group.

The *sth1-F793S* mutant is an effective null with unique allele-specific effects

Previous studies of *STH1* have reported four temperature sensitive *sth1* alleles (*sth1-1*, *sth1-2*, *sth1-3*, and *sth1-L1346A*) (Du et al., 1998; Huang et al., 2004). The *sth1-1*, *sth1-2*, and *sth1-3* alleles each have mutations in the sequence region corresponding to the ATPase domain, although distinct from the *sth1-F793S* allele. To determine whether these other *sth1* alleles perturb Nup localization, we conducted indirect immunofluorescence microscopy for Nup116 localization. After four hours at 37˚C, Nup116 remained predominantly at the nuclear rim in each of these strains (Figure 2.4A), whereas Nup116 mislocalized under similar conditions in the strain expressing *sth1-F793S* (Figure 2.2B). Similar results were obtained after nine hours at 37˚C, with only slight mislocalization of Nup116 detectable in cells expressing *sth1-3* (data not shown). Therefore, the *sth1-F793S* allele had a specific effect on Nup localization.

We further characterized the *sth1-F793S* mutant by testing for whether known multicopy suppressors of *sth1-3* allele also suppressed the temperature sensitive phenotype and Nup mislocalization of the *sth1-F793S* allele. Genes encoding members of the cell wall integrity pathway (*MID2, RHO2, ROM2. PKC1*, and *WSC1*) have been

41

previously shown to multicopy suppress the temperature sensitive growth phenotype of the *sth1-3* allele (Chai *et al.,* 2002). However, the growth defect (data not shown) and Nup60-GFP mislocalization in the *sth1-F793S* mutant were not rescued by overexpression of any of these genes (Figure 2.5). Therefore, the *sth1-F793S* allele may be affecting distinct or multiple functions of RSC that are not compensated by the cell wall integrity pathway alone.

Next, we compared the *sth1-F793S* allele and the *sth1-3* allele for growth on different carbon sources and in the presence of thiabendazole (TBZ) (microtubule-depolymerizing agent) or hydroxyurea (HU) (ribonucleotide reductase inhibitor) (Figure 2.4B). While the parental strains of each mutant exhibit slightly different growth phenotypes, growth of the *sth1-F793S* mutant was dramatically enhanced on non-glucose carbon sources as compared to both respective parental strains and to the *sth1-3* mutant. The enhanced growth phenotype specific to the *sth1-F793S* mutant might be due to changes in transcription as a result of RSC depletion. Similar to the previously described effects on other *sth1* mutant alleles (Hsu et al., 2003; Koyama et al., 2002), the *sth1-F793S* mutant showed enhanced sensitivity to HU, while TBZ was less effective on the *sth1-F793S* mutant (Figure 2.4B, lower two rows). The allele-specific drug sensitivities indicate differential functions for RSC in double strand break repair, microtubule function and kinetochore structure, events distinct from transcription (Chai et al., 2002; Chai et al., 2005; Liang et al., 2007; Shim et al., 2007; Shim et al., 2005; Tsuchiya et al., 1998).

Given the similarities between the Nup mislocalization in the *sth1-F793S* and *TetO7-sth1* mutants, we evaluated protein stability in the *sth1-F793S* cells by
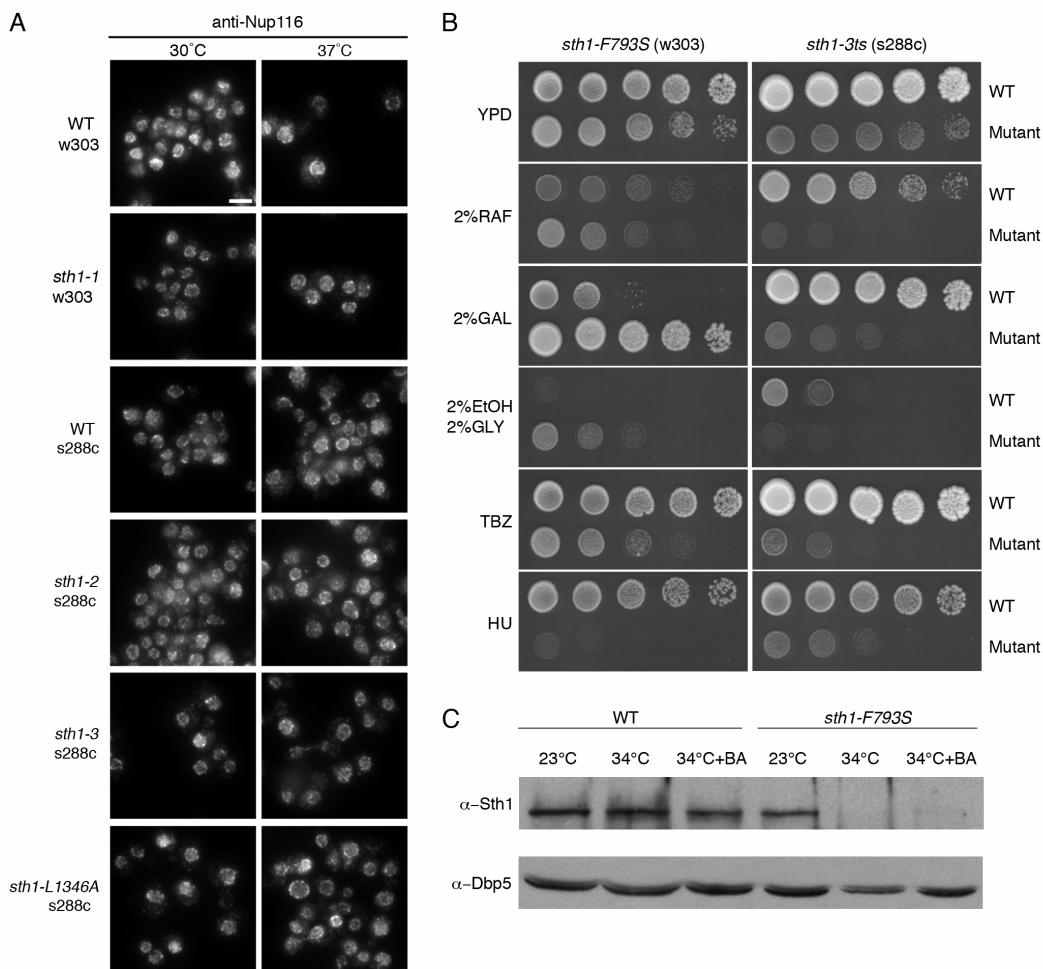
Figure 2.4. The *sth1-F793S* allele is distinct from other *sth1* alleles. (A) NPC mislocalization defect is specific to the *sth1-F793S* allele. Indirect immunofluorescence microscopy for Nup116 localization was conducted on logarithmically growing parental (WT) and designated *sth1* mutant cells cultured at 30˚C or 37˚C for 4 hours. Size bar, 5 mm. (B) The growth phenotypes of the *sth1-F793S* allele are distinct from those for the *sth1-3* allele. Serial diluted *sth1-F793S* and *sth1-3* mutant cells and the corresponding wild type (WT) strains, W303 (SWY518) and S288C (YOL183) respectively, were spotted onto YP agar plates with different carbon sources, thiobendazole (TBZ) (60 mg/ml), or hydroxyurea (HU) (50 mM). The plates were incubated at semi-permissive growth temperatures (30°C for *sth1-F793S*; 35°C for *sth1-3*) and monitored for growth after 2 days. (C) The *sth1-F793S* allele is an effective null at 34°C. The wildtype (SWY518) and *sth1-F793S* (SWY4143) strains were grown for 5 hours at 23°C or 34°C in the presence or absence of 0.4% BA. Total cell lysates were separated by SDS-PAGE and immunoblotted with a rabbit anti-Sth1 polyclonal antibody.

43
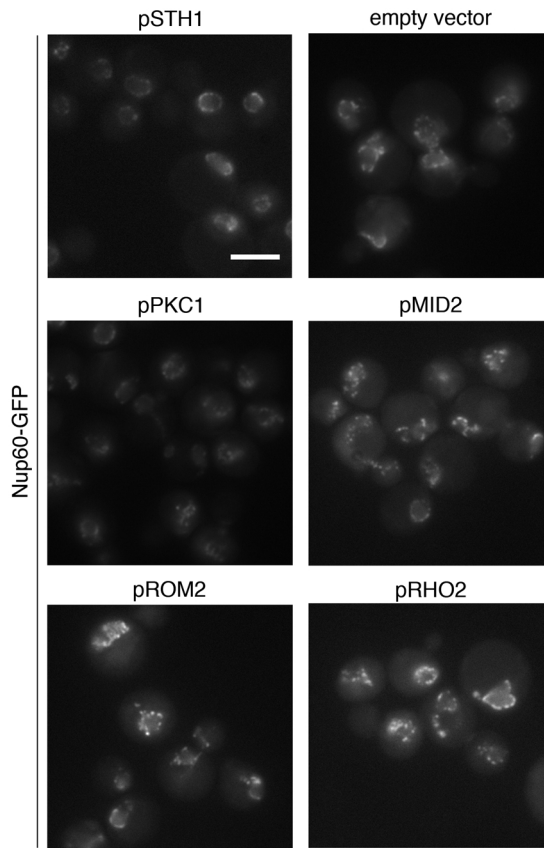
Figure 2.5. Members of the cell wall integrity pathway do not multicopy suppress nucleoporin mislocalization in the *sth1-F793S* mutant. Nup60-GFP localization was observed after a five-hour shift to 34°C in the *sth1-F793S* mutant (SWY4182) transformed with 2-micron based multicopy suppressor plasmids from the Yeast Genomic Tiling Collection (*pSTH1*, empty vector, *pPKC1*, *pMID2*, *pRHO2*, and *pROM2*). Size bars, 5 **µ**m.

immunoblotting. Wild type Sth1 protein levels were unchanged after shifting to growth at 34°C for 5 hours; however, the sth1-F793S protein was not detectable after temperature shifting (Figure 2.4C). Others report that the sth1-3 protein is stable and has wild type ATPase activity (Du et al., 1998). Thus, at 34°C, the *sth1-F793S* allele is an effective null with distinct cellular perturbations.

Analysis of additional RSC complex members for NPC perturbations

By the nature of our genetic screening strategies, all of the RSC components identified represented essential genes. To investigate other subunits, we directly examined the available null strains for nonessential RSC components (Figure 2.6). Indirect immunofluorescence microscopy for anti-Nup116 and anti-GLFG Nups was conducted. Nups localized in a normal perinuclear punctate pattern in *rsc1D*, *rsc2D*, and *rsc14D* mutant cells. In *htl1D* cells, moderate mislocalization was detected after shifting to the nonpermissive temperature. Visual scanning of the Z-plane showed severe nuclear morphology perturbations coincident with the pattern of Nup mislocalization (Figure 2.6). The most striking mislocalization was observed in the *rsc7D* mutant, where Nups were markedly redistributed to cytoplasmic foci after shifting to growth at the nonpermissive temperature (Figure 2.1D). Overall, multiple independent members of the RSC complex were linked to proper NPC localization.
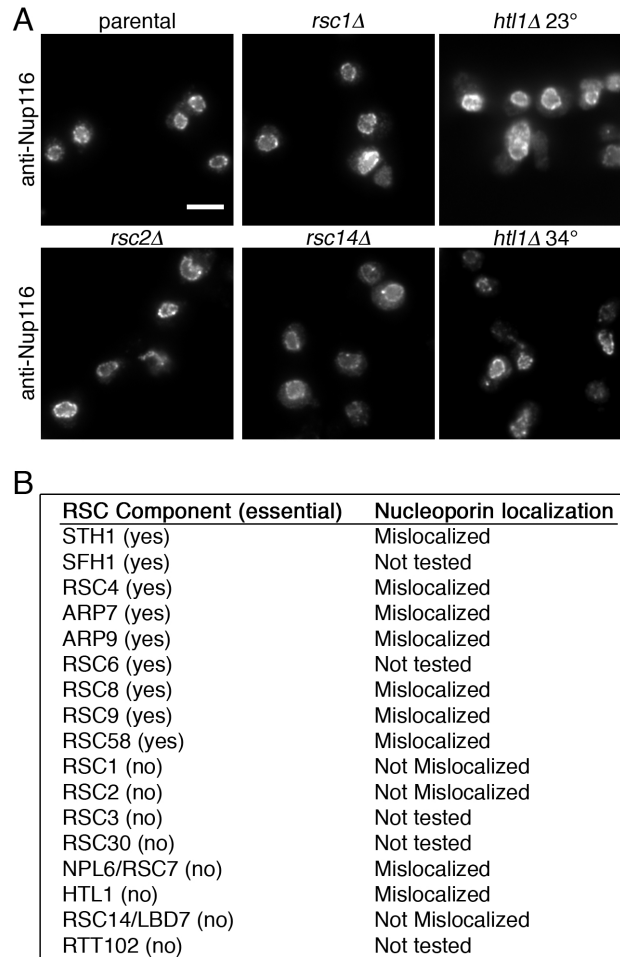
Figure 2.6. Nups mislocalize to varying degrees in *rsc* mutant strains. (A) Indirect immunofluorescence microscopy for Nup116 localization in *rsc1Δ, rsc2Δ, rsc14Δ* and *htl1Δ* strains at 23°C and in the *htl1Δ* strain after shifting for 5 hours at 34°C. (B) Nup localization phenotypes for each of the RSC components are summarized. Size bars, 5 μm.

Ultrastructure analysis of nuclear membrane defects in *sth1-F793S, TetO₇-STH1* and *TetO₇-RSC58* mutant cells

To further investigate the NPC defects in these *TetO₇-RSC* and *sth1-F793S* mutants, thin section transmission electron microscopy (TEM) was conducted. The *sth1-F793A* mutant and wild type parental strains were evaluated before and after growth for five hours at 34°C, whereas the *TetO₇-STH1* and *TetO₇-RSC58* strains were processed after ten hours of growth in the absence and presence of doxycycline. In the wild type parental strain and before temperature shifting (data not shown) or doxycycline treatment, the nuclei, NEs and NPCs of all the strains were not perturbed (Figure 2.7). In the control cells, the NPCs appeared as electron dense structures spanning the NE of a single distinct nucleus (Figure 2.7A, D, G). In contrast, striking ultrastructural perturbations were observed in the temperature arrested *sth1-F793S* cells (Figure 2.4B,C) and the doxycycline-treated *TetO₇-STH1* (Figure 2.7E,F) and *TetO₇-RSC58* cells (Figure 2.7H,I). Relative to parental or control cells, in all three mutants, there was significant cytoplasmic membrane proliferation that appeared to originate from the ER and/or NE. Extensive sheets of membrane were present, often in multiple layers, around the cell periphery/plasma membrane, and in intertwined honeycombs. There was also an accumulation of distinct 40-50 nm cytoplasmic vesicles. The nucleus itself was often difficult to clearly identify. When an apparent nuclear cross-section was observed, a few electron dense structures representing NPCs were detected. The time frame after temperature or doxycycline shifting for the appearance of these ultrastructural defects was coincident with the Nup mislocalization defects described above (Figures 2.1, 2.2).
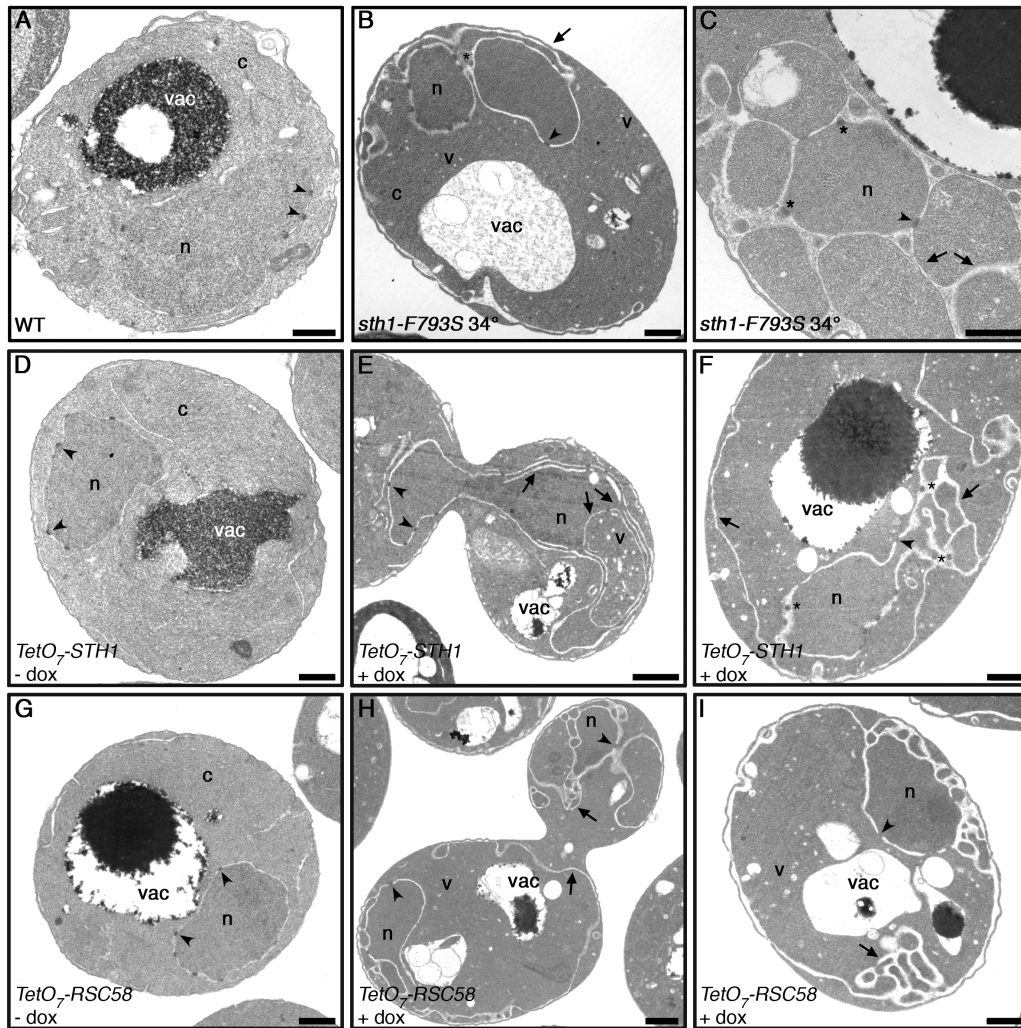
Figure 2.7. The *sth1-F793S* and *TetO₇-RSC* mutant cells have severe NE perturbations at the nonpermissive or repressive conditions. (A-C) Logarithmically growing parental cells (A, SWY2089) or *sth1-F793S* mutant cells (B-C, SWY3202) were shifted to the 34°C for 5 hours, then processed for TEM. (D-I) Logarithmically growing *TetO₇-STH1* (D-F) and *TetO₇-RSC58* (G-I) cells were cultured in the absence (D, G) or presence (E, F, H, I) o 10 mg/ml doxycycline for 10 hours, then processed for thin layer TEM. n, nucleus; c, cytoplasm; vac, vacuole; v, vesicle; arrowhead, NPC; *, NPC-like structure; arrow, membrane. Size bars, 0.5 mm.

GFP-Nup mislocalization in *rsc* mutants requires new protein synthesis and transcription

As a test for defects in new NPC assembly versus perturbations in the stability of existing NPCs, we have previously assayed the effect of cycloheximide treatment on Nup mislocalization in *npa* mutants (Ryan et al., 2003; Ryan et al., 2007). Mutants that perturb pre-existing factors or NPC components will not require translation for the phenotype and will show mislocalization in the presence of cycloheximide. In contrast, mislocalization due to perturbations in *de novo* NPC or NE biogenesis will require translation of assembly or structural factors for accumulation of perturbed GFP-Nups, and thus will not show GFP-Nup mislocalization in cycloheximide. This is true for the NPC assembly defects documented in the RanGTPase cycle mutants *prp20-G282S (npa14-1), ntf2-H104Y (npa11-1), rna1-S116F (npa13-1), gsp1-P162L (npa15-1), kap95-E126K (npa16-1)* and *apq12Δ* (Ryan et al., 2003; Ryan et al., 2007; Scarcelli et al., 2007). In *sth1-F793S (npa18-1)* and *rsc7D* mutant cells treated with cycloheximide, the GFP-Nups remained associated in a predominantly nuclear rim localization after incubation at the nonpermissive temperature (Figure 2.8A). Marked mislocalization was not detected. Similarly, treatment of *TetO$_7$-RSC8* cells with cycloheximide during nonpermissive growth conditions also prevented Nup mislocalization (Figure 2.8B). These data indicate that the defects in the *sth1-F793S*, *rsc7D*, and *TetO$_7$-RSC8* mutant strains required ongoing translation.

As the RSC complex is functionally linked to gene expression (Angus-Hill et al., 2001; Badis et al., 2008; Damelin et al., 2002; Hartley and Madhani, 2009; Kasten et al., 2004; Mas et al., 2009; Ng et al., 2002; Parnell et al., 2008; Soutourina et al., 2006) we speculated that some of the defects in the *sth1-F793S* mutant might be linked to altered
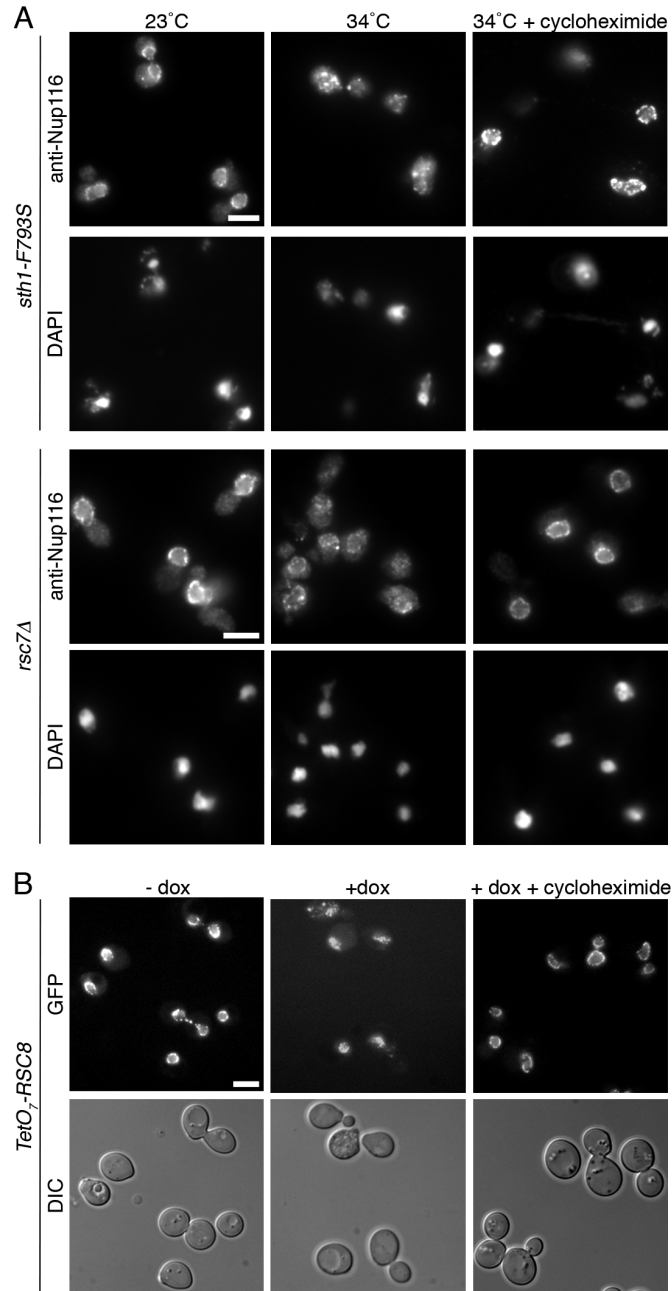
Figure 2.8. Translation is required for RSC NE/NPC perturbations. (A) Indirect immunofluorescence microscopy for anti-Nup116 C-terminal antibody localization was conducted for *sth1-F793S* and *rsc7D* mutant cells. Logarithmically growing cells were cultured at 23°C or 34°C for 5 hours, in the presence or absence of 10 mg/ml cycloheximide. (B) Direct fluorescence microscopy was conducted for GFP-Nic96 and Nup170-GFP localization in logarithmically growing cells *TetO7-RSC8* cells cultured in the presence or absence of 10 mg/ml doxycycline and 10 mg/ml cycloheximide for 8 hours. Corresponding DIC images are shown below each panel. Size bars, 5 mm.

expression of RSC-controlled genes that encode proteins involved in NE and/or NPC

biogenesis. To globally assess the role of transcription in the *sth1-F793S* Nup

mislocalization phenotype, we used a RNA polymerase II temperature sensitive mutant.

The *RBP4* gene encodes a non-essential RNA polymerase II subunit (Woychik and

Young, 1989); however, the *rbp4D* is temperature sensitive for growth above 32°C and

after 45 minutes at 37°C, 96% of RNA polymerase II transcription is lost (Miyao et al.,

2001; Woychik and Young, 1989). The *sth1-F793S rbp4D* double mutant was evaluated

for NPC localization by monitoring GFP-tagged Nic96, Nup60, or Nup133 (Figure 2.9).

After shifting to growth at 34°C for 5 hours, the respective GFP-tagged Nups remained

localized at the nuclear rim and mislocalization was not detected. GFP-tagged Nups also

remained rim localized in the *rpb4Δ* single mutant (data not shown). This observation

was further confirmed using thiolutin, an inhibitor of global RNA synthesis. Treatment

with thiolutin blocked GFP-tagged Nic96 mislocalization in *TetO$_7$-STH1* cells grown in

the presence of doxycycline (Figure 2.10) and GFP-tagged Nic96, Nup60, Nup133

mislocalization in the *sth1-F793S* mutant (data not shown). Taken together, both ongoing

transcription and translation were required for the NPC/NE defects.

Control experiments were also conducted to assay for effects on mRNA stability

in the *sth1-F793S* Nup mislocalization phenotype. Quantitative-PCR was used to

evaluate *NUP* and *ACT1* relative mRNA levels between wildtype and *sth1-F793S* mutant

cells. At the permissive growth temperature, *NUP60-GFP* and *NIC96-GFP* mRNA levels

did not vary more than 1.5 fold between wild type and *sth1-F793S* cells. After a three

hour shift to 34°C in the presence of thiolutin, the *NUP* mRNAs examined were actually

stabilized relative to *ACT1* in the *sth1-F793S* cells (*NUP60-GFP* up to 5 fold, and

51
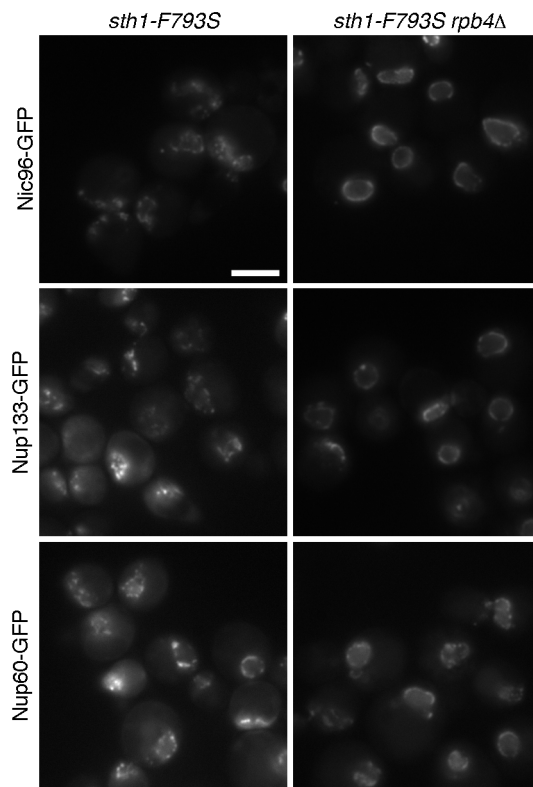
Figure 2.9. Nup mislocalization in *sth1-F793S* cells requires ongoing transcription. The *RPB4* deletion allele was integrated into the *sth1-F793S* strains expressing GFP-tagged Nic96 (SWY4243), Nup133 (SWY4245), or Nup60 (SWY4247). These strains and the corresponding parental *sth1-F793S RPB4* strains (SWY4244, SWY4246, and SWY4248, respectively) were shifted to 34°C for 5 hours. Representative live-cell, direct fluorescence images of GFP-Nup localization are shown. Size bar, 5 mm.
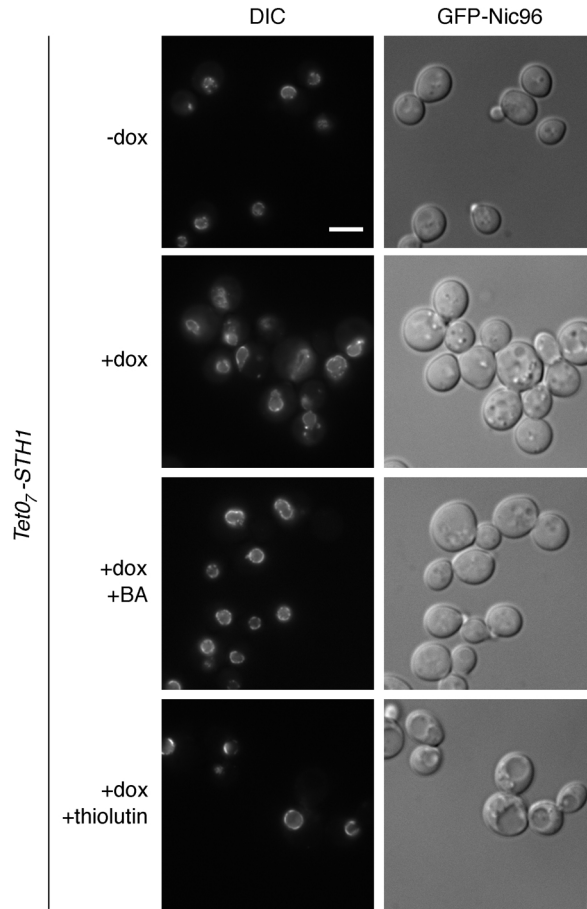
Figure 2.10. Benzyl alcohol and transcriptional shut-off block GFP-Nic96 mislocalization in *TetO7-STH1* cells grown in the presence of doxcycline. Direct fluorescence microscopy of GFP-Nic96 after twelve hours of growth in the absence or presence of doxycycline (10 **μ**g/ml) with addition of thiolutin (3 **μ**g/ml) or BA (0.4%). Size bars, 5 **μ**m.

NIC96-GFP up to 21-fold). Therefore, the lack of Nup mislocalization upon

transcriptional shutoff was not due to decreased mRNA stability of the *NUP* transcripts

tested.

GFP-Nup mislocalization in the *sth1-F793S* mutant does not require cell division

To evaluate whether the transcriptional and translational shut-off were acting

indirectly to block Nup mislocalization by inhibiting *sth1-F793S* cell division, we tested

for mislocaization in nocodazole arrested cells. The *sth1-F793S* mutant was treated with

15μg/ml of nocodazole for two hours, resulting in greater than ninety-percent of the cells

as large budded and held in G2-M. At this time point, the cultures were shifted to 34°C

for three hours. The cell population remained at greater than sixty-five percent large-

budded/G2-M. Importantly, Nup60-GFP was mislocalized to the same level in both

arrested and un-arrested control cultures (Figure 2.11). This suggested that Nup

mislocalization in *sth1-F793S* cells does not require cell division, and confirmed that the

lack of mislocalization in the cycloheximide, *rpb4Δ* and thiolutin experiments is linked to

inhibition of translation or transcription.

Increasing membrane fluidity blocks *sth1-F793S* mutant NPC/NE defects

Nup mislocalization and NE/ER defects have been reported in mutants defective

in the RanGTPase cycle (Ryan et al., 2003), in the COPII complex for ER/Golgi

trafficking (Ryan and Wente, 2002b), in NPC proteins (Aitchison et al., 1995), in lipid

biogenesis factors (Siniossoglou, 2009), or NE/ER membrane proteins (Dawson et al.,

2009; Scarcelli et al., 2007). We also identified additional components in some of these

54
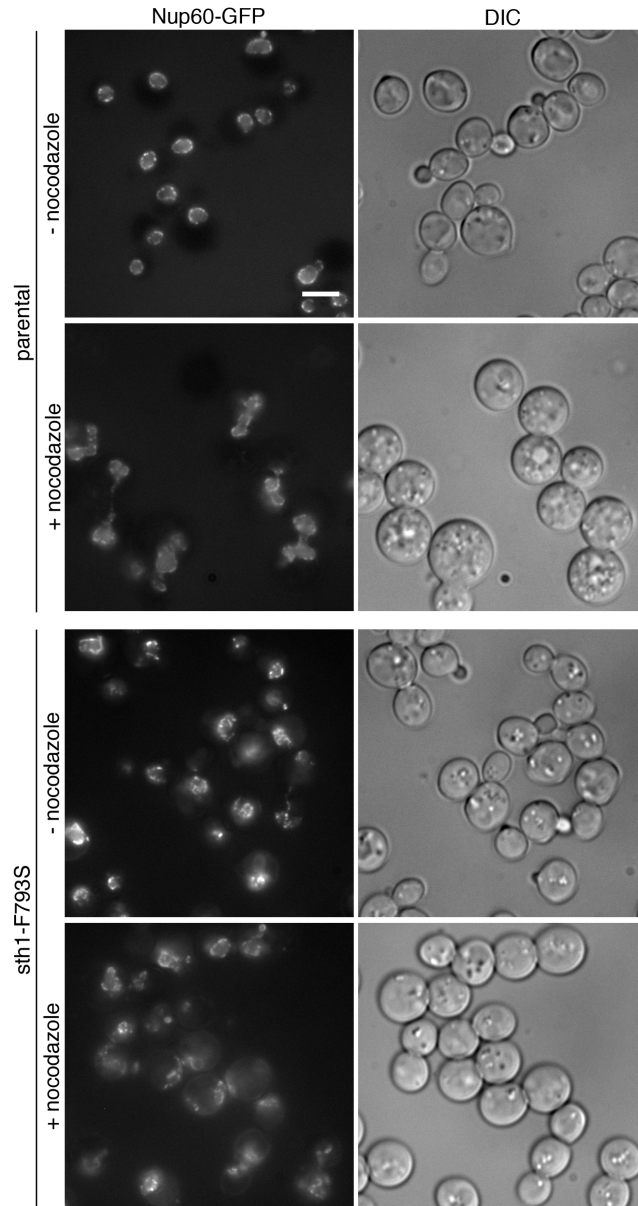
Figure 2.11. Nup mislocalization in the sth1-F793S strain occurs independent of cell division. Direct fluorescence microscopy of Nup60-GFP localization in wild type (SWY4374) or *sth1-F793S* (SWY4182) cells grown in the presence or absence of nocodazole at 23°C for two hours and then shifted to 34°C for three hours. DIC images reveal arrested G2/M cell morphology in nocodazole (15 **µ**g/ml) treated cultures. Size bars, 5 **µ**m.

pathways in the *TetO₇-orf* screen reported here (Figure 2.1A, Table 2.1). To directly test for links to secretion in *sth1-F793S* cells, we assayed for secreted invertase activity. The *sth1-F793S* cells displayed 53% of wild type invertase activity relative to our parental control strain. In comparison, *sec23-S383L (npa1-1)* and *sec13-G176R (npa2-1)* mutants had 3% and 30% of wild type invertase activity levels, respectively. We also tested for genetic interactions between the *sth1-F793S* mutant and the *sec13-G176R* or *sec23-S383L* mutant alleles. Of note, a *sth1-F793S sec13-G176R* double mutant and the *sth1-F793S sec23-S383L* double mutant were both viable and showed no synthetic fitness defects (SWY3436, SWY3437; Table 2.1). The same results were found for a *sth1-F793S prp20-G282S* double mutant which was viable and showed growth identical to the *sth1-F793S* mutant (SWY3409; Table 2.1). We concluded that the defects in the *sth1-F793S* mutant were not due to indirect severe perturbations on the levels of secretory or RanGTPase cycle factors. We used an independent assay to investigate whether NE membrane composition or fluidity was connected to the *sth1-F793S* mechanism of perturbation. Benzyl alcohol (BA) is an established membrane fluidizer (Colley and Metcalfe, 1972; Gordon et al., 1980) that has recently been used in *S. cerevisiae* to examine the role of Apq12 in NPC assembly (Scarcelli et al., 2007) and in *A. nidulans* to analyze functional roles for the An-Nup84-120 complex at the NE (Liu et al., 2009). To test this with the *sth1-F793S* mutant, 0.4% BA was added to the cells coincident with the shift to the nonpermissive growth temperature. Nuclear rim localization of GFP-tagged Nic96, Nup170, Nup60, Nup133, and Pom34 were independently evaluated in respective strains by direct fluorescence microscopy (Figure 2.12). Strikingly, no Nup mislocalization was observed in the BA-treated *sth1-F793S* cells. GFP-Nic96 was also

not mislocalized when *TetO$_7$-STH1* cells were treated with BA during growth in the presence of doxcycline (Figure 2.10). Moreover, TEM examination of the BA-treated, temperature-shifted *sth1-F793S* cells revealed that the ultrastructural NE defects were also absent (Figure 2.13). Immunoblotting was conducted and showed that the sth1-F793S protein was still unstable in the BA-treated cells (Figure 2.4C). Thus, the RSC role in mediating proper NE morphology and NPC localization was compensated for by alteration in NE dynamics.

Hyperosmotic growth conditions alleviate the *sth1-F793S* temperature sensitivity and NE/NPC defects

In our analysis of phenotypes for the *sth1* mutants under different growth conditions, we observed that the *sth1-F793S* mutant temperature sensitive phenotype was rescued on 1M sorbitol (Figure 2.14A). This osmotic remediabilty phenotype is often observed for mutants with defective cell wall synthesis, and suggests that sorbitol provides cushioning and protection from cell lysis. Alternatively, altered growth under hyperosmotic conditions may require Hog1 mitogen-activated protein kinase (MAPK) signaling. Hog1 MAPK signaling is activated upon changes in external osmolarity and promotes cell survival through the production of intracellular glycerol to counter water loss and disruptions in ion homeostasis(Saito and Posas, 2012). To determine if the growth phenotype required active Hog1 MAPK signaling we combined the *sth1-F793S* mutant with a *hog1Δ* mutant and tested for growth rescue on 0.4M NaCl. The *sth1-F793S* temperature sensitivity was rot rescued, and required Hog1 MAPK signaling (Figure 2.14B).
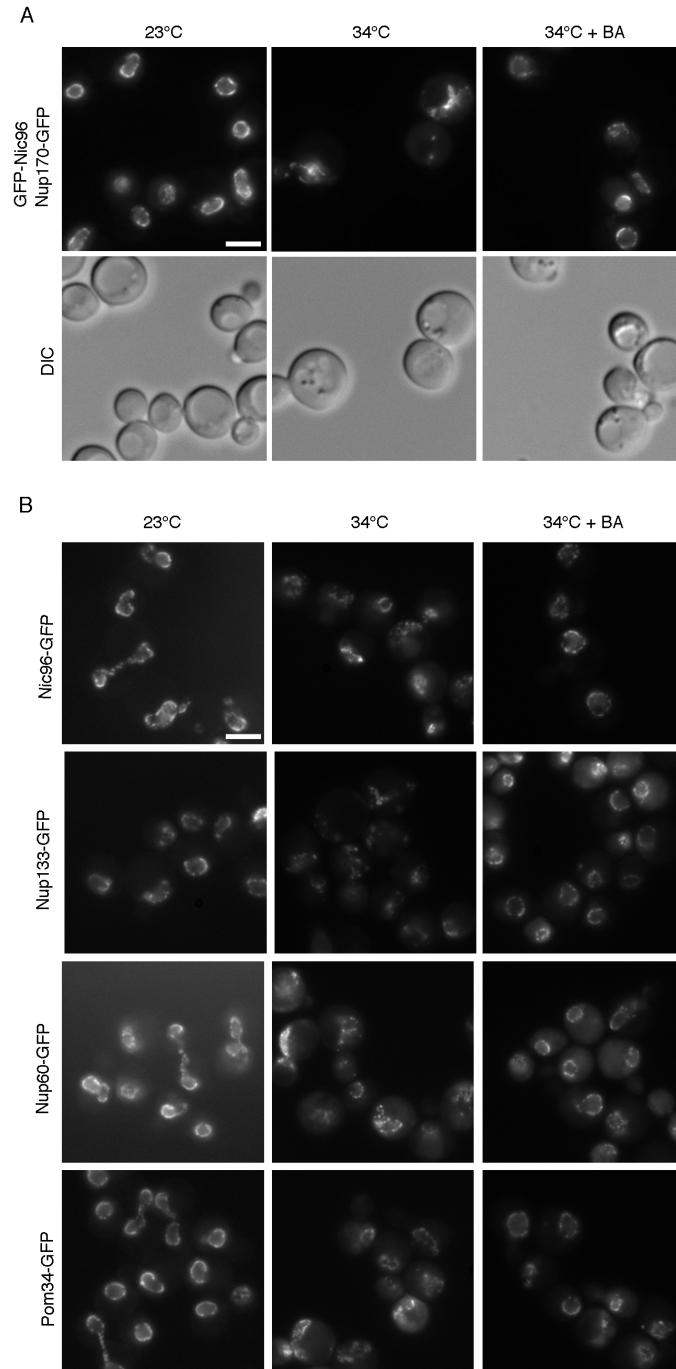
Figure 2.12. Benzyl alcohol treatment prevents GFP-Nup mislocalization in *sth1-F793S* cells. Logarithmically growing cultures of the *sth1-F793S GFP-nic96 nup170-GFP* (SWY3202) strain (A) and the *sth1-F793S* (SWY4143) strains with GFP-tagged Nic96, Nup60, Nup133, or Pom34 (B) were grown for 5 hours at 23°C (left column) and then shifted to 34°C in the absence (middle column) or presence (right column) of 0.4% BA. Representative live-cell, direct fluorescence images of GFP-Nup localization are shown. For (A), the corresponding DIC images are shown. Size bars, 5 mm.

58
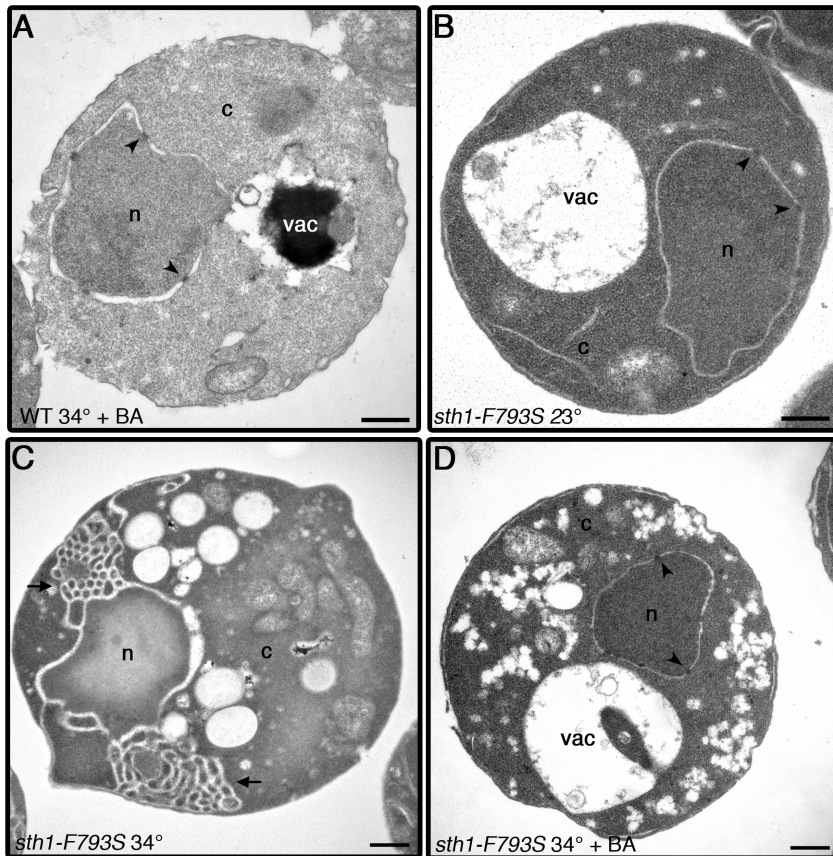
Figure 2.13. The *sth1-F793S* NE and nuclear morphology perturbations are prevented by benzyl alcohol. Logarithmically growing wild type (WT, SWY518) (A), *sth1-F793S* (SWY4143) (B-D) were incubated for 5 hours at 23°C (B) or at 34°C (A, C, D) in the absence (C) or presence (A, D) of 0.4% BA. Samples were processed for TEM. n, nucleus; c, cytoplasm; vac, vacuole; arrowhead, NPC; arrow, membrane. Size bars, 0.5 mm.

We next determined whether the *sth1-F793S* mutant recovered from the defects NE morphology with electron microscopy and observed intact NE uniform shape and unaltered membranes (Figure 2.14C). Thus, the Hog1 MAPK response enhances stability of sth1-F793S protein and leads to functional Sth1 protein that complements both growth and NE phenotypes at the non-permissive temperature.

Discussion

In our independent *TetO$_7$-orf* and *npa* genetic screens, we find that perturbation of Sth1 and a number of other RSC components results in altered Nup localization, perturbed NE organization and significant cytoplasmic membrane proliferation. The comparable phenotypes between the *sth1-F793S (npa18-1)*, the *TetO$_7$-STH1*, the *TetO$_7$-RSC*, and the *rsc7D* mutant strains indicate that the Nup/NE perturbations result from RSC complex loss-of-function. This conclusion is further corroborated by the loss of detectable sth1-F793S protein at the nonpermissive temperature in the mutant strain. Such defects in NE/NPC structure have not been previously documented in RSC mutants. Others have identified that the *rsc7(npl6)* mutant allele leads to defective localization of nuclear proteins, and also have reported a genetic interaction between *rsc7* and *nup84* mutants (Bossie *et al.*, 1992; Damelin *et al.*, 2002). We speculate that the RSC complex mutant phenotypes reflect a functional connection between proper chromatin remodeling and NE/NPC structure.

On a more general level, we have demonstrated the utility of the *TetO$_7$-orf* collection for GFP-based screening of perturbations in specific cell functions. Our prior
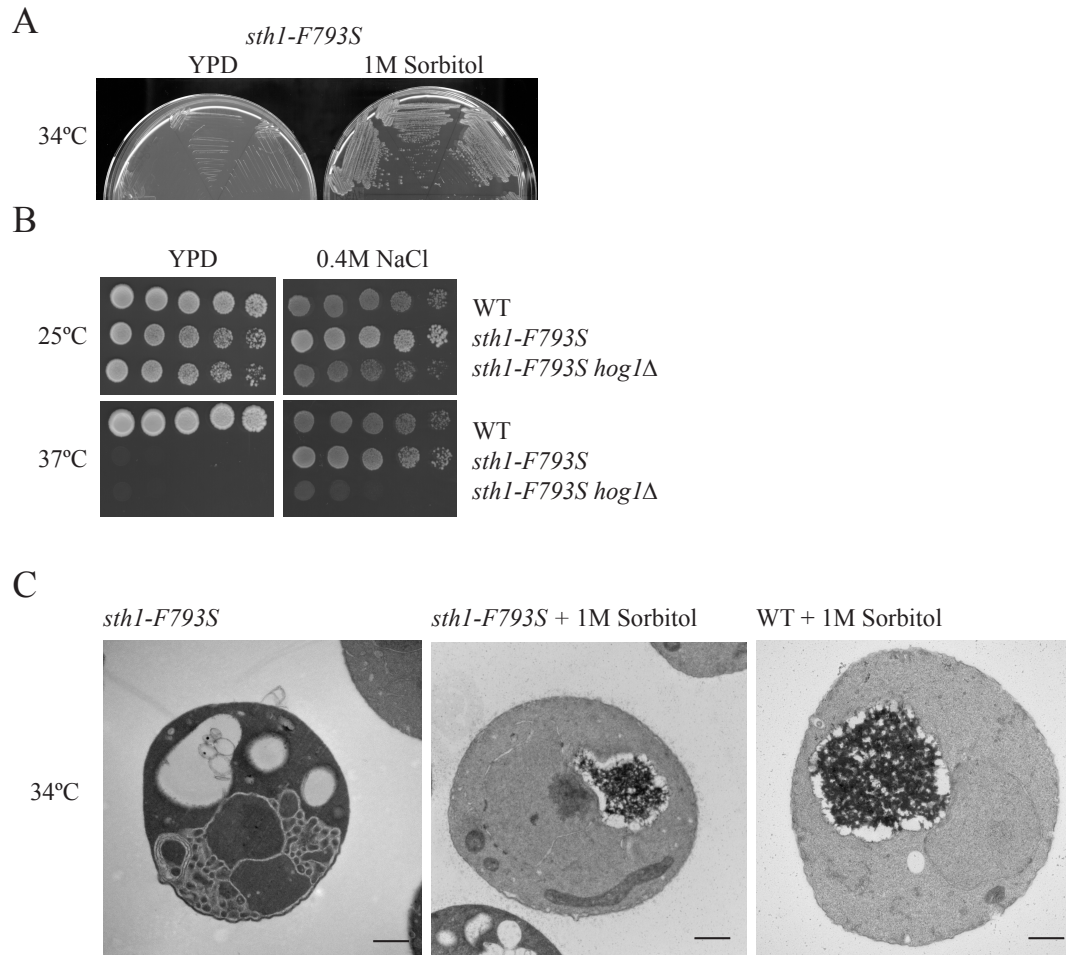
Figure 2.14. Osmotic remediability of the *sth1-F793S* mutant. A. *sth1-F793S* growth on YPD and 1M sorbitol plates at the non-permissive temperature. B. Serial dilutions of wildtype, *sth1-F793S*, and *sth1-F793S hog1Δ* on YPD and 0.4M NaCl plates grown at 25°C and 37°C. C. Electron micrographs of *sth1-F793S*, *sth1-F793S* +1M Sorbitol, and wiltype +1M sorbitol grown at 34°C. Scale bar 0.5μm

npa mutant screen was not to saturation and it would be technically challenging to achieve full genomic coverage based on the number of genes we have found with indirect perturbations in NE/NPC structure (e.g. the secretory pathway) (Ryan and Wente, 2002b). Taking the *TetO₇-orf* and *npa* screens together, we have now repeatedly identified genes in the same functional classes, indicating a nearly comprehensive assessment of the role of essential factors. In this study, we have further identified components of the lipid biosynthesis and secretory pathways for proper Nup localization. Others have shown that mutation of *FAS3/ACC1*, a gene required for long chain fatty acid synthesis, results in NE/NPC defects (Schneiter et al., 1996). The same lipid-membrane effects might be the basis for the *TetO₇-LCB2*, *TetO₇-FAS2*, and *TetO₇-CDS1* defects in GFP-Nic96 localization. We also identified connections here to the proteasome and enzymes required for GPI-anchoring. Future analysis of the NE and NPC defects in these mutants could give insight into the mechanisms by which the global nuclear architecture is coordinated and regulated.

Our results with the RSC complex mutants also potentially impact on prior interpretations of RSC-associated functions. Multiple studies have shown that RSC functions in DNA double strand break repair (Chai et al., 2005; Liang et al., 2007; Shim et al., 2007; Shim et al., 2005). Interestingly, the functional integrity of two different Nup subcomplexes is required for double strand break repair by homologous recombination (Palancade et al., 2007), and at least the Nup84 subcomplex is also required for anchoring telomeres and efficient DNA double strand break repair (Therizols et al., 2006). Studies also report that *nup170* mutants have defects in chromosome segregation (Iouk et al., 2002; Kerscher et al., 2001). Such striking NE and NPC perturbations, and severely

perturbed nuclear morphology, in the *sth1-F793S* and *TetO₇-RSC* cells could have indirect effects on DNA damage responses and gene expression. Additional work will be required to reveal whether the some of the RSC-associated phenotypes are due to altered NE/NPCs.

We propose that there are at least two possible mechanistic explanations for the NE/NPC defects in the RSC complex mutants. First, the lack of RSC activity could result in decreased expression of a factor(s) directly required for proper NE/NPC structure and/or biogenesis, or decreased expression of a factor(s) that maintains membrane fluidity. Others have reported that defects in the RSC complex result in pleiotropic effects attributed to either misregulated transcription or lack of chromatin access for other proteins (reviewed in (Saha et al., 2006)). RSC controls the transcriptional activation and repression of a broad subset of genes, with different RSC mutants having different transcriptional defects (Angus-Hill et al., 2001; Badis et al., 2008; Damelin et al., 2002; Hartley and Madhani, 2009; Kasten et al., 2004; Ng et al., 2002; Parnell et al., 2008; Soutourina et al., 2006). We observed that both new protein synthesis and ongoing transcription were required for the GFP-Nup perturbation, suggesting that the defects were not caused by loss of gene expression. Furthermore, we find similar NE/NPC defects in several different RSC mutants, and the *TetO₇-orf* screen also identified the *TetO₇-SPT16* and *TetO₇-TAF6* strains as having weak Nup localization defects. An independent study has examined strains with deleted non-essential genes and identified nuclear morphology defects in *arp5Δ*, *bre1Δ* and *seh1Δ* strains, all encoding components of histone remodeling and modifying complexes and NPC, respectively (Fabre *et al.*, 2002). A common silencing defect was identified among the deletion strains with altered

63

nuclear morphology, pointing towards an interdependence between maintenance of

silenced chromatin and NE structure. This indicates that the NE/NPC perturbation could

be a function of the global chromatin state as opposed to a specific transcriptional defect.

Our biochemical and genetic analysis of potential transcriptional targets with NPC/NE

connections also suggested that the *sth1-F793S* mutant is not linked to severe indirect

defects in secretion or the RanGTPase cycle. Furthermore, to date our tests of known

multicopy suppressors of *sth1* mutants have not found any that rescue the altered nuclear

morphology or temperature sensitivity of the *sth1-F793S* mutant. Therefore, although we

cannot rule out specific changes in gene expression, we speculate that the NE/NPC

defects are not simply indirect perturbations due to altered transcription levels.

As an alternative model, the RSC complex activity might be required for

generating the correct chromatin state for contacts with the NE and/or association with a

NE/NPC assembly factor. It has recently been shown that post-mitotic NPC assembly

requires the chromatin-interacting factor MEL-28/ELYS for recruitment of the metazoan

Nup107-160 complex (Franz et al., 2007; Rasala et al., 2006; Rasala et al., 2008). In

yeast, the RSC complex has been connected to the yeast Nup84 complex by its shared

link to non-homologous end-joining (NHEJ) with Nup133 and Nup120 (as well as

Nup60) (Palancade et al., 2007). In addition, the reported synthetic lethality of a *nup84D

rsc7D* double mutant (Wilson et al., 2006) further suggests that proper function of the

Nup84 complex is dependent on the integrity of RSC. In this light, the connection of the

RSC chromatin-remodeling complex to proper NE structure is especially intriguing. We

speculate that the loss of RSC function could decouple the chromatin/NE interface,

leading to a chromatin or NE stress response. Structural and/or chromatin-associated

roles of Nups and Poms might be inhibited, while lipid biosynthetic pathways might signal to the NE to expand to re-establish chromatin connections. Indeed, several reports have shown that the nucleosome occupancy of RSC changes in response to stress (Damelin et al., 2002; Mas et al., 2009; Ng et al., 2002). This hypothesis is supported by our observation that increasing membrane fluidity prevented the NE and NPC perturbations in the *sth1-F793S* cells, even though the sth1-F793S protein was still absent.

Recent studies have documented connections between NPCs/Nups and transcriptional regulation (Brown and Silver, 2007; Casolari et al., 2004; Dilworth et al., 2005; Ishii et al., 2002; Rodriguez-Navarro et al., 2004; Schmid et al., 2006). For example, two NPC nuclear basket Nups (Nup2 and Nup60) have been linked to this transcriptional regulation by their association with chromatin-bound Prp20, the RanGEF (Dilworth et al., 2005). Interestingly, the membrane perturbations in the *sth1-F793S* and *TetO$_7$-RSC* mutants are similar to that previously reported for *nup1* mutant cells (Bogerd et al., 1994) which are defective for a NPC nuclear basket Nup (Rout et al., 2000). There are also reported genetic interactions amongst components of the Nup84 complex and the Rap1 transcriptional activation complex, and most components of the Nup84 complex have the capacity to activate transcription (Menon et al., 2005). Additionally, genome-wide analysis of protein:DNA binding interactions has shown that Nups preferentially bind to transcriptionally active genes and induction of the *GAL1* and *INO1* genes results in their translocation to the nuclear rim (Casolari et al., 2004). These peripherally recruited genes also exhibit transcriptional memory coincident with their retention at the periphery for hours after the initial activation (Brickner *et al.* 2007). This transcriptional

memory and sustained peripheral anchoring requires H2AZ and the chromatin-remodeling complex, SWR1. These data suggest that RSC might activate transcription of genes at the nuclear periphery through interactions with NPC. Taken together, we conclude that a general mechanism may exist whereby the RSC complex generates a correct chromatin state for NE/NPC association, whether for transcriptional activation and/or for NE/NPC structure and biogenesis.

Previous work has implicated the RSC chromatin-remodeling complex in the activation of genes responsive to hyperosmotic stress. The osmotically induced Hog1 MAPK enters the nucleus and recruits the RSC complex to promoters and ORF regions where RSC then remodels nucleosomes for efficient transcription. Though multiple RSC mutants exhibit salt sensitivity, the *sth1-F793S* mutant is resistant to osmotic stress and surprisingly shows a growth rescue when grown on hyperosmotic medium at the non-permissive temperature (Figure2.9A). Several possible mechanisms may help to explain this observation. First, heat shock proteins may be induced under salt and promote proper folding of sth1-F793S protein at the non-permissive temperature. Similarly, osmotic stress may result in a post-translational modification (PTM) that enhances sth1-F793S stability and function. We investigated whether RSC subunits underwent dramatic PTMs with a TAP-pulldown under untreated and 0.4M NaCl conditions followed by PTM analysis with 2D-DIGE and mass spectrometry. Our 2D-DIGE analysis identified likely PTMs, though we were unable to find significant changes between the untreated and treated samples (data not shown). Also, although the mass spectrometry detected multiple peptides that were phosphorylated and ubiquitinated, the coverage was not suitable for quantifying differences. Thus, more sensitive equipment such as the orbitrap,

velos, or a multidimensional approach would be better suited for continuing with these experiments. An alternative explanation, is that the initial chromatin state that is established when cells are exposed to osmotic stress may be locked in and bypass any further requirements for sth1-F793S protein once shifted to the non-permissive temperature. We envision that this chromatin state may represent a global nuclear organization to coordinate expression of genes required to survive under hyperosmotic conditions. The following chapter addresses the changes in nuclear structure under hyperosmotic stress and the resulting influences on gene expression.

MATERIALS AND METHODS

Yeast strains, plasmids, genetics and media

All *S. cerevisiae* strains used in this study are listed in Table 2.2. The original *npa18-1* strain (SWY3201) was backcrossed with the parental strain SWY2090 to yield SWY3202 (temperature sensitive at 34˚C and GFP-Nup mislocalization). A *LEU2/CEN* library (American Type Culture Collection) was transformed into the SWY3202 strain, and colonies were incubated at the permissive temperature, 23˚C, for 36 hours, and then shifted to 34˚C. Plasmid DNA was recovered from each resulting colony and analyzed by restriction digest. The library plasmid inserts from two independent isolates were sequenced. The minimal overlapping region harbored only two complete open reading frames (ORFs), *STH1* and *YIL127C*. Wild type *STH1* and *YIL127C,* with respective flanking promoter regions, were independently subcloned into the *Xba*I and *Xho*I sites of pRS315 (Sikorski and Hieter, 1989) by polymerase chain reaction amplification using library plasmid template and the following forward and reverse primers: *STH1*, (5’)

67

CAAGTCTAGACCTGTCGATTAACTGAGC (3'), (5')

GTAACTCGAGCTAGAAAGAGTATTAGAGG (3'); *YIL127C*, (5')

ACGTTCTAGACGAACAACTTAAGGAGGGAG (3'), (5')

GCAACTCGAGTTCACATTGATGAGCACGTG (3'). The resulting p*STH1* (pSW3051)

and p*YIL127C* (pSW3049) plasmids were transformed into SWY3202. To analyze the

sth1 allele in SWY3202, genomic DNA from the mutant strain was amplified using *STH1*

flanking oligonucleotides and the high-fidelity polymerase *Pfu* (Stratagene). Products

from two independent PCR reactions were purified and sequenced.

All strains were cultured in either rich (YPD: 1% yeast extract, 2% peptone, 2%

dextrose) or synthetic minimal (SM) media lacking appropriate amino acids and

supplemented with 2% dextrose. All yeast genetic techniques and molecular cloning were

performed according to standard procedures (Sambrook et al., 1989a; Sherman et al.,

1986). Cell viability assays were performed on treated and untreated *sth1-F793S* and the

TetO_7-STH1 mutant strains. After growth under permissive and nonpermissive conditions

(three and twelve hours, respectively), the mutant strains were plated onto YP plates at

100 cells per plate, incubated at 23°C for two days and quantified for colony forming

units. Serial dilutions of mid-log phase W303, SWY4143, S288C and BLY49 were

spotted onto YP plates supplemented with 2% glucose, 2% galactose, 2% raffinose or 2%

ethanol/2% glycerol. These strains were also spotted onto YPD plates containing

thiabendazole (TBZ; 60 μg/ml) or hydroxyurea (HU; 50 mM). The plates were imaged

after 3 days incubation at the semipermissive temperatures of the respective mutant

alleles. Multicopy suppressor plasmids from were obtained from the Yeast Genomic

Tiling Collection through Open Biosytems (Jones *et al*., 2008).

TetO₇-promoter GFP-nic96 strain collection generation

The yeast Tet-promoters Hughes Collection (referred to here as the *TetO₇-orf* strain collection was obtained from Open Biosystems (Mnaimneh et al., 2004). This collection contains 813 strains of the 1105 reported total essential genes. By a series of strain crosses and selections, *GFP-nic96* was incorporated into each *TetO₇-orf* strain that was reported as having a slow growth phenotype on doxycycline. Strain Y3656 was crossed with SWY2090 (Table 2.1). The resulting strain, SWY3191, was crossed with strains from the *TetO₇-orf* strain collection. Strains were mated on YPD for a minimum of six hours, and diploids were selected by pinning three successive times onto SM Lys⁻His⁻ media. For sporulation, strains were incubated on YPD for 15 hours at 30°C, and then transferred by pinning to SPO media (1% potassium acetate, 0.1% yeast extract, 0.05% glucose, 14 mg/L histidine, 71 mg/L leucine). Diploids were allowed to sporulate at 23°C for at least four days. *MATα* haploids were selected by streaking each strain to SM Arg⁻ Leu⁻ Can⁺ (60 mg/L canavanine sulfate) media. Strains with the *TetO₇* promoter were selected by streaking on YPD media containing G418 (200 mg/ml active units). Strains expressing the tetracycline transactivator (tTA) and *GFP-nic96* were further identified by growth on SM Ura⁻ His⁻ Leu⁻ media. Resulting strains had the genotype *MATα can1Δ::MFA1pr-HIS3::MFαpr-LEU2 GFP-Nic96:HIS3 URA3::CMV-tTA gene::kanᴿ-tetO7-TATA leu2 his3 (LYS or lys; TRP or trp; ADE2 or ade2-1::ADE2:ura3).* Some *GFP-nic96 TetO₇-orf* strains were not obtained due to apparent technical difficulties with incorporating *GFP-nic96* into the given background.

Screening the GFP-nic96 TetO₇-orf strain collection

GFP-Nic96 localization was screened visually in 531 *GFP-nic96 TetO₇-orf* strains after growth in doxycycline containing media. Specifically, the strains described as having constitutive slow growth (CSG), or having a weak, moderate, or severe growth defect in media containing 10 mg/ml doxycycline (Table 2.1) were inoculated directly into YPD media containing 10 mg/ml doxycycline and cultured overnight (13-15 h) at 30°C. For strains with a growth phenotype described as "very severe" or "very severe/(almost) no growth on doxycycline" (Mnaimneh et al., 2004), log-phase cultures in YPD were treated with 10 mg/ml doxycycline for approximately five hours. Some of the strains with "very severe" growth defects grew sufficiently in the presence of doxycycline overnight, and were screened under these conditions.

Fluorescence, indirect immunofluorescence, and electron microscopy

Yeast strains with GFP-tagged Nups were examined from cultures by direct fluorescence microscopy. For cycloheximide, thiolutin, and benzyl alcohol experiments, logarithmically growing cultures were treated with 10mg/ml cycloheximide, 3mg/ml thiolutin, or 0.4% benzyl alcohol, and then temperature shifted for five hours at 34°C or treated with 10mg/ml doxycycline for eight to twelve hours. Cell cycle arrest experiments included a two hour pre-incubation with nocodazole (15µg/ml) followed by a three hour shift to 34°C. Arrest was monitored with quantification of the percentages of G2 arrested cells in treated and untreated cultures, both before and after the temperature shift. For indirect immunofluorescence microscopy, cells from logarithmically growing cultures were pelleted, fixed for 10 minutes at room temperature with 3.7% formaldehyde, 10%

methanol in 100 mM potassium phosphate pH 6.5, and processed as previously described (Wente and Blobel, 1993). Samples were incubated with affinity purified, rabbit anti-Nup116 C-terminal polyclonal antibody (Iovine et al., 1995) (1:50). Bound antibody was detected by incubation with Alexa 594 goat anti-rabbit secondary antibody (1:400). Additional samples were incubated with mouse anti-Nup159 monoclonal antibody (1:10, gift of G. Blobel and M. Rout) and bound antibody was detected with Alexa 594 goat anti-mouse secondary antibody (1:200).

A final stain for five minutes with 0.1 mg/ml DAPI in PBS, 1% BSA was conducted before mounting onto slides with 90% glycerol, 1 mg/ml *p*-phenylenediamine, PBS, pH 9.0. Light microscopy was performed with an Olympus BX50 microscope with a UPlanF1 100x/1.30 oil immersion objective. Images were collected with Photometrics CoolSnapHQ camera and MetaVue v4.6 software, and processed with Adobe Photoshop 9.0 software. For electron microscopy, 2×10^8 logarithmically growing cells were harvested from the specific culture conditions and processed as previously described (Wente and Blobel, 1993). Samples were analyzed on a Philips CM-12 120 keV electron microscope. Images were acquired with an Advanced Microscopy Techniques (AMT) Advantage HR or MegaPlus ES 4.0 camera, and processed with Adobe Photoshop 9.0 software.

Invertase assays

Cells were prepared as described (Ryan and Wente, 2002b), except that 20 ml of cell suspension was used for each assay. Strains assayed included SWY2089 (parental), SWY3378 (*sth1-F793S (npa18-1)*), SWY2324 (*sec13-G176R (npa2-1)*), and SWY2325

71

(*sec23-S383L (npa1-1)*). The percentage of activity in each sample was calculated relative to the activity of the wild type control strain. All assays were performed on three replicate cultures.

Immunoblotting

Cultures were grown to early log phase at 23°C, and then shifted to growth at 34°C in the presence or absence of 0.4% benzyl alcohol. Total cell lysates were prepared by bead beating in lysis buffer (20 mM Tris pH. 6.5, 5mM MgCl2, 2% Triton X-100, 150mM NaCl) and resolved by SDS-PAGE. The blots were incubated with either affinity purified rabbit anti-Dbp5 polyclonal antibody (1:1000, (Bolger et al., 2008)) (as a loading control) or a rabbit anti-Sth1 polyclonal antibody (1:100, (Saha et al., 2002)), followed by incubation with HRP-conjugated anti-rabbit antibodies (Jackson) and detection via SuperSignal West Pico ECL (Pierce).

Quantitative PCR

Cells were grown to early log phase and shifted to 34°C with the addition of thiolutin (3μg/ml). After 3 hours, cells were rinsed with ice-cold sterile water and frozen in liquid nitrogen. RNA was isolated from equivalent cell numbers with hot phenol (Geng and Tansey, 2008). Oligo(d)T reverse-transcription was performed with TaqMan Reverse-Transcription Kit (Applied Biosystems) and quantitative PCR was performed in triplicate using the Bio-Rad iCycler and iQ SYBR Green Supermix (Bio-Rad). The comparative C_T method was used to quantify fold changes in *NUP-GFP* transcripts relative to *ACT1*. Gene-specific primers for *GFP* and *ACT1* were validated across 6 logs

of input cDNA. *ACT1*, (5') CTCCACCACTGCTGAAAGAGAA (3'), (5')

CGAAGTCCAAGGCGACGTAA (3'), *GFP*, (5') AGTGGAGAGGGTGAAGGTGA

(3'), (5') GTTGGCCATGGAACAGGTAG (3').

2.2 Yeast strains used in this study.

Strain	Genotype	Source
TetO$_7$ collection	*MAT**a** CAN1 his3 leu2 met15 URA3::CMV-tTA orf::kanR-tetO$_7$-TATA*	Open Biosystems Mnaimneh *et al.*, 2004
Y3656	*MAT**a** can1D::MFA1pr-HIS3::MFa1pr-LEU2 ura3D0 lys2D0 leu2D0 his3D1*	Tong *et al.*, 2004
W303	*MAT**a** ade2-1 can1-100 his3-11,15 leu2-3,112 trp1-1 ura3-1*	Thomas *et al.*, 1989
S288C	*MAT**a** ura3-52 his3Δ200 ade2-101 lys2-801*	Mortimer and Johnston, 1986
SWY2090	*MAT**a** GFP-nic96:HIS3 nup170-GFP:URA3 trp1-1 ura3-1 his3-11,15 leu2-3,112 can1-100 ade2-1::ADE2:ura3*	Ryan and Wente, 2002
SWY2324	*MATα sec13-G176R (npa2-1) GFP-nic96:HIS3 nup170-GFP:URA3 lys2 ura3-1 his3-11,15 leu2-3,112 can1-100 ade2-1::ADE2:ura3*	Ryan and Wente, 2002
SWY2325	*MATα sec23-S383L (npa1-1) GFP-nic96:HIS3 nup170-GFP:URA3 lys2 ura3-1 his3-11,15 leu2-3,112 can1-100 ade2-1::ADE2:ura3*	Ryan and Wente, 2002
SWY2518	*MAT**a** prp20-G282S (npa14-1) trp1-1 ura3-1 his3-11,15 leu2-3,112 can1-100 ade2-1::ADE2:ura3*	Ryan *et al.*, 2003
SWY3191	*MAT**a** can1D::MFA1pr-HIS3::MFa1pr-LEU2 GFP-nic96:HIS3 ura3 lys2 leu2 his3 ADE2*	Y3656 × SWY2090
SWY3201	*MATα sth1-F793S (npa18-1) GFP-nic96:HIS3 nup170-GFP:URA3 lys2 ura3-1 his3-11,15 leu2-3,112 can1-100 ade2-1::ADE2:ura3*	original *npa* screen isolate Ref. (Ryan and Wente, 2002a)
SWY3202	*MAT**a** sth1-F793S (npa18-1) GFP-nic96:HIS3 nup170-GFP:URA3 lys2 trp1-1 ura3-1 his3-11,15 leu2-3,112 can1-100 ade2-1::ADE2:ura3*	backcross of SWY3201 × SWY2090
SWY3243	*MATα sth1-F793S (npa18-1) GFP-nic96:HIS3 nup170-GFP:URA3 lys2 ura3-1 his3-11,15 leu2-3,112 can1-100 ade2-1::ADE2:ura3*	backcross of SWY3201 × SWY2090
SWY3244	*MAT**a** sth1-F793S (npa18-1) GFP-nic96:HIS3 nup170-GFP:URA3 trp1-1 ura3-1 his3-11,15 leu2-3,112 can1-100 ade2-1::ADE2:ura3*	backcross of SWY3201 × SWY2090
SWY3249	*MAT**a** sth1-F793S (npa18-1) trp1-1 ura3-1 his3-11,15 leu2-3,112 can1-100 ade2-1::ADE2:ura3*	SWY3243 × SWY518
SWY3250	*MATα sth1-F793S (npa18-1) lys2 ura3-1 his3-11,15 leu2-3,112 can1-100 ade2-1::ADE2:ura3*	SWY3243 × SWY518
SWY3378	*MAT**a** sth1-F793S (npa18-1) GFP-nic96:HIS3 nup170-GFP:URA3 trp1-1 ura3-1 his3-11,15 leu2-3,112 can1-100 ade2-1::ADE2:ura3*	SWY3243 × SWY2090
SWY3409	*MAT**a** sth1-F793S (npa18-1) prp20-G282S (npa14-1) lys2 ura3-1 his3-11,15 leu2-3,112 can1-100 ade2-1::ADE2:ura3*	SWY3250 × SWY2518
SWY3436	*MATα sec13-G176R (npa2-1) sth1-F793S (npa18-1) lys2 ura3-1 his3-11,15 leu2-3,112 can1-100 ade2-1::ADE2:ura3 GFP-nic96:HIS3 nup170-GFP:URA3*	SWY2324 × SWY3378
SWY3437	*MATα sec23-S383L (npa1-1) sth1-F793S (npa18-1) lys2 ura3-1 his3-11,15 leu2-3,112 can1-100 ade2-1::ADE2:ura3 GFP-nic96:HIS3 nup170-GFP:URA3*	SWY2325 × SWY3378
SWY4143	*MAT**a** sth1-F793S (npa18-1) trp1-1 ura3-1 his3-11,15 leu2-3,112 can1-100 ade2-1::ADE2:ura3*	SWY3250 backcrossed 5 times to SWY518
SWY4182	*MAT**a** sth1-F793S (npa18-1) nup60-GFP:HIS3 trp1-1 ura3-1 his3-11,15 leu2-3,112 can1-100 ade2-1::ADE2:ura3*	*nup60-GFP:HIS3* integrated into SWY4143
SWY4183	*MAT**a** sth1-F793S (npa18-1) nup133-GFP:HIS3 trp1-1 ura3-1 his3-11,15 leu2-3,112 can1-100 ade2-1::ADE2:ura3*	*nup133-GFP:HIS3* integrated into SWY4143
SWY4184	*MAT**a** sth1-F793S (npa18-1) nic96-GFP:HIS3 trp1-1 ura3-1 his3-11,15 leu2-3,112 can1-100 ade2-1::ADE2:ura3*	*nic96-GFP:HIS3* integrated into SWY4143
SWY4185	*MAT**a** sth1-F793S (npa18-1) pom34-GFP:HIS3 trp1-1 ura3-1 his3-11,15 leu2-3,112 can1-100 ade2-1::ADE2:ura3*	*pom34-GFP:HIS3* integrated into SWY4143
SWY4243	*MAT**a** sth1-F793S (npa18-1) rpb4::KAN^R nic96-GFP:HIS3 trp1-1 ura3-1 his3-11,15 leu2-3,112 can1-100 ade2-1::ADE2:ura3*	*rpb4::KAN^R* integrated into SWY4184
SWY4245	*MAT**a** sth1-F793S (npa18-1) rpb4::KAN^R nup133-GFP:HIS3 trp1-1 ura3-1 his3-11,15 leu2-3,112 can1-100 ade2-1::ADE2:ura3*	*rpb4::KAN^R* integrated into SWY4183
SWY4247	*MAT**a** sth1-F793S (npa18-1) rpb4::KAN^R nup60-GFP:HIS3 trp1-1 ura3-1 his3-11,15 leu2-3,112 can1-100 ade2-1::ADE2:ura3*	*rpb4::KAN^R* integrated into SWY4182
SWY4374	*MAT**a** nup60-GFP:HIS3 ade2-1 can1-100 his3-11,15 leu2-3,112 trp1-1 ura3-1*	*nup60-GFP:HIS3* integrated into W303
SWY4375	*MAT**a** nic96-GFP:HIS3 ade2-1 can1-100 his3-11,15 leu2-3,112 trp1-1 ura3-1*	*nic96-GFP:HIS3* integrated into W303
BLY47	*MATα sth1-1ts ade2-1 can1-100 his3-11,15 leu2-3,112 trp1-1 ura3-1*	Du *et al.*, 1998
BLY48	*MATα sth1-2ts ura3-52 his3Δ200 lys2-801 suc2*	Du *et al.*, 1998
BLY49	*MAT**a** sth1-3ts ura3-52 his3Δ200 ade2-101*	Du *et al.*, 1998
BLY491	*MATα sth1-L1346A ura3-52 lys-801 his3Δ200*	Huang *et al.*, 2004

CHAPTER 3

REGULATION OF HOG1-ACTIVATED STOCHASTIC GENE EXPRESSION AND THE SUBNUCLEAR LOCALIZATION OF HOT1 BY CASEIN KINASE II

Introduction

Whether the structural arrangements of the genome contribute to complex transcriptional variations with different types of cells, and in response to environmental stimuli remains a central question in biology.   The genome within the nucleus is functionally organized to allow for coordinated events of gene expression, RNA processing, genomic repair, and replication. Several properties of nuclear structure including the gene positioning and subnuclear localization of active transcriptional machinery are predicted to influence the efficiency of transcriptional events (Edelman and Fraser, 2012; Misteli, 2013; Mitchell and Fraser, 2008). The cellular signaling pathways that regulate the dynamics of nuclear organization and impact gene expression in response to environmental stress remain largely undefined.

In *Saccharomyces cerevisiae*, Hog1 MAPK (mitogen-activated protein kinase) signaling coordinates a global transcriptional response to osmotic stress that is kinetically unparalleled (Capaldi et al., 2008; Rep et al., 2000). Several hundred genes exhibit altered levels of transcription within minutes after exposure to moderate osmotic stress (0.4M NaCl). Rapid signaling activates the Hog1 MAPK, which then enters the nucleus and directs a combination of transcriptional activators to initiate the transcriptional response (de Nadal et al., 2011; Saito and Posas, 2012). Within a population of identical cells, Hog1 MAPK activation results in the stochastic activation of target genes and a variable expression pattern across a population of cells (Neuert et al., 2013; Pelet et al.,

2011). Several factors are known to contribute to stochastic gene activity, including chromatin-remodeling events, the duration of Hog1 nuclear activity, and the intracellular concentration of the transcription factor, Hot1 (Neuert et al., 2013; Pelet et al., 2011). I have chosen this system to determine if the subnuclear organization of transcription impacts stochastic gene activity and to identify the cellular cues that influence the dynamic organization of transcription events.

My findings redefine the current view of stochastic gene expression in the HOG MAPK pathway and identify a novel role for nuclear organization. Under osmotic stress, I observed dynamic changes in nuclear organization, resulting in localization of the Hot1 transcription factor to subnuclear foci that overlap with the Hot1 target gene *STL1*. Surprisingly, I found that Hot1-GFP foci form constitutively when Casein Kinase II (CK2) is inhibited. Stochastic activity of *STL1* results in bimodal expression in a wild type population of cells under moderate osmotic stress. However, in *ck2* mutant strains, this bimodality is lost and *STL1* is expressed in all cells. I have, thus identified a novel function for CK2 in regulating the dynamic localization of a transcription factor, and propose that the organization of transcription events represents an additional regulatory factor influencing stochastic gene expression.

Results

Osmotic stress leads to subnuclear localization of transcription factors and gene loci

I began my analysis of subnuclear organization in the Hog1 MAPK transcriptional response by localizing GFP-tagged Hot1, Msn2 and Sko1 transcription factors and the Hog1 MAP kinase under conditions of moderate osmotic stress (0.4M

NaCl) (Figure 3.1A). In all cases, the proteins exhibited altered localization patterns. As previously described, Hog1 and Msn2 change from predominantly cytoplasmic to nuclear localization (O'Rourke et al., 2002). Both Sko1 and Hot1 remain nuclear, however Hot1 strikingly redistributed to distinct subnuclear foci. I asked whether this localization was specific to Hot1 and examined the heat shock transcription factor, Hsf1, for altered localization under osmotic stress. Hot1 and Hsf1 are maintained at similar protein levels, but only Hot1 localization was altered under osmotic stress (data not shown). From these initial localization studies, I directed further analysis toward the requirements and functions of Hot1-foci in the Hog1 MAPK transcriptional response.

Hot1-foci resembled the clustering of transcription events to transcription factories that have been described in mammalian cells. Mammalian transcription factories are sites for enrichment of both transcription factors and associated target genes (Edelman and Fraser, 2012; Schoenfelder et al., 2010). To test for similarities between the Hot1-foci and transcription factories, I colocalized the Hot1-responsive gene *STL1* and Hot1 in untreated and 0.4M NaCl treated cells (Figure 3.1B). To visually track the *STL1* gene, I inserted 128 LacO-repeats downstream in the 3'UTR of *STL1* and expressed mCherry-LacI. The mCherry-LacI signal corresponds to the positioning of the *STL1* gene locus within the nucleus. In untreated cells, few Hot1-foci are observed (1-2 foci per cell). After 0.4M NaCl stress, Hot1-foci increase to 6-10 per cell. I observe frequent overlap between *STL1* gene loci and the Hot1 foci in both treated and untreated cells, with more rare occasions of non-overlapping loci-foci are observed. Since mammalian transcription factories are present even under conditions where transcription is absent (Ghamari et al., 2013; Mitchell and Fraser, 2008), I sought to determine the
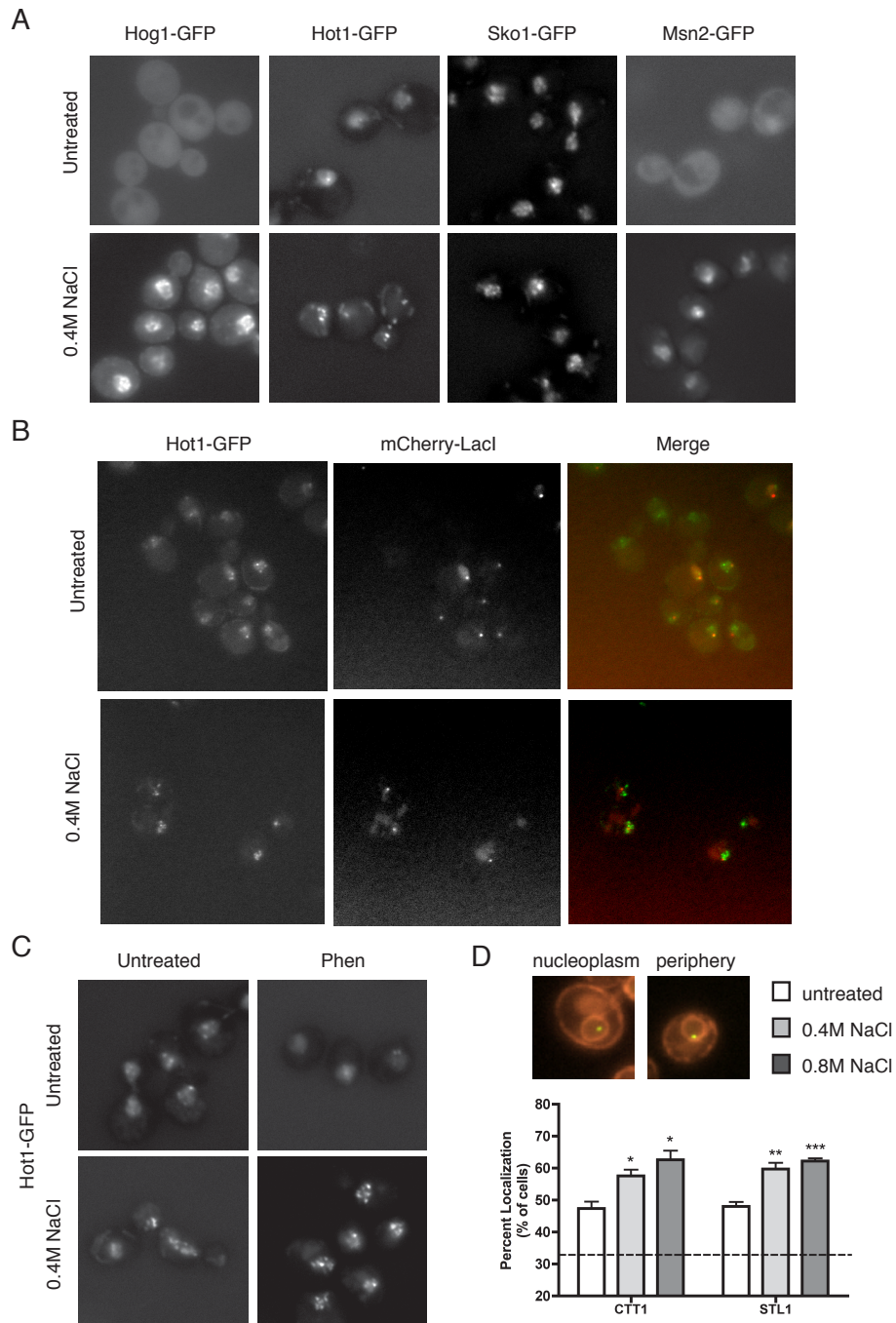
Figure 3.1. Subnuclear localization of the Hot1 transcription factor to foci that overlap with gene targets under hyperosmotic conditions (A) C-terminal GFP-fusions of Hog1, Hot1, Sko1, and Msn2 were visualized by live cell microscopy in YPD and after 5 minutes of 0.4M NaCl stress. (B) The *STL1* gene locus was localized by expression and targeting of mCherry-LacI to a 128-LacO array inserted into the 3'UTR of *STL1*. Cells were imaged from untreated and 0.4M NaCl treated cultures for Hot1-GFP and mCherry-

requirements for transcription, I inhibited RNAPII transcription with 1,10-phenanthroline

and observed no affect on Hot1 foci formation (Figure 3.1C). Thus both Hot1-foci and

transcription factories represent subnuclear foci that are enriched in transcription factors

and gene targets, and each form independent of RNAPII transcription.

Prior reports for many inducible responses in *S. cerevisiae* have observed localization of

genes to the nuclear periphery coinciding with optimal transcriptional activity (Brickner

et al., 2007) . Furthermore, the *CTT1* promoter contains a consensus for the gene

recruitment sequence (GRSI) motif that functions to recruit *INO1* to the nuclear periphery

under conditions of inositol starvation. To determine whether *CTT1* and *STL1* are

enriched for peripheral localization, I visualized the gene loci with GFP-LacI and LacO-

array repeats. I quantified the percent of cells with overlapping *CTT1* and *STL1* signal

with the nuclear periphery marker DsRED-HDEL (Figure 3.1D). In untreated cells, both

genes occupied the periphery in approximately 50% of the cells (Figure 3.1D). After

treatment with either 0.4M (15min) and 0.8M NaCl (30min) I observed a 10-15%

increase in peripheral localization for *CTT1* and *STL1* (Figure 3.1D). In summary, salt-

dependent nuclear rearrangements occur where the Hot1 transcription factor localizes to

subnuclear foci, the *STL1* gene target and salt-responsive genes *CTT1* and *STL1* enrich at

the nuclear periphery.

LacI. (C) Hot1-GFP localization in cells pretreated with 0.001% v/v DMSO and
100µg/ml phenanthroline in YPD and after 5 minutes of 0.4M NaCl stress. (D) LacI-GFP
was expressed and targeted to 128-LacO arrays in *STL1* and *CTT1* 3'UTR. Cells were
shifted to YPD + 0.4M NaCl for 15min and 0.8M NaCl for 30min. Live cell microscopy
was performed to score changes in nuclear position of the gene loci. Loci that fully
overlapped or were exterior to the HDEL-DsRed signal were scored as peripheral. All
remaining loci were scored nucleoplasmic. The dotted line represents the percent of
peripheral localization of a gene locus with random positioning within the nucleus.
Results averaged from three independent experiments (n>50 cells). Bars represent
standard deviation, * $p<0.05$, ** $p<0.01$.

Hot1 foci form independent from Hog1 MAPK signaling

I next examined the requirements for Hog1 signaling inputs. The localization of Hot1-GFP was examined in untreated and 0.4M NaCl treated cultures in strains defective in Hog1 kinase activity and Hog1 nuclear import. To determine whether signaling through the Hog1 pathway was required I localized Hot1-GFP in a *hog1Δ* mutant. To my surprise, Hot1-GFP showed wildtype localization patterns (Figure 3.2A). To rule out potential cross talk adaptations in the absence of Hog1 protein, I deleted the *NMD5* gene that encodes for the Hog1 nuclear import factor. In the *nmd5Δ* strain where Hog1 is active, but is unable to enter the nucleus, hot1-foci again were unaltered (Figure 3.2A). Lastly, I localized Hot1-GFP in an analog sensitive mutant of Hog1, *hog1-as (T100A).* After 10minutes of addition of the ATP analog, 1NM-PP1, I added 0.4M NaCl and observed Hot1-GFP localization to foci (Figure 3.2A). The percent of cells with Hot1-foci were the same as in wildtype cells in all mutants in both untreated and treated conditions (Figure 3.2B). To determine whether constitutive activation of Hog1 would be sufficient to induce Hot1-foci I overexpressed a dominant form of Ssk2 MAPKKK, *SSK2ΔN* (Figure 3.2C). Though Hog1 accumulated in the nucleus, Hot1 remained diffuse nuclear (Figure 3.2D). My analysis indicates that Hog1 signaling input is neither necessary nor sufficient for Hot1-foci formation.

Casein Kinase II prevents Hot1 localization to foci

My findings that Hot1-foci form independent of Hog1 signaling input prompted us to ask whether additional cellular signaling pathways regulate Hot1 localization. I investigated nuclear kinases and phosphatases in a candidate-based approach and

80
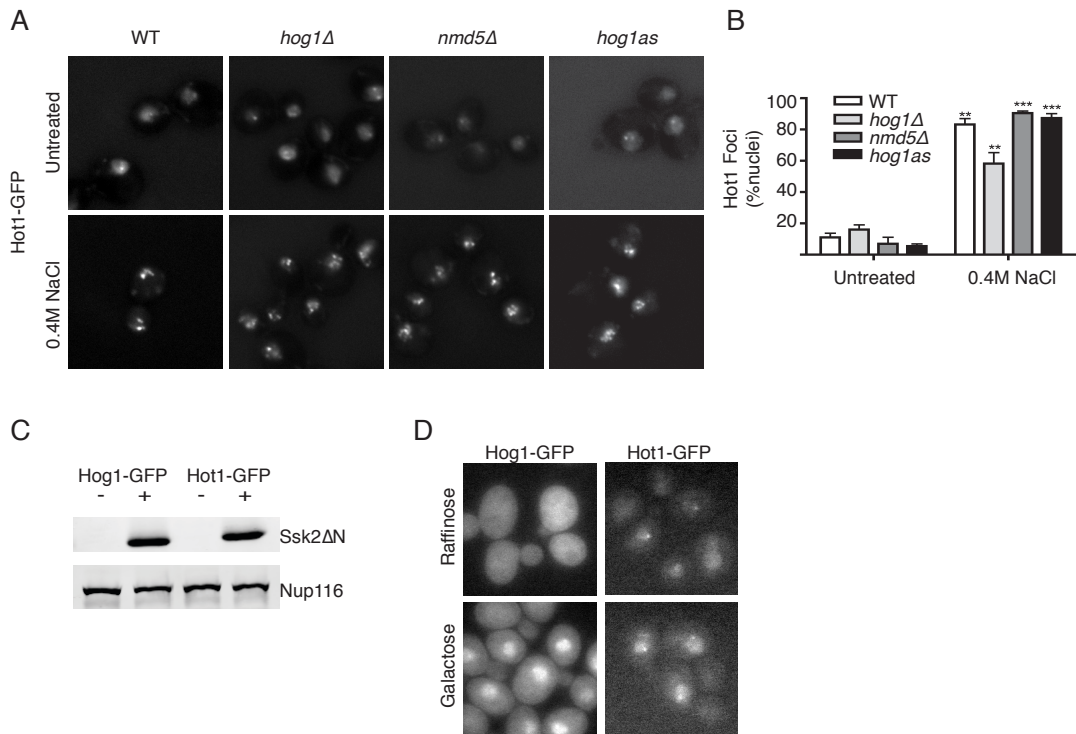
Figure 3.2. Hot1 localization to foci occurs independent from Hog1 MAPK signaling (A) Hot1-GFP localization by live cell microscopy in strains deleted for *HOG1*, *NMD5*, and in a strain with a *hog1as* allele inhibited with 1NM-PP1 (2μM). (B) Quantification for Hot1-GFP foci in *hog1Δ*, *nmd5Δ*, and *hog1as* mutant strains relative to wild type untreated and under hyperosmotic stress (0.4M NaCl). Bars represent standard deviation, **p<0.01, *** p<0.001 relative to wild type untreated. (C) Western blot for *SSK2ΔN* overexpression. – represents SM+raffinose + represents SM+galactose. (D) Images for Hot1=GFP and Hog1-GFP in SM+raffinose and in SM+galactose for *SSK2ΔN* overexpression.

identified altered localization of Hot1 upon genetic disruption and treatment with the TBBt inhibitor of Casein Kinase II (CK2). CK2 is a nuclear kinase that is a tetramer comprised of two alpha catalytic (Cka1, Cka2) and two beta regulatory (Ckb1, Ckb2) subunits. Upon deletion of each of the CK2 subunits, Hot1-foci form constitutively in 80% of cells under normal growth conditions, mirroring Hot1-foci under hyperosmotic stress in wildtype cells (Figure 3.3A-B). The percentage of cells with Hot1-foci also increased with higher concentrations of TBBt inihibitor (Figure 3.3C-D). Given my previous observations for Hot1-foci localization to the *STL1* target gene, I determined whether the constitutive Hot1-foci overlap with *STL1*. In a *cka2Δ* strain, Hot1-foci colocalized to the *STL1* gene in both untreated and 0.4M NaCl treated cells (Figure 3.3E). Therefore, I find that CK2 negatively regulates Hot1-foci formation. Additionally, in *ck2* mutants, the constitutive Hot1-foci colocalize with the Hot1-gene target, *STL1*.

Hot1 interacts with Casein Kinase II and is a direct substrate for phosphorylation

To determine the specificity of CK2-dependent regulation of Hot1-foci, I tested whether Hot1 might be directly regulated through CK2 phosphorylation. *In vivo* interactions provide a predictive measure for potential CK2 substrates (Meggio and Pinna, 2003). Therefore, I first performed a coimmunoprecipitation experiment in cells expressing Cka1-GFP and Hot1-TAP. I observed a significant enrichment of Hot1-GFP from Cka1-GFP immunoprecipitates in both untreated and treated conditions, indicating that the Hot1-CK2 association occurs independent of Hog1 MAPK signaling (Figure 3.4A). To address whether Hot1 was a direct substrate for CK2, I performed an *in vitro*

82
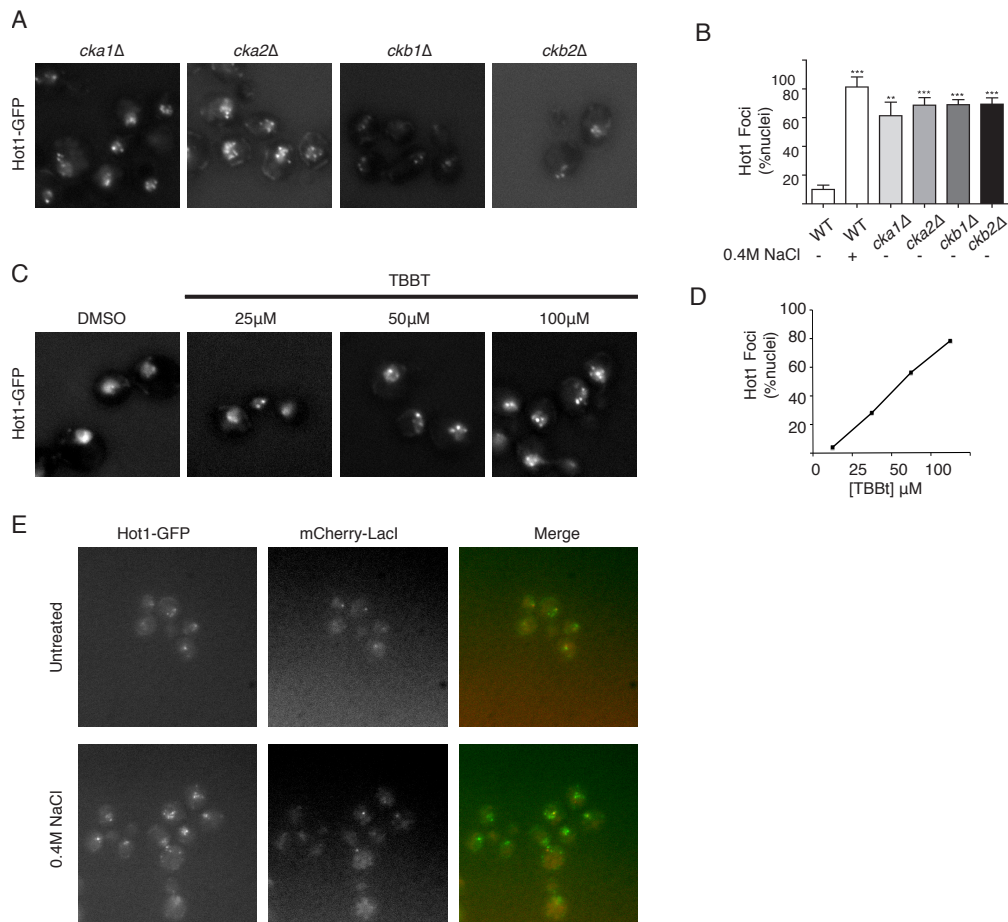
Figure 3.3: Casein kinase II disruption results in constitutive Hot1 foci (A) Hot1-GFP localization by live cell microscopy in strains deleted for genes encoding Casein Kinase II subunits, *CKA1, CKA2, CKB1,* and *CKB2*. (B) Hot1-GFP locaized to clusters after 10min of TBBt treatment at the listed concentrations. (C) Quantification for Hot1-GFP foci in Casein Kinase II delete strains untreated relative to wildtype untreated and under hyperosmotic stress (0.4M NaCl). Bars represent standard deviation, *** p<0.001 relative to wiltype untreated. (D) Dose-response for Hot1-GFP foci upon TBBt treatement. (E) The *STL1* gene locus was localized by expression and targeting of mCherry-LacI to a 128-LacO array inserted into the 3'UTR of *STL1*. Cells were imaged from untreated and 0.4M NaCl treated cultures for Hot1-GFP and mCherry:LacI.
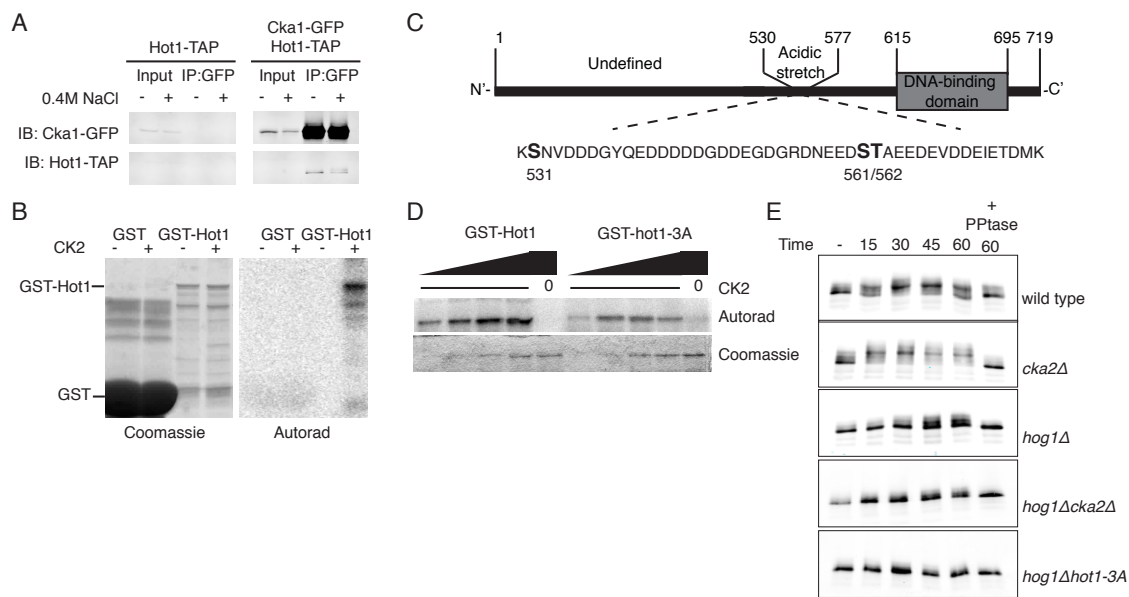
Figure 3.4: Hot1 interacts with Casein Kinase II and is a directly phosphorylated by Casein Kinase II *in vitro* (A) Immunoprecipitations for Cka1-GFP and subsequent immunoblots for Hot1-TAP. Cultures were either untreated or treated with 0.4M NaCl for 10 minutes. Lysates were immunoprecipitated for Cka1-GFP, and subsequently blotted for Cka1-GFP and Hot1-TAP. (B) *In vitro* kinase assays with human Casein Kinase II and recombinant GST and GST-Hot1. Right, coomassie stained gel for total input. Left, radiograph for incorporated [γ-^{32}P]. (C) Domain map for Hot1 depicting the undefined structure of the N-terminus (1-530), the acidic stretch with CK2 consensus sites (530-577), and the DNA-binding domain (615-695). (D) An *in vitro* kinase assay with CK2 and increasing (0.125, 0.25, 0.5 and 1μg) amounts of GST-Hot1 or GST-hot1-3A protein. (E) *In vivo* phosphorylation of Hot1-GFP in untreated and treated (0, 15, 30, 45, 60 min) wildtype, *hog1Δ, cka2Δ, hog1Δcka2Δ,* and *hog1Δhot1-3A* strains. Lambda phosphatase collapse was performed for 60min time point. Anti-GFP western blot for GFP-BP enriched Hot1.

phosphorylation assay. GST-Hot1 was expressed and purified from *E. coli* and incubated with recombinant human CK2 and $[\gamma^{32}P]$-ATP. A phosphorylation event specific to GST-Hot1 was detected upon addition of CK2, confirming that Hot1 is indeed a direct substrate for CK2 (Figure 3.4B).

Given the *in vitro* evidence for CK2 phosphorylation of Hot1, I used an *in silico* based approach to scan Hot1 primary sequence for CK2 consensus sites. The CK2 minimum consensus is S-x-x-E/D and often includes an enrichment of aspartic acid and glutamic acid residues spanning amino acids n+4 through n-7 (Meggio and Pinna, 2003). Three highly acidic CKII consensus sites (S532, S560 and T561) were identified in the C-terminus just upstream of the putative DNA-binding domain (615-695) (Figure 3.4C). A phosphodead version of Hot1 with three alanine substitutions at S531/S561/S562 was recombinantly expressed and tested for phosphorylation in my *in vitro* kinase assay. This *hot1-3A* protein was less phosphorylated, indicating that these sites are modified by CK2 (Figure 3.4D). I next determined whether the phosphorylation of Hot1 was altered *in vivo* in several mutant contexts (Figure 3.4E). In wild type cells, Hot1 phosphorylation peaks between 30 and 45 minutes and is reduced after 60 minutes of 0.4M NaCl stress. Slightly elevated levels of phosphorylation were observed in *cka2Δ* cells, where the majority of phosphorylation was lost in *hog1Δ* cells. I did however observe Hot1 phosphorylation at 45 and 60 minutes in the *hog1Δ* cells that corresponds to the time points where Hot1-mediated transcription is inactivated. I predicted that these were CK2 phosphorylation events, and in a *hog1Δcka2Δ* double mutant Hot1 phosphorylation at these later time points was reduced. Using a *hog1Δ* combined with a CK2 phosphodead mutant, *hot1-3A,* I assessed whether these sites corresponded to the CK2 phosphorylation

events. Again, I observed a loss of Hot1 phosphorylation, suggesting these sites are directly phosphorylated by CK2. Taken together, these observations show that Hot1 is a direct *in vivo* target of phosphorylation by CK2 at time points that correlate with the inactivation phase of the Hog1 MAPK transcriptional response.

Casein Kinase II impacts stochastic expression of *STL1*

Previous work has uncovered highly dynamic and heterogeneous expression of Hot1-regulated genes within a population of cells (Neuert et al., 2013; Pelet et al., 2011). This stochastic gene behavior is thought to result from the short temporal window of Hog1 nuclear activity and the ability of chromatin remodelers to transition the chromatin to an active state. Still, it is likely that there are additional unknown factors at play. Transcription factories in vertebrate cells represent localized compartments enriched for gene activity associated with select transcription factors (Cisse et al., 2013; Ghamari et al., 2013; Iborra et al., 1996; Schoenfelder et al., 2010). Models have suggest that the organization of transcription events in transcription factories may provide a mechanism for concentrating necessary components to switch to an 'on' or active state of expression (Misteli, 2013). Therefore, I were interested in whether CK2 regulation of Hot1 localization influenced the stochastic behavior of the Hot1-dependent gene, *STL1*. Given that the absence of CK2 Hot1 localizes to constitutive foci, and CK2 phosphorylation of Hot1 occurs during the inactivation phase of Hot1 transcription, I predicted that CK2 would provide negative feedback on Hot1-dependent gene expression.

I employed a single cell analysis of *STL1* expression with flow cytometry to detect production of Stl1-GFP expressed from the endogenous *STL1* locus. Under 0.4M

NaCl stress I observed clear bimodal expression pattern in a wild type population at

(Figure 4.5A). As expected, the production of Stl1-GFP was Hot1 and Hog1-dependent,

where no response was observed in cells lacking Hot1 and cells expressing the *hog1as*

allele in the presence of 1NM-PP1 (Figure 4.5A). In the absence of the two alpha

catalytic CK2 subunits, Cka1 and Cka2, the bimodal expression shifted to a more

unimodal expressing population of cells. I then performed a dose-response for *STL1*

expression comparing wild type and *cka2Δ* cells and failed to observe a concentration of

NaCl where *cka2Δ* cells exhibited a bimodal response (Figure 4.5B). Similarly in a time

course experiment comparing WT and *cka2Δ* cells, I were unable to detect a bimodal

response in *cka2Δ* population within the time intervals of 15, 30, 45 and 60 minutes after

0.4M NaCl stress. (Figure 4.5C).

Using this time course experiment, I then determined whether direct CK2

phosphorylation of Hot1 influenced the bimodal expression pattern with cells expressing

the hot1-3A phosphodead version of Hot1 (Figure 4.5D). In the *hot1-3A* mutant

population, the strong peak of non-expressing cells decreased and shifted to a unimodal

pattern of *STL1-GFP* expression. Taken together, these results show that CK2 negatively

regulates Hog1-mediated gene expression through a mechanism involving

phosphorylating Hot1 and enhances the biomodal expression pattern observed for *STL1*.

Discussion

Multiple epigenetic mechanisms contribute to cell variations in gene

expression. The accessibility of a gene to transcriptional machinery is influenced by
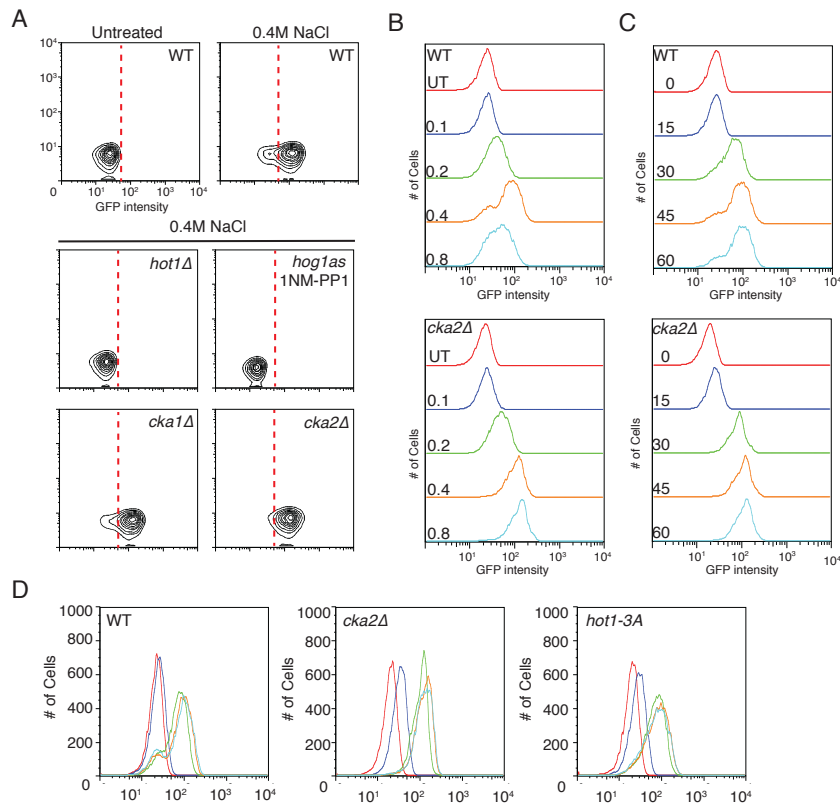
Figure 4.5: CK2 phosphorylation of Hot1 promotes bimodal expression of *STL1*. (A) Contour plots of Stl1-GFP expression in cells untreated and after 60min of 0.4M NaCl stress. The red dotted line separates Stl1-GFP non-expressing and expressing cells, where less then 0.05% of wildtype (WT) cells express Stl1-GFP in untreated conditions. (B) Dose response of Stl1-GFP expression wild type and *cka2Δ* populations of cells after treatment with the indicated NaCl concentrations for 60min. (C) Time course for expression of Stl1-GFP after 0.4M NaCl stress in the wildtype (WT) and *cka2Δ* populations of cells. (D) Time course of Stl1-GFP expression in wildtype (WT), *cka2Δ* and *hot1-3A* cells from untreated (UT) to 60minutes of 0.4M NaCl stress.

the local chromatin as well as gene positioning within respect to different transcriptional compartments.   The transcription of inducible genes in *S. cerevisiae* is regulated through positioning to distinct gene territories; however, an in-depth understanding of the cellular signaling events that regulate gene positioning is still missing. My analyses of Hog1-activated transcription under conditions of osmotic stress indicates previously unrecognized roles for Casein Kinase II (CK2) that regulate the subnuclear organization of transcriptional events and account for the heterogeneity of gene expression within a population.

Subnuclear foci for osmotic gene transcription

Transcription factories in mammalian cells are sites enriched in transcriptional components and co-regulated genes. These subnuclear compartments are proposed to coordinate transcriptional events that result in cell-specific patterns gene expression.   My results indicate the presence of similar transcriptional compartments in *S. cerevisiae* that form under osmotic stress. The Hot1-transcription factor localizes to subnuclear foci that colocalize to the *STL1* gene target in the first minutes following exposure to osmotic stress. Surprisingly, Hot1 localization to foci occurs independent from Hog1 MAPK activity. Previously, the localization of Hot1 to gene promoters was described to occur independent from Hog1 phosphorylation (Alepuz et al., 2003; Alepuz et al., 2001). However, the localization of Hog1 to Sko1 and Hot1 gene targets is required to recruit chromatin-remodeling machinery and for the global reallocation of RNAPII to a subset of 28 osmotically-responsive genes co-occupied by Hog1, Sko1 and Hot1 (Cook and

O'Shea, 2012; Mas et al., 2009). Given that 6-10 Hot1-foci are observed in osmotically stressed cells, it is possible that these foci represent sites for clustering of these 28 gene targets. A high local concentration of Hot1 may also be required due to the low protein abundance of Hot1 (128copies/cell) and relative to the ~29 Hot1-target genes. Furthermore, Hot1-foci may serve to localize Hog1 activity through mechanisms that ensure nuclear enrichment and retention. Additionally, the subnuclear compartmentalization of Hog1-gene expression provides a strategy for isolating the activity of Hog1 to osmotic gene targets, and to the exclusion of housekeeping genes.

The dynamic regulation and composition of Hot1-foci

The composition and dynamics of subnuclear compartments in metazoans vary across cell types and upon changing environmental conditions (Biamonti and Vourc'h, 2010; Mao et al., 2011b). Under osmotic stress, the formation of several distinct nuclear bodies have been described (Schoborg et al., 2013; Valgardsdottir et al., 2008; Vidal et al., 2013). In *S. cerevisiae*, hyperosmotic foci containing components of the filamentous and pheromone MAPK pathways form to inhibit the inappropriate activation of the respective downstream targets (Vidal et al., 2013).   However, these foci exhibit Hog1-dependency and are inhibited by alpha factor, two processes that I were unable to link to Hot1-foci. Rather, I have identified a novel regulatory role for CK2 in the formation of Hot1 foci. My data suggests that CK2-dependent phosphorylation may remove Hot1 from foci during the inactivation of Hog1 MAPK gene expression. My identification of CK2 as cellular input regulating subnuclear organization provides evidence for the previously controversial role of CK2 in osmotic stress (Bidwai et al., 1995; de Nadal et

al., 1999; Tenney and Glover, 1999). Regulation of vertebrate CK2 may have conserved roles in regulating the dynamics of nuclear bodies observed in other eukaryotes.

The factor(s) required for the dynamic assembly of Hot1 foci remain unidentified. It is possible that a phosphatase acts to reverse CK2 phosphorylation of Hot1 upon osmotic stress, resulting in the robust localization of Hot1 to foci. Additionally, CK2 is able to phosphorylate sites that are adjacent to prior phosphorylation events suggesting that an additional kinase may be involved in assembly of Hot1 foci that also primes Hot1 for inactivation by CK2. Another mechanism may involve inactivation of the otherwise constitutive activity of CK2 under osmotic stress, allowing for temporary relief of Hot1 inhibition. My continuing studies will further investigate these possibilities.

I predict that additional components localize to Hot1-foci that avoid detection by conventional live cell fluorescent microscopy. The visualization of limited components in vertebrate transcription factories is only recently becoming possible (Cisse et al., 2013; Ghamari et al., 2013). My continued experiments are aimed to identify protein components through mass spectrometry of Hot1 protein-interaction partners. Genomic regions that are enriched for association with Hot1-foci can also be evaluated with ChIP and chromatin conformation capture experiments.   These strategies will help inform my current model of Hot1-foci representing active transcriptional compartments.

Nuclear organization of transcription and stochastic gene activity

The current models for cell-to-cell variations in Hog1 MAPK gene expression account for Hog1 as the sole kinase input with additional contributions of factors required to remove chromatin obstructions at target promoters and Hog1 nuclear retention time.   I

have provided a novel input to this model suggesting that nuclear organization into Hot1-foci provides an additional factor favoring Hog1-activation of transcription. These Hot1-foci are Hog1-independent suggesting that they occur upstream of Hog1-recruitment or in parallel to the Hog1 events at the promoter. Hog1-independent regulation of the Hot1-foci formation may provide additional mechanisms to prevent inappropriate activation and limit expression to conditions when Hog1 is properly localized to the nucleus in the context of osmotic stress. I have observed that in *ck2* mutants, Hot1 constitutive localization to foci correlates with the uniform activation of *STL1* target gene within a population of cells. I propose a model whereby Hot1-foci poise localized gene targets for coordinated transcriptional activation by Hog1. Thereby, my model further suggests that stochastic activity of genes relies on the local availability of transcriptional components.

MATERIALS AND METHODS

Yeast strains, growth conditions and plasmids

Yeast strains listed in Table 3.1 are of the BY4743 designer deletion S288C background. Knockouts, endogenous tagging and dellito perfetto point mutations were constructed with standard LiAc transformation procedures. Strain crosses were performed to obtain various combinations of alleles. The *GFP-LacI/LacO CTT1* and *STL1* strains were made as described in (Brickner et al., 2010), with *LEU2:DsRED-HDEL* as a nuclear periphery marker. All *S. cerevisiae* strains were grown in YPD (2% peptone, 2% glucose, 1% yeast extract) or SC dropout medium at 30°C. For osmotic stress, a stock solution of YPD+4M NaCl was added to the final concentrations indicated. Inhibitors were used at 100μM Latrunculin A, 20μg/ml Nocodozole, 100μg/ml

Phenanthroline, and 200μM TBBt. The plasmids used in this study are listed in Table

3.2. Standard molecular cloning techniques were used as in (Sambrook et al., 1989b).

Flow cytometry

Overnight cultures were inoculated to grow for at least 15hrs to an OD600 of 0.5

and further treated for various timepoints at indicated NaCl concentrations. Samples

were harvested by diluting into 10mM Tris, 1mM EDTA pH 8.0 + 1μg/ml

cyclohexamide and immediately measured for GFP fluorescence using a Guava easyCyte

Flow cytometer. For each sample, 20,000 cells were collected within gated SSC and FSC

population that excluded doublets and small debris. Data was graphed using FlowJo

software.

***In vitro* kinase assay**

GST-HOT1 expression was induced in Rosetta cells with 200μM IPTG at 16°C

overnight. The cells were lysed in binding buffer (20 mM HEPES at pH 7.5, 300 mM

NaCl, 3 mM $MgCl_2$, 10% w/v glycerol, 10mM EDTA, 1xPI (Roche), and 0.1mM PMSF)

with sonication. The lysates were centrifuged for 15 min at 15,000 rpm and the soluble

fraction was loaded onto 200μl of glutathione sepharose beads (GE life sciences) and

bound for 4hrs at 4°C. The beads were washed three times with binding buffer and three

times with kinase buffer (20mM Tris-HCl, 50mM KCl, 10mM $MgCl_2$ pH 7.5).

Phosphorylation reactions were performed in 500μL of kinase buffer and supplemented

with 20μM cold ATP, 20μCi γ^{32}PATP and 1000 units of human Casein Kinase II (NEB)

for 1hr at 30°C. Reactions were terminated by resuspending and boiling in 2X SDS

buffer. Samples were further analyzed by SDS PAGE, coomassie staining and autoradiography. Additionally, GST-Hot1 and GST-hot1-3A were purified with glutathione sepharose beads (GE life sciences) and dialyzed into kinase buffer for subsequent phosphorylation with human Casein Kinase II (NEB).

Immunoprecipitations and immunoblotting

Hot1-TAP and Cka1-GFP expressing cultures grown to OD_{600} =0.6 were treated with and without 0.4M NaCl for 10min. Cultures were immediately washed in ice-cold ddH_2O and pellets were snap frozen in liquid nitrogen. Pellets were lysed by bead beating in lysis buffer (50mM Tris HCl, 150mM NaCl, 5mM EDTA 0.1% Triton X-100, 10% glycerol, 1x protease inhibitors (Roche), 0.1mM PMSF, 1mM Na3NO4, 50mM NaF, pH7.5). Lysates were clairified at 13,000rpm for 6min and supernatant was incubated on camelid GFP-nanobody, GFP-binding protein (GBP)-conjugated sepharose beads at 4°C for 1hr. GBP-beads were washed three times in wash buffer (50mM Tris, 150mM NaCl, 0.1%Triton X-100, pH 7.5) and then boiled in 2X SDS buffer. Further analysis with SDS PAGE and western blotting was performed with rabbit anti-GFP antibody. Hot1-GFP pullouts were performed for *in vivo* phosphorylation analysis of Hot1 identically as described above.

Microscopy

Cultures for imaging were diluted from saturated overnight starter cultures to OD_{600} = 0.05 and grown at 30°C for 5hrs to reach OD_{600} = 0.4-0.6. To quantify the LacO-array experiments HDEL was used as a marker of the nuclear periphery and GFP-LacI foci were quantified as peripheral (HDEL-GFP overlap) or nucleoplasmic. For each

experiment, 100 cells were quantified (n=3). Quantification of Hot1-foci was performed in untreated cells and after a 5-minute shift to 0.4M NaCl. Nuclei were scored for 1 or >1 Hot1-foci in 50 cells for each experiment (n=3). Images were acquired with a personal DeltaVision microscope system (Applied Precision, IX70 Olympus) using a 100X NA 1.40 UPlanSApo objective, and Photometrics CoolSnap HQ2 camera. Images were processed with softWoRx imaging software and DeltaVison's constrained three-dimensional deconvolution method to remove out of focus light. Further linear adjustments were made for brightness and contrast in ImageJ or Adobe Photoshop CS6. Remaining images were acquired with a standard microscope (BX50; Olympus) equipped with a motorized stage (Model 999000, Ludl), UPlanF1 100× NA 1.30 oil immersion objective, and digital charge coupled device camera (Orca-R2; Hamamatsu). Any additional image processing used NIS-Elements (Nikon), ImageJ (NIH) or Adobe Photoshop CS6.

Table 3.1. Yeast strains used in this study.

Strain	Genotype	Source
S288C	*MATa/α his3Δ1/his3Δ1 leu2Δ0/leu2Δ0 LYS2/lys2Δ0 met15Δ0/MET15 ura3Δ0/ura3Δ0*	BY4743 Brachmann *et al.,* 1998
GFP collection	*MATa GFP:spHIS5 his3Δ1 leu2Δ0 LYS2 met15Δ0 ura3Δ0*	Open Biosystems Mnaimneh *et al.*, 2004
TAP collection	*MATa TAP:spHIS5 his3Δ1 leu2Δ0 LYS2 met15Δ0 ura3Δ0*	Thermo Scientific Ghaemmaghami *et al., 2003*
Null Strain collecion	*MATa ::KAN^r his3Δ1 leu2Δ0 LYS2 met15Δ0 ura3Δ0*	Thermo Scientific G. Giaever *et al.*, 2002
SWY5835	*MATa ura3Δ0:STL1-LacOx128:URA3 Hot1-GFP:spHIS5 leu2Δ0 lys2Δ0 met15Δ0 pRS425:mCherry-LacI*	this study
SWY4927	*MATa STL1-LacOx128:URA3 his3:GFP-LacI-HIS3 leu2:DsRed-HDEL:LEU2 lys2Δ0 met15Δ0*	this study
SWY4929	*MATa CTT1-LacOx128:URA3 his3:GFP-LacI-HIS3 leu2:DsRed-HDEL:LEU2 LYS2 met15Δ0*	this study
SWY5656	*MATa HOT1-GFP:spHIS5 hog1-as his3Δ1 leu2Δ0 LYS2 met15Δ0 ura3Δ0*	this study
SWY5456	*MATa HOT1-GFP:spHIS5 nmd5::HIS3 leu2Δ0 LYS2 ura3Δ0*	PSY1199 Ferrigno et al., 1998
SWY4826	*MATα HOT1-GFP:spHIS5 hog1::KAN^r his3Δ1 leu2Δ0 LYS2 met15Δ0 ura3Δ0*	this study
SWY5451	*MATa HOT1-GFP:spHIS5 cka1::KAN^r his3Δ1 leu2Δ0 LYS2 met15Δ0 ura3Δ0*	this study
SWY5452	*MATa HOT1-GFP:spHIS5 cka2::KAN^r his3Δ1 leu2Δ0 LYS2 met15Δ0 ura3Δ0*	this study
SWY5453	*MATα HOT1-GFP:spHIS5 ckb1::KAN^r his3Δ1 leu2Δ0 lys2Δ0 MET15 ura3Δ0*	this study
SWY5454	*MATa HOT1-GFP:spHIS5 ckb2::KAN^r his3Δ1 leu2Δ0 LYS2 met15Δ0 ura3Δ0*	this study
SWY5508	*MATa HOT1-TAP:spHIS5 CKA1-GFP:spHIS5 his3Δ1 leu2Δ0 LYS2 met15Δ0 ura3Δ0*	this study
SWY5660	*MATa hot1-3A-GFP:spHIS5 his3Δ1 leu2Δ0 LYS2 met15Δ0 ura3Δ0*	this study
SWY5690	*MATa hot1-3A-GFP:spHIS5 hog1::KAN his3Δ1 leu2Δ0 LYS2 met15Δ0 ura3Δ0*	this study
SWY5842	*MATa HOT1-GFP:spHIS5 cka2::KAN^r hog1::KAN^r his3Δ1 leu2Δ0 LYS2 met15Δ0 ura3Δ0*	this study
SWY5833	*MATa cka2::KAN^r ura3Δ0:STL1-LacOx128:URA3 HOT1-GFP:spHIS5 leu2Δ0 lys2Δ0 met15Δ0 pRS425:mCherry-LacI*	this study
SWY5572	*MATa STL1-GFP:spHIS5 his3Δ1 leu2Δ0 LYS2 MET15 ura3Δ0*	this study
SWY5575	*MATα STL1-GFP:spHIS5 cka1::KAN^r his3Δ1 leu2Δ0 LYS2 MET15 ura3Δ0*	this study
SWY5576	*MATa STL1-GFP:spHIS5 cka2::KAN^r his3Δ1 leu2Δ0 LYS2 MET15 ura3Δ0*	this study
SWY5643	*MATα STL1-GFP:spHIS5 hog1::KAN^r his3Δ1 leu2Δ0 LYS2 MET15 ura3Δ0*	this study
SWY5655	*MATa STL1-GFP:spHIS5 hog1-as his3Δ1 leu2Δ0 LYS2 MET15 ura3Δ0*	this study
SWY5659	*MATa hot1-3A STL1-GFP:spHIS5 his3Δ1 leu2Δ0 LYS2 met15Δ0 ura3Δ0*	this study

Table 3.2. Plasmids used in this study.

Plasmid	Encoded gene	Source
pFA6a-*GFP-HISMX6*	*GFP-spHIS5*	Longtine et al 1997
pASF144	pRS304:*GFP-LacI*	Straight *et. al* 1996
p6LacO128	pRS306:*LacO128*	Brickner and Walter. 2004
pCORE-UK	*URA3/KAN^r*	Storici and Resnick. 2006
pSW3632	pRS306:*CTT1-3'UTR:LacO128*	This study
pSW3633	pRS306:*STL1-3'UTR:LacO128*	This study
pSW3850	pRS426:*GAL:SSK2ΔN-HA*	This study
pSW3883	pGEX-5x3:*GST-HOT1*	*This study*
pSW3917	pGEX-5x3:*GST-hot1-3A*	This study
pSW3948	pRS425:*HIS3:mCherry-LacI*	This study
pSW3889	pRS415:*hot1-3A-GFP*	This study

CHAPTER 4

DISCUSSION AND FUTURE DIRECTIONS

The nucleus is a fascinating organelle divided into distinct structural compartments that function in events of DNA transcription, replication and repair. Our findings in *Saccharomyces cerevisiae* have led us to important insights into roles for chromatin organization and gene expression in the dynamic regulation of nuclear structure. In our early work, genetic screens provided compelling evidence for the functions of the RSC chromatin-remodeling complex in maintaining nuclear structure. This study further revealed additional requirements for transcription and membrane dynamics in NE homeostasis, which likely contribute to the global defects in nuclear structure observed in *rsc* mutants. In a later study, I revealed exciting roles for the subnuclear organization of transcription in the stochastic activation of genes in response to osmotic stress. First, I observed the striking localization of the Hot1 transcription factor to subnuclear foci under conditions of osmotic stress, which colocalized with the Hot1-gene target, *STL1*. Furthermore, I provided evidence that the formation of Hot1-foci correlates with a more robust transcriptional activation of *STL1* within a population of cells. Finally, I identified inhibitory roles for Casein Kinase II in regulating both Hot1 activity and localization. This work has generated many new ideas for future studies exploring the functional impacts for the dynamic regulation of nuclear structure. Within this chapter, I will present future experiments to follow up on several remaining questions from my current studies. Later sections are devoted to highlighting the frontiers in nuclear cell biology that I find most compelling.

A model for the functional role for Hot1-foci in stochastic gene activity

My data suggest a model wherein Hot1-foci represent active transcription factories for Hog1-regulated gene expression (Figure 4.1). With approximately 100 copies of Hot1 protein in the nucleus, I predict that the foci concentrate Hot1 in the vicinity of target promoters. To coordinate Hot1-dependent transcription I envision clustering of the 20 known Hot1 target genes to the observed 4-6 Hot1-foci/cell. The formation of Hot1-foci occurs independent from Hog1, and likely represents a parallel mechanism that coordinates the transcriptional response to osmotic stress. I predict that localization of a gene to Hot1-foci represents a stochastic switch in transcriptional activation. When a gene is localized to Hot1-foci it is switched 'on' and genes that are not localized to Hot1-foci remain 'off'. Finally my results shed light onto a previously undescribed mechanism of Hot1 inhibition wherein Casein kinase II negatively regulates both Hot1 transcriptional activity and localization to subnuclear foci.

Incorporating published results into my model

The O'Shea and Posas groups have thoroughly investigated the mechanisms for Hog1-activated gene transcription (Capaldi et al., 2008; Cook and O'Shea, 2012; de Nadal and Posas, 2010; Nadal-Ribelles et al., 2012; O'Rourke et al., 2002). These studies have focused on the ordered events of promoter recruitment and in defining subsets of genes regulated by each transcriptional activator (Sko1, Hot1 and Msn2/4). One perplexing finding is that neither Hot1 nor Sko1 require Hog1-phosphorylation to
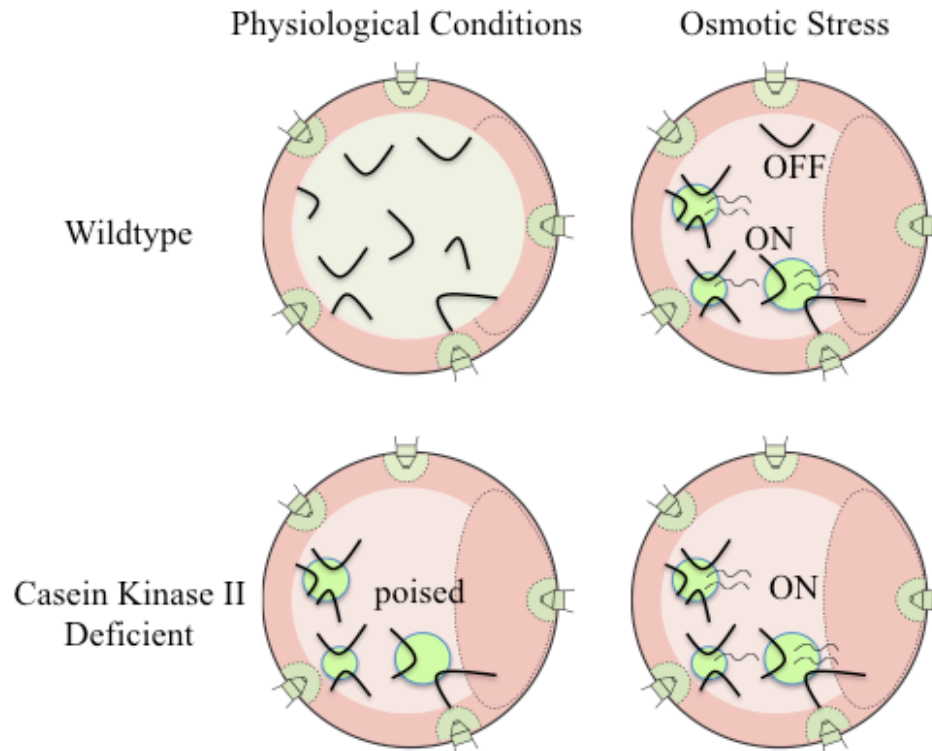
FIGURE 4.1. Model for the stochastic activation of genes positioned to Hot1-foci. The clustering of Hot1 gene targets to Hot1-foci is a stochastic event that is required for transcriptional activation. Hot1 target genes that are positioned to Hot1-foci are switched ON, where those genes that are not localized to Hot1-foci remain OFF. In Casein Kinase II deficient cells, gene targets positioned to constitutive Hot1-foci and are poised for transcriptional activation.

recognize and bind to promoters. (Alepuz et al., 2003; Cook and O'Shea, 2012). Rather the critical role for Hog1 is to recruit RNAPII, which occurs after the transcription factors have already bound to the promoters of Hog1-responsive genes. Therefore, a Hog1-independent mechanism accounts for the localization of transcription factors to the target genes.

I report Hog1-independent Hot1-foci enrich at the *STL1* gene locus, and propose that these transcription factor foci represent the initial promoter recruitment events. Since Hot1-foci are constitutive in *ck2* mutants, I predict that in these mutants Hot1 would exhibit stress-independent recruitment to *STL1* along with 19 additional Hot1-gene targets identified by the O'Shea group. However, the enrichment of Hot1 to gene promoters is not sufficient to induce transcription, as *ck2* mutants do not show constitutive *STL1* transcription. Additional Hog1-dependent events, including chromatin remodeling at the promoter and recruitment of RNAPII are still necessary for activation of *STL1*.

My model further suggests that Hot1-foci represent an additional rate-limiting step in the stochastic activation of Hog1-responsive genes (Figure 4.2). Previous studies have identified additional factors impacting stochastic activation including RSC chromatin remodeling at the promoter and Hog1-nuclear residence time. My model places the formation of Hot1-foci upstream to these events. Epistasis experiments combining *ck2* mutants and *rsc* chromatin-remodeling mutants could further determine whether these are two distinct switches. If the *cka2Δrsc3Δ* double mutants result in a bimodal expression pattern, then this would suggest that two stochastic events regulate expression of *STL1*. However, a unimodal expression pattern would indicate that the

localization of Hot1 to subnuclear foci represents the major stochastic event regulating *STL1* expression.

Outstanding Questions

Cellular cues regulating the dynamics of Hot1-Foci

I have identified a clear inhibitory role for CK2 in regulating the localization of Hot1 to nuclear foci. To determine whether CK2 plays a direct or indirect role in regulating Hot1 localization and activity I employed an *in silico* approach to identify the sites of CK2 phosphorylation on Hot1. Three highly predicted CK2 consensus sites were altered to encode phospho-dead (Hot13A) and phosphor-mimetic (Hot13D) versions of Hot1. If CK2 phosphorylation of Hot1 directly inhibits Hot1 localization to foci, I predicted that Hot13A would localize to constitutive nuclear foci and the Hot13D to not localize to foci. Surprisingly, both versions showed identical localization patterns as wildtype Hot1. I propose three hypotheses based on these results: (1) additional sites are modified by CK2 that were not predicted based on the *in silico* approach (2) an interaction between CK2 and Hot1 more strongly influences Hot1 localization then the phosphorylation event, and remains unaffected in the Hot13A and Hot13D mutants or (3) CK2 does not directly target Hot1.

I am currently testing these hypotheses with several different approaches. As an unbiased method to identify CK2 phosphorylation events, I am using mass spectrometry of purified Hot1 from untreated and osmotically-induced cells. Along with these experiments, I am analyzing *in vivo* phosphorylation of Hot1 in *hog1Δ, cka2Δ* and *hog1Δcka2Δ*. I have observed a Hog1-independent phosphorylation event of Hot1 that
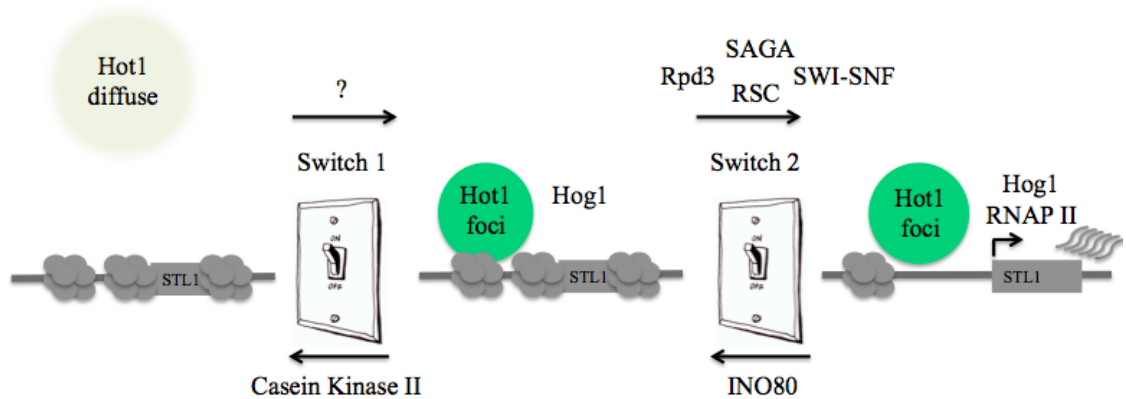
FIGURE 4.2. Stochastic events influencing Hot1 regulated gene expression. I propose that the localization of *STL1* to Hot1-foci represents 'Switch 1' regulating the stochastic expression of *STL1*. Casein Kinase II turns off Switch 1. Switch 2 represents the previously described stochastic events of chromatin remodeling and modifying events open up the promoter for transcription by RNAPII. Further epistasis experiments will be required to resolve whether these switches represent two distinct stochastic events of Hot1 regulated gene expression.

occurs after 45minutes of moderate osmotic stress and correlates with the inactivation of Hot1 transcription. I predict that this is a CK2 phosphorylation event and will be absent in *hog1Δcka2Δ* cells. Additionally, I am performing domain-mapping experiments to determine whether a stretch of acidic amino acids on Hot1 is a CK2-interaction domain. Deletion of this domain is predicted to result in constitutive Hot1-foci formation and loss of Hot1 inactivation by CK2.

I have yet to identify an additional factor that promotes the formation of Hot1-foci upon osmotic stress. Initially, I predicted a role for an activating phosphatase in the removal of potential inhibitory CK2 phosphorylation sites on Hot1. Candidate phosphatases with described nuclear roles and are documented to reverse CK2 phosphorylation events were investigated for the absence of Hot1-foci under osmotic stress. These included the PP2A regulatory subunits (*cdc55Δ, rts1Δ, rrd1Δ*), the PP4 catalytic subunit and regulatory subunits (*pph3Δ and psy2Δ, psy4Δ,* respectively) and the calcenurin phosphatase (*cnb1Δ*). No change in foci formation was detected among the mutants (data not shown). Remaining experiments will follow up with additional phosphatases that have identified roles in Hog1 MAPK signaling such as the PP2C phosphatases (*ptc2Δptc3Δ)*, PPZ phosphatases (*ppz1Δppz2Δ*) and the plasma membrane phosphatases (*psr1Δpsr2Δ*). If these efforts are unsuccessful in identifying a Hot1 phosphatase, an unbiased global analysis may be necessary. Additionally, analysis with double mutants or broad phosphatase inhibitors may be useful approaches as many phosphatases perform redundant roles.

Another potential mechanism for Hot1 activation and formation of Hot1-foci is though phosphorylation by a CK2-priming kinase. CK2 is a serine-threonine kinase that

targets upstream of acidic amino acid residues (pS/T-X-X-E/D) or to previously phosphorylated residues (pS/T-X-X-pS/T) (Meggio and Pinna, 2003). An activating kinase might signal for Hot1-foci formation, which would prime Hot1 for subsequent phosphorylation and inactivation by CK2. Several known Hog1-phosphorylation sites in Hot1 could potentially serve to prime CK2 phosphorylation. However, I have ruled out Hog1 as a potential CK2-priming kinase, based on two observations. First, Hot1-foci form independent of Hog1 and second I observe phosphorylation corresponding to CK2-inactivating phosphorylation in a *hog1Δ*. It is also possible that the yeast Mec1 kinase may prime Hot1. Several mass spectrometry studies identified Hot1 phosphorylation events occur at Mec1 consensus S/T-Q motifs (Albuquerque et al., 2008). Also, the vertebrate osmotic transcription factor TonEBP/NFAT5 requires phosphorylation by the vertebrate Mec1 kinase for activation (Irarrazabal et al., 2004). My mass spectrometry experiments will evaluate these possibilities, and determine whether CK2 phosphorylation sites require a priming phosphorylation event.

Another potential mechanism for osmotically-induced Hot1-foci may be in the temporary inactivation of CK2. CK2 is universally considered a constitutive kinase (Meggio and Pinna, 2003), and currently there is no *in vivo* evidence for stress-regulated CK2 activity. However, several *in vitro* studies provide evidence that CK2 activity is inhibited with increasing salt concentrations. Elevated (0.5M NaCl) salt concentrations result in a shift from protomer to monomer forms of CK2 and a loss in an auto-phosphorylation event of the regulatory subunits (Pagano et al., 2005; Valero et al., 1995). Additionally, a phosphoproteomic study to identify phospho-peptides enriched in 0.4M NaCl reported a decrease in auto-phosphorylation of Ckb1 (S77, S98) (Soufi et al.,

2009). Based on these findings, I propose an additional mechanism for Hot1-foci

formation that results from the temporary inactivation of CK2 as intracellular NaCl

concentrations increase. As the cell recovers and internal osmolite concentrations return

to normal levels, restored activity of CK2 may promote the inactivation of Hot1.

Composition of Hot1-foci

In my model, I propose that Hot1-foci represent transcription factories for Hog1-

regulated gene expression. This implies that the transcriptional machinery is also

recruited to Hot1-foci. I have extensively screened though components of the RSC

chromatin-remodeling complex, FACT complex, SAGA, TREX, TREX2, NPC, CK2 and

candidate phosphatases but have yet to identify a component that localizes to foci under

osmotic stress. Under moderate stress (0.4M) I observe granular staining of Sko1, Msn2

and Hog1 and also more punctate staining under higher conditions (1M NaCl) of osmotic

stress. Live cell microscopy may not be the best method to identify additional

components of Hot1-foci for several reasons that have also hindered the live cell

visualization of mammalian transcription factories. First, my ability to detect Hot1-foci

may be due to the low expression levels of Hot1, where proteins expressed at higher

levels may prevent the resolution of distinct foci. Also, other components may associate

dynamically or only a post-translationally modified subset of proteins may localize to

Hot1-foci.

Until recently, the visualization of mammalian transcription factories was only

possible though immunofluorescence on fixed samples with antibodies recognizing active

RNAPII or nascent transcripts labeled with nucleotide analogs. The primary issue was

the inability to distinguish between inactive and active forms of RNAPII signified by phosphorylation events on C-terminal domain (CTD) of the largest subunit of RNAPII. A recent study circumvented this issue and visualized transcription factories through the localization of the Cdc9 kinase that associates at early stages of transcription with initiating RNAPII (Ghamari et al., 2013). I am currently analyzing the yeast RNAPII CTD kinases for foci formation under osmotic stress. Additionally, advanced imaging experiments using PALM were able to resolve RNAPII clusters that increased in dwell time upon stimulated transcription (Cisse et al., 2013). Though these recent approaches were successful in observing transcription factories in living cells, live cell microscopy screening is not a suitable approach for identifying additional components of Hot1-foci.

My current approach is to biochemically screen for components of Hot1-foci through the identification of Hot1-interaction partners with mass spectrometry. Hog1 and CK2 will provide positive controls for factors that are known to interact with Hot1. Additionally, I predict I will enrich for Sko1 or Msn2/4 if Hot1-foci represent clustering of all Hog1-mediated transcription events. This approach has the potential to identify novel factors involved in assembly of Hot1-foci and gene positioning and clustering to Hot1-foci. Proteins that bind insulators and exhibit boundary activity may be required for gene positioning and clustering to Hot1 foci. Other potential candidates include validated and predicted targets of CK2; Yta7, Abf1, and Bdf1/Bdf2, as well as protein complexes that mediate long-range chromatin interactions in metazoans such as cohesin and mediator (Kagey et al., 2010; Loven et al., 2013; Sawa et al., 2004; Upton et al., 1995). These components can be further validated by localization to Hot1-foci and for their requirements in Hot1-foci formation.

I am also interested in identifying the composition of gene targets that are positioned to Hot1-foci. The simplest approach is to first perform Hot1 ChIP experiments in *ck2* mutants for the 20 previously identified Hot1-target genes (Cook and O'Shea, 2012). If *ck2* mutants show promising enrichment of Hot1 interactions with Hot1-targets, additional clustering genes can be identified by Hot1 ChIP-chip/seq, a ChIP chip/seq approach using *LacI/STL1:LacO-array*, or a DamID analysis with *DAM-LacI/STL1:LacO-array*. I also predict that Sko1 and Msn2-4 gene targets will position to Hot1-foci. Alternatively, recent studies have highlighted the roles for promoter-encoded gene recruitment sequences (GRS) and the Put3 transcription factor in specifying interchromosomal gene clustering (Brickner et al., 2012). A bioinformatics approach could be used to identify these identify shared sequence elements within the promoters of Hot1-associating genes that function like a GRS. If these preliminary experiments validate my model, then circularized chromosome conformation capture (4C) with *STL1*, or a Hi-C experiments could be used to identify a salt-specific global chromatin arrangement that coordinates Hog1-MAPK gene expression. Processing global 3C datasets poses a major challenge, however the simple genome of *S. cerevisiae* makes these experiments more approachable. The Hog1-MAPK pathway would provide an ideal system to begin elucidating how global chromatin landscapes change to coordinate stress-activated gene expression programs.

Functions for Hot1-foci

In an individual cell, expression from two identical *STL1* promoters is uncorrelated suggesting that a cell intrinsic factor accounts for the stochastic activation of

osmotically-induced genes (Pelet et al., 2011). I hypothesize that gene positioning to Hot1-foci is this intrinsic factor where *STL1* localized to Hot1-foci is active, but *STL1* not localized to Hot1-foci is inactive. To directly test whether *STL1* localization to Hot1-foci impacts *STL1* activity, I must co-localize Hot1-GFP with nascent *STL1* mRNA. There are several current methods to visualize nascent RNAs including the MS2 mRNA tagging system and single mRNA fluorescence in situ hybridization (FISH).

I have developed a system to visualize *STL1* transcripts in live cells by tagging the *STL1* 3'UTR with MS2 hairpin sequences from the MS2 bacteriophage and co-expressing a GFP-tagged MS2 coat protein (MCP-GFP) that binds to the MS2 hairpins (Haim-Vilmovsky and Gerst, 2009). Unfortunately, I have not observed *STL1-MS2* transcripts within the nucleus. Events of release from the transcriptional site and mRNA export may occur prior to visible accumulation of MCP-GFP on the *STL1-MS2* transcript. The Singer group has observed *MDN1* transcripts at the transcription site with a 5'UTR mRNA tag (Larson et al., 2011), suggesting that I may need to switch to a 5'UTR *MS2-STL1*. If nascent transcripts co-localize to Hot1-GFP foci, then active transcription occurs in Hot1 foci. To further demonstrate that the *STL1* is inactive when not localized to Hot1-GFP foci, I can perform a triple-labeling experiment with the *MS2-STL1, STL1:LacO-array,* and Hot1-GFP. Alternatively, RNA FISH experiments to label *STL1* transcript coupled with immunofluorescence of Hot1-GFP would also begin address this question. I have avoided localizing Hot1 by immunofluorescence due to observed artifacts upon fixation that result in Hot1-foci in the absence of 0.4M NaCl. To proceed with these experiments, I would have to optimize fixation conditions to match unfixed localization patterns. Optimization of one of these two approaches will be required to

directly test whether the localization of a gene to Hot1-foci determines the transcriptional activity.

Other nuclear foci have been described in *S. cerevisiae* and Drosophila that arise under conditions of osmotic stress, which sequester nuclear proteins and inhibit their roles in gene expression and chromatin organization (Schoborg et al., 2013; Vidal et al., 2013). In *S. cerevisiae*, the kinases and transcription factors of the mating/filamentous MAPK pathways localize to subnuclear foci under osmotic stress (Vidal et al., 2013). Feedback mechanisms exist in the upstream signaling events to insure signaling between the mating/filamentous MAPK cascade and Hog1 MAPK cascade remain insulated and that crosstalk does not lead to inappropriate activation of Fus3/Kss1 and Hog1 MAPKs. Following this rationale, the authors of this study (Vidal et al., 2013) hypothesized that under osmotic stress the mating/filamentous MAPK components were sequestered in nuclear foci to prevent an inappropriate transcriptional crosstalk. Surprisingly, these mating/filamentous MAPK foci require Hog1 MAPK signaling, where Hot1-foci form independent of Hog1. Additionally, the mating/filamentous pathway foci are inhibited with pre-treatment of alpha-factor, while Hot1-foci are not. These results suggest that Hot1-foci and mating/filamentous foci are distinct, and further suggests that transcriptionally activate and inactive domains within the nucleus provide an additional mechanism for insulation between the two MAPK pathways.

In Drosophila, assemblies of insulator proteins (BEAF-32, u(Hw), Mod(mdg4)67.2, CP190, and dCTCF) at peripheral sites that are devoid of DAPI-stained chromatin form under conditions of osmotic stress (Schoborg et al., 2013). These insulator bodies are highly dynamic and reversible and, like Hot1-foci, form independent

of Hog1 (p38) MAPK signaling. The authors propose that the removal of insulator proteins from the chromatin allows for the rearrangements of chromatin domains to promote the osmotic transcriptional response. Based on these predictions, I speculate that insulator bodies are distinct from TonEBP nuclear stress bodies in human cells and Hot1-foci observed in yeast. Alternatively, it is possible that these subnuclear bodies are one in the same with insulator proteins potentially functioning to bridge chromatin associations within the Hot1-foci and nuclear stress bodies. Continued research will be required to distinguish between these possibilities.

It is unclear whether *S. cerevisiae* would require such dramatic removal of insulator proteins for the rearrangement of chromatin. Yeast chromatin is highly mobile and behaves as a tethered polymer. Rare restricted movements occur at centromeres and telomeres that are anchored to the nuclear envelope and within DNA localized to the nucleolus (Albert et al., 2013). Overall these dynamics do not change when a global transcriptional program is induced with rapamycin (Albert et al., 2013). However, it is unknown whether insulator proteins in *S. cerevisiae* (RNAPIII, cohesins, Cha4, Rap1, Tbf1, Reb1) are dynamically regulated to allow for movements of telomeres, *HMR/HML* loci, centromeres, telomere clusters, and rDNA (West et al., 2002). It is an interesting possibility that sequestration of insulator proteins may alter the global dynamics of chromatin organization to facilitate stress-activated transcriptional programs.

Exploring frontiers in nuclear structure and function

The field of nuclear cell biology is truly burgeoning. Current studies are transitioning from descriptive accounts of nuclear structure to a deeper understanding of

the functionality of higher order nuclear organization. Technology is leading us in this transition. Chromatin domains and cell specific genome conformations are beginning to be unveiled with DamID and 3C methodologies. Clever use of bacterial operators and transcriptional repressors (LacO-LacI and TetO-TetR) to label specific regions of the genome has allowed us to observe patterns of gene positioning in living cells. In the following section, I have proposed new screening ideas and technologies that I believe will help to drive new discoveries to further uncover nuclear structure-function relationships.

A major advantage for studying basic cellular processes in *Saccharomyces cerevisiae* is the ease of performing genetic screens. A genetic screen to identify the largely uncharacterized mechanisms for gene positioning and interchromosomal interactions would be valuable. I propose a strategy to screen for interchromosomal interactions with a modified split ubiquitin two-hybrid system (Figure 4.3) (Laser et al., 2000). In this system, LacI-C_{ub}–RUra3p and TetR-N_{ub} fusions would be expressed in a strain with corresponding LacO and TetO arrays at two gene loci known to cluster. Under conditions of gene clustering the proximity of the LacI-C_{ub}–RUra3p and TetR-N_{ub} would reconstitute ubiquitin. Cleavage by ubiquitin specific proteases would then result in free RUra3p (R, arginine that signals for degradation by the N-end rule pathway) that is rapidly degraded. Under conditions of interaction, the cells would die on URA and be resistant to 5' FOA. With this method, screening through yeast deletion library and mutant collections for growth on URA and 5' FOA sensitivity could identify novel factors required for clustering.

This modified split ubiquitin two-hybrid would also be a useful system for

monitoring the relationship between stochastic gene positioning and stochastic gene activity at the level of a single cell. Rather then RUra3p, RGFPp could be fused to the LacI-C_{ub}. Low levels of cellular GFP would indicate frequent events of gene clustering, where high levels would indicate few events of gene clustering. Flow cytometry or automated imaging could be used to quantify the results. Coupling this gene-clustering reporter with a fluorescent reporter to measure gene expression would provide single-cell readout for the correlation between gene clustering and gene activity. This system could also be useful for measuring memory of gene clustering events. The Brickner lab has identified an MRS (memory recruitment sequence) in the promoter of *INO1* that is required for prolonged positioning at the nuclear periphery and a faster transcriptional reactivation (Brickner et al., 2012). If gene-clustering events exhibit memory, then the levels of RGFPp will remain low after transcriptional repression. Again these experiments could be coupled to a reporter for gene expression to correlate memory of clustering to transcriptional memory at the level of a single cell.

Nature has provided a molecular toolkit for the nuclear cell biologist, including fluorescent proteins, the LacO-LacI and the MS2-MCP for live cell visualization of DNA and RNA molecules. Recently, breakthrough discoveries have revealed the utility of the bacterial Class II clustered regularly interspaced palindromic repeats (CRISPR) system for site-specific genome editing in eukaryotes. In this system, a ribonucleoprotein complex of a catalytic Cas9 protein and CRISPR guide RNA is directed to complementary DNA sequences within the genome and performs a site-specific cleavage event. Numerous groups have validated the CRISPR/Cas9 system in multiple model organisms including Drosophila, zebrafish, budding yeast, human cells, and mice

Gene clustering → no growth on –URA
5' FOA insensitive
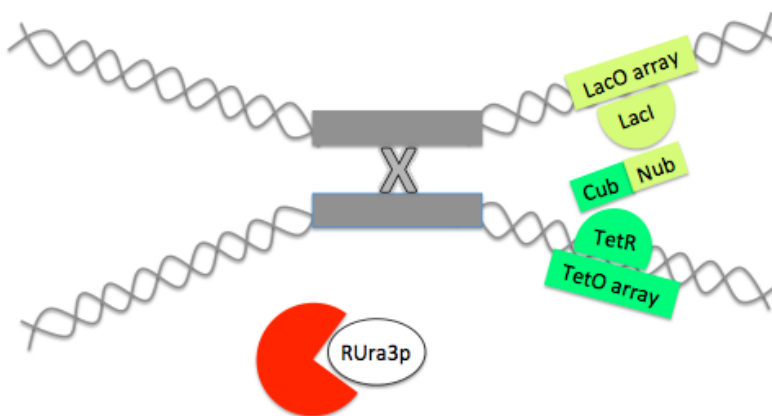
No interaction → growth on –URA
5 'FOA sensitive

FIGURE 4.3. Modified split ubiquitin yeast two-hybrid to screen for gene clustering. In cells where gene-clustering events occur, Cub-Nub interactions result in the degradation of RUra3p, no growth on –URA media and 5' FOA resistances. When gene-clustering factors are absent, the loss Cub-Nub interactions will result in the stabilization of RUra3p, growth on –URA and 5' FOA sensitivity. Alternatively, replacing RUra3p with RGFPp would allow for fluorescence-based readout of gene-clustering events.

(Bassett et al., 2013; DiCarlo et al., 2013; Hwang et al., 2013; Mali et al., 2013; Wang et al., 2013)

Before CRISPR/Cas9, it was nearly impossible to track endogenous genes in metazoan cells and consequently gene-positioning studies were limited to fixed samples using DNA fluorescent in situ hybridization (FISH). Using CRISPR/Cas9 technology I can now endogenously tag metazoan genes with the LacO Arrays. Alternatively, I propose an even simpler 'CRISPR FISH' method for tracking endogenous genes (Figure4.4). Recently, catalytically inactive Cas9 (dCas9) fused to transcriptional activators and repressors was shown to specifically target to endogenous genes and regulate expression (Gilbert et al., 2013). In theory, a GFP-dCas9 fusion and CRISPR guide RNAs can be used to GFP-label specific sequences in the genome. Potentially multiple gene loci could be monitored in one cell using CRISPR/Cas variants that recognize different proto-spacer adjacent motifs (PAMs) (Mojica et al., 2009). CRISPR FISH could also be introduced into an organism to track endogenous gene positioning during development or in different disease models. The dCas9-activator/repressor fusions described above could be used to recruit chromatin-modifying and remodeling enzymes to alter the chromatin context of particular regions in the genome to study the epigenetic inputs of gene positioning. I am only beginning to understand the utility of the CRISPR/Cas9 system, but predict that this technology will revolutionize my methods of studying nuclear structure in metazoans.

Lastly, a remaining frontier in nuclear cell biology is in uncovering the roles for non-coding RNAs (ncRNAs) in regulating the assembly of nuclear bodies and dynamics of gene positioning. In vertebrates, ncRNAs are stable components of nuclear bodies and

have major roles in seeding the assembly of nuclear bodies (Mao et al., 2011b). Artificial tethering the SatIII and NEAT1 ncRNAs to sites within the genome are sufficient for the assembly of nuclear stress bodies and paraspeckles, respectively (Shevtsov and Dundr, 2011). Additionally, X-chromosome inactivation involves the localized spreading of the XSIT ncRNA to neighboring chromatin and the recruitment of silencing complexes (Engreitz et al., 2013). These examples provide a model where the transcription of ncRNAs influence the dynamics and biogenesis of nuclear bodies.

In *S. cerevisiae*, multiple examples of inducible genes are associated with ncRNAs that are transcribed in the antisense direction, from bidirectional promoters or from an upstream promoter (Bumgarner et al., 2009; Martens et al., 2004; Neil et al., 2009; van Werven et al., 2012). Known functions for ncRNAs are in stimulating or repressing transcription of an associated ORF, through processes that alter the local chromatin environment and RNAPII promoter accessibility (Wu et al., 2012). Still there may be remaining functions for ncRNAs in the regulation of yeast nuclear architecture. There is evidence for chromatin loops influencing the transcription of ncRNAs from bi-directional promoters (Tan-Wong et al., 2012). Perhaps ncRNAs with inhibitory effects on gene transcription may prevent the formation of chromatin loops. Additionally, ncRNAs in vertebrates are proposed to act as sponges that bind and localize transcriptional and mRNA processing machinery. I have yet to identify what seeds Hot1-foci formation, but this process could either be activated or antagonized by the presence of a ncRNA. An annotated ncRNA *SUT498* is transcribed antisense to the *STL1* gene (Xu et al., 2009). There may be roles for *SUT498* in the stochastic activation of *STL1* and the localization of *STL1* to Hot1-foci. I predict that the antisense transcription of *SUT498*
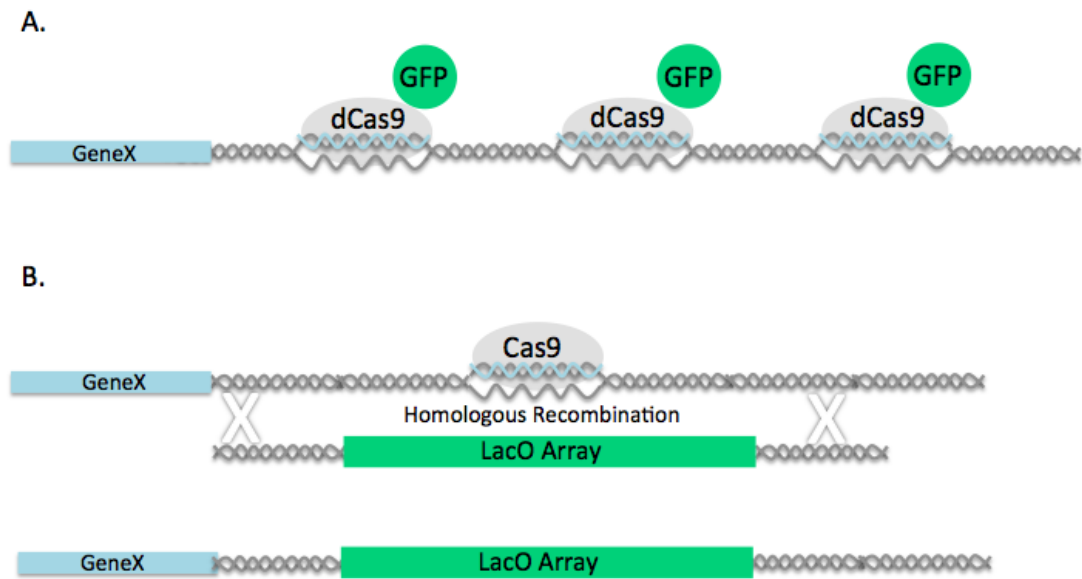
FIGURE 4.4. New CRISPR methods for visualizing gene positioning in metazoans. A. CRISPR FISH method using guide RNAs to target GFP-tagged catalytically dead Cas9 (dCas9) to endogenous genes. B. Genome editing with the CRISPR-Cas9 system to insert LacO arrays in the 3'UTR of endogenous genes.

antagonizes Hot1 binding to the *STL1* promoter and potentially the localization the *STL1* gene locus to Hot1 foci. A similar model has been predicted for the *ICR1* ncRNA regulation of *FLO11* expression in yeast, where transcription of ICR1 inhibits the Flo8 transcription factor from binding to the promoter of *FLO11(Bumgarner et al., 2012)*. Furthermore, I predict that *ck2* mutants will have lower or no expression of *SUT498* due to constitutive localization of *STL1* to Hot1 foci. This could provide a system to investigating the links between ncRNAs, stochastic activity and higher order nuclear structure.

Relating my studies to human disease

Physicians rely heavily on features of nuclear morphology in the diagnosis of several human diseases. Nuclear envelopathies and laminopathies -characterized by abnormal folding and blebbing of the NE- are result from mutations in multiple genes that encode for nuclear lamina-associated proteins (Butin-Israeli et al., 2012; Worman et al., 2010). These mutations result in devastating diseases such as muscular dystrophies, premature aging and increased incidences cancer. Abnormalities in nuclear structures such as enlarged nuclei, irregular nuclear membrane and prominent nucleoli indicate a progression and severity of multiple cancer types, including cervical (pap smear) and breast (nuclear pleomorphism grading scale) (Chow et al., 2012). Reports have even revealed deteriorations in nuclear structure and permeability in the normal aging processes. Though these examples emphasize the importance of nuclear structure in disease, our knowledge of the molecular events that contribute to the progression of these diseases is limited. Throughout my PhD training, I have considered the relevance of my

work in the broader context of human disease. Briefly, I will speculate on how the results of our two studies relate to current research in cancer and autoimmune disease.

The nuclear envelope malformations and disrupted lipid homeostasis observed upon genetic disruption of gene components of the RSC chromatin-remodeling complex resembles the progressive abnormalities in nuclear structure observed in human cancers. Recently, cancer genome sequencing efforts have identified a full spectrum of mutations within components of the human SWI/SNF and highlighted broad requirements for the tumor suppressor functions of SWI/SNF (Kadoch et al., 2013; Shain and Pollack, 2013). The mechanisms of SWI/SNF tumor suppressor activity of SWI/SNF has been linked to roles in chromatin segregation and gene expression (Dykhuizen et al., 2013; Tolstorukov et al., 2013). SWI/SNF has additional roles in homologous recombination and repair of DNA double strand breaks (Seeber et al., 2013). With the pleotropic functions of SWI/SNF, it is difficult to identify whether SWI/SNF plays a direct role in maintaining proper nuclear structure or whether nuclear structure defects are an indirect result of the accumulation of DNA damage, aneuploidy or aberrant gene transcription. Our studies suggest that in *S. cerevisiae rsc* mutants, altered gene expression and lipid homeostasis rapidly results in abnormal nuclear structure. Potentially, the abnormal nuclear structure observed in human cancers with mutations in SWI/SNF may precede or coincide with increasing genomic instability. Further work is necessary to determine the precise tumor suppressor functions of SWI/SNF, and whether abnormal nuclear structure in cancers is tightly correlated with SWI/SNF mutations. This information will possibly hold therapeutic value and result in better outcomes for cancer patients.

In my studies of nuclear organization upon osmotic stress in *S. cerevisiae,* I observed the localization of Hot1 to subnuclear foci. TonEBP/NFAT5, the human transcription factor responsive to osmotic stress, is required for the formation of subnuclear foci termed nuclear stress bodies (Valgardsdottir et al., 2008). TonEBP/NFAT5 induces the transcription of SatIII RNAs from pericentric chromatin and transitions the local heterochromatin to more active acetylated chromatin. The SatIII RNAs are proposed to recruit transcriptional and mRNA processing machinery ultimately resulting in the biogenesis of specialized stress-induced transcription factories (Biamonti and Vourc'h, 2010). Similar to the roles for Hot1-foci, TonEBP nuclear stress bodies may ultimately coordinate a gene expression program that results in the stochastic expression of genes and variable transcriptional responses to promote survival under stressful environmental conditions. Very recently, researchers have implicated high salt diets and the TonEBP/NFAT5 transcription factor in the development of autoimmune diseases (Kleinewietfeld et al., 2013; Wu et al., 2013). In an *in vitro* system that simulated the differentiation of naïve T cells, increasing NaCl concentrations stimulated production of a strong population of T_H17 autoimmune cells (Kleinewietfeld et al., 2013). The mechanisms that contribute to stochastic fate decisions during development are largely unknown, but many predict that subnuclear positioning of genes plays an important role. It is possible that the localization of genes to nuclear stress bodies in naïve T cells may influence the stochastic decisions during the differentiation of subpopulations of helper T cells. Additionally, my identified role for CK2 in Hot1-localization to foci may potentially be conserved in localizing TonEBP/NFAT5 to mammalian nuclear stress bodies. These studies and others can begin to better define the

requirements for nuclear architecture in cell fate decisions, and potentially reveal

additional pathways that can be targeted to treat autoimmune diseases.

Closing

From yeast to man, nuclear organization plays a major role in modulating genome

function. Our studies have described underlying mechanisms regulating genome

organization in *S. cerevisiae*. Surprisingly, I have found that nuclear organization

accounts for differential gene expression in cells with identical genomes. Continuing

studies in the dynamic regulation of nuclear organization will begin to uncover

mechanisms for regulated gene expression in response to environmental stress and

throughout development, and in the misregulation of gene expression in human disease.

TRAFFICKING TO UNCHARTED TERRITORY OF THE NUCLEAR ENVELOPE

The nuclear envelope (NE) in eukaryotic cells serves as the physical barrier between the nucleus and cytoplasm. Until recently, mechanisms for establishing the composition of the inner nuclear membrane (INM) remained uncharted. Current findings uncover multiple pathways for trafficking of integral and peripheral INM proteins. A major route for INM protein transport occurs through the nuclear pore complexes (NPCs) with additional requirements for nuclear localization sequences, transport receptors, and Ran-GTP. Studies also reveal a putative NPC-independent vesicular pathway for NE trafficking. INM perturbations lead to changes in nuclear physiology highlighting the potential human disease impacts of continued NE discoveries.

Introduction

Linking structure to function is a critical goal for understanding the physiological impacts of the nuclear envelope (NE) in eukaryotic cells. At the most basic level, the NE double lipid bilayers provide a physical barrier dividing the cytoplasm and nucleus. The inner nuclear membrane (INM) and outer nuclear membrane (ONM) fuse at discrete sites to form pores that perforate the NE. The structures anchored in these pores, nuclear pore complexes (NPCs), form transport channels for the diffusion of small molecules and the

selective trafficking of macromolecules greater than ~40kDa (Hetzer, 2010; Tetenbaum-Novatt and Rout, 2010). As such, the NE and NPCs are fundamentally responsible for the compartmentalization of the nucleus and cytoplasm and the resulting separation of function.

Beyond serving as a physical barrier with selective transport channels, the NE harbors multiple critical cellular activities. The NE provides a scaffold for the organization of chromatin into selective zones of heterochromatin and euchromatin, and a platform for genomic transcription and repair (Strambio-De-Castillia et al., 2010; Van de Vosse et al., 2011). In addition, the NE bridges cytoskeletal communications to the chromatin for signaling events (Razafsky and Hodzic, 2009) and in yeast the NE anchors the cell division machinery (Ding et al., 1997; Jaspersen and Winey, 2004). These NE functions are inherently dependent on establishing novel INM and ONM protein and lipid compositions.

With the ONM being continuous with the endoplasmic reticulum (ER), mechanisms that set up the ONM composition are considered synonymous with those for the ER. In contrast, the INM harbors a unique protein composition and requires specific trafficking mechanisms (Antonin et al., 2011; Lusk et al., 2007). The proteins of the INM are synthesized in the cytoplasm, the cytoplasmic ER, or the ONM and must then be localized to the INM. For example, the INM is associated with the nuclear lamins, intermediate filament proteins that are translated in the cytoplasm, imported into the nucleus, and assembled into a lamina network at the INM. Lamin functions are topics of intense investigation and extensively reviewed elsewhere (Dechat et al., 2010; Gruenbaum et al., 2005). Importantly, efforts directed towards defining the INM protein

composition estimate as many as ~80 proteins reside at the INM (Schirmer et al., 2003). Common structural domains categorize subsets of INM proteins into proteins families; for example, the LEM, SUN and KASH-domain families (Gruenbaum et al., 2005; Wilson and Foisner, 2010). The LEM-domain family of proteins contributes to chromatin organization, where as the SUN and KASH-domain families together are components of a complex that links the nucleoskeleton to the cytoskeleton (the LINC complex). However, the majority of INM proteins lack functional characterization (Schirmer et al., 2005).

Taken together, the physical complexity of the INM suggests a significant uncharted territory for NE functions and highlights the importance of understanding INM trafficking mechanisms. We summarize here new insights into how INM composition is established and provide a perspective on how proper trafficking and INM composition impacts the NE environment and nuclear shape and size. We further review intriguing links between the INM and viral life cycles that suggest the potential discovery of novel routes to the INM.

Section I: Connections between NPCs and the INM

To date, trafficking of proteins from the cytoplasmic compartment to the INM is thought to occur exclusively through NPCs. Significant work has advanced insights into NPC architecture and transport mechanisms (as reviewed in (Brohawn et al., 2009; Hoelz et al., 2011)). In total, each NPC is comprised of >400 individual nucleoporin (Nup) polypeptides that derive from approximately 30 different types of Nups (Alber et al., 2007). The Nups associate into discrete subcomplexes that are present in 8-fold radial and

bilateral symmetry along the respective central NPC axis and the NE plane (Alber et al., 2007). The resulting structural building blocks include an inner ring, an outer ring, a linker complex, and pore membrane proteins (Poms) as diagramed in Figure 1A. Nearly one third of the Nups share a common unstructured domain with multiple phenylalanine-glycine (FG) repeats separated by characteristic space sequences (Terry and Wente, 2009). These FG domains fill or line the central NPC channel (Alber et al., 2007), coincidentally forming the basis of the NPC permeability barrier and facilitating NPC translocation via direct FG interactions with transport receptors (Bayliss et al., 2002; Iovine et al., 1995; Liu and Stewart, 2005; Radu et al., 1995). On each respective NPC face, asymmetric filamentous structures (cytoplasmic fibrils, nuclear basket) extend from the core structure and harbor functions that help define transport directionality (Brohawn et al., 2009; Tetenbaum-Novatt and Rout, 2010).

The central channel of the NPC is estimated to be ~50 nm in diameter based on cryo-electron tomography experiments (Frenkiel-Krispin et al., 2010). In addition, eight peripheral channels of ~9 nm diameter might exist between the NE and NPC substructures (Baur et al., 2007). These peripheral channels are predicted to structurally accommodate the cytoplasmic domains of integral INM proteins and allow for maintained membrane insertion while integral INM proteins traverse the NPC pore membrane (Figure A.1A).

Paradoxically, there is increasing evidence for roles of INM protein localization in mediating new NPC assembly into an intact NE (as reviewed in (Doucet and Hetzer; Fernandez-Martinez and Rout, 2009)). For example, the integral membrane protein
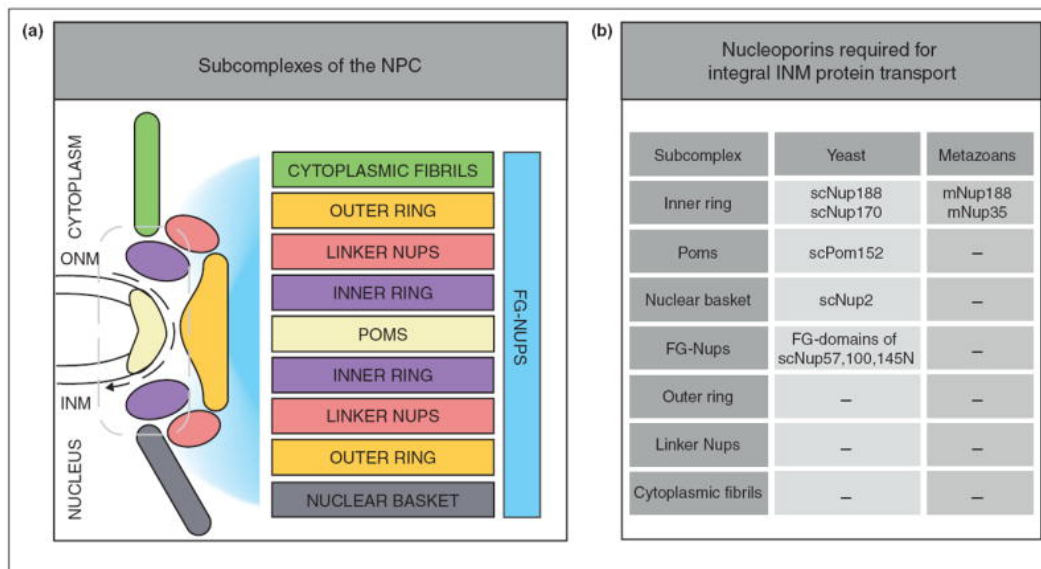
Figure A.1. Subcomplexes of the NPC and requirements for integral INM protein transport. (A) The ~30 Nups of the NPC assemble into subcomplexes which serve as the building blocks of the NPC (Alber et al., 2007). The symmetric subcomplexes include the inner ring (purple), outer ring (yellow), Poms (beige), linker Nups (red) and a central set of FG-Nups (blue). The asymmetric subcomplexes include the cytoplasmic fibrils (green) and nuclear basket (dark gray), which extend into the cytoplasm and nucleus and also harbor FG-Nups. The space between the inner ring subcomplex and Poms represents a putative peripheral channel (gray dashed box) for transit of integral INM proteins (black dashed line). (B) Select proteins of the FG-Nup family (scNup100, scNup57, scNup145N), the inner ring (scNup170, scNup188, mNup53, mNup188), the Poms (scPom152) and the nuclear basket (scNup2) have been implicated in integral INM protein transport (Deng and Hochstrasser, 2006; King et al., 2006; Meinema et al., 2011; Zuleger et al., 2011).

mPom121 is selectively targeted to the INM prior to its localization to the pore

membrane at steady state, and this INM localization step is required for NPC assembly

(Doucet and Hetzer; Mitchell et al., 2010; Shaulov et al., 2011; Talamas and Hetzer;

Yavuz et al.). Other INM proteins impacting NPC assembly are the LEM-domain

proteins in *S. cerevisiae* (sc) scHeh1/Heh2 and the metazoan (m) SUN-domain protein

mSUN1 (Talamas and Hetzer; Yewdell et al.). These INM proteins potentially have roles

in the generation and stabilization of membrane curvature required for INM and ONM

fusion during nuclear pore formation. With these known examples, it is clear that INM

proteins are both trafficked though the NPC and play active roles in NPC assembly,

providing a curious chicken and egg scenario. It is also intriguing to consider that such

coupled dependence for INM protein localization and NPC biogenesis might contribute

to the unknown mechanism by which NPC number per nucleus is determined.

Section II: NPC-dependent trafficking mechanisms for INM proteins

Three basic classes of proteins are selectively targeted to the INM: peripheral

INM proteins anchored through protein-protein interactions, peripheral INM proteins that

associate with the INM outer leaflet via amphipathic helices or post-translational

modifications, and integral INM proteins. For peripheral INM proteins, localization from

the cytoplasm to the nucleus is governed by the same paradigms as that for soluble

nuclear proteins (as reviewed in (Cook et al., 2007; Lusk et al., 2007; Stewart, 2007)),

followed by INM association once in the nucleus (Figure A.2A). These peripheral INM

proteins harbor short amino acid spans termed nuclear localization sequences (NLSs),

which are recognized by nuclear import receptors known as karyopherins (Kaps) or
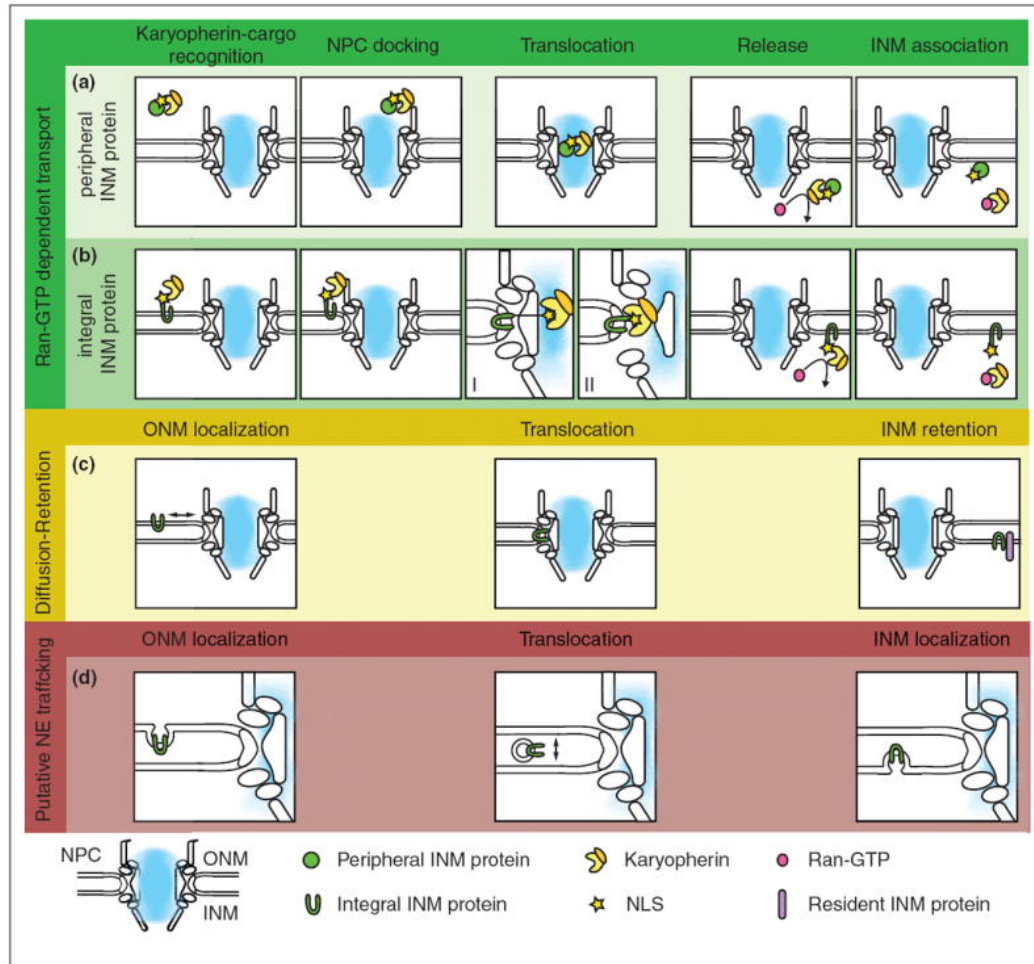
Figure A.2. Pathways for the localization of INM proteins. (A, B) The Ran-GTP dependent pathways for peripheral and integral INM localization require an NLS (yellow star), karyopherins (scKap60/Kap95 or mImp-α/β, yellow/orange caps), Ran-GTP (pink circle), and FG-Nups of the NPC channel (blue region). (A) Peripheral INM proteins are transported similar to soluble proteins; however, after Ran-GTP mediated release, the peripheral INM proteins anchor to the INM through lipid modifications, amphipathic alpha helices, or protein-protein interactions with integral INM proteins. (B) Integral INM proteins remain embedded in the NE throughout translocation. (B-I) The integral INM protein may contain a long intrinsically disordered linker domain allowing for karyopherin transit through the central FG-Nup channel (King et al., 2006; Meinema et al., 2011). (B-II) Alternatively, the karyopherins may translocate with structural remodeling of the NPC needed to accommodate the cargo-karyopherin complex. (C) A diffusion-retention mechanism contributes the localization of peripheral and integral INM proteins through protein-protein interactions with INM proteins (purple) (Gardner et al., 2011; Zuleger et al., 2011). (D) A putative NE trafficking pathway might exist, which utilizes a vesicular trafficking pathway through the NE lumen that is NPC-independent. The illustration represents NE lumenal vesicles as observed during Herpes Simplex Virus nuclear egress (Johnson and Baines, 2011), and potential dynamics of vesicles observed in mutant phenotypes with *S. cerevisiae* (*sc-acc1-1-7*) (Schneiter et al., 1996) and metazoans (m-torsinA and LAP1) (Kim et al., 2010).

128

importins. There are 14 Kap family members in *S. cerevisiae*, and over 20 in metazoan cells (Mosammaparast and Pemberton, 2004), each of which interacts with a distinct NLS or nuclear export sequence (NES) encoded in different cargo (Pemberton and Paschal, 2005).

Kap-mediated mechanisms for import require direct Kap binding both to the cargo NLS and to the FG-Nups (Lee et al., 2005). Kap binding to the FG-Nups mediates docking at the cytoplasmic filaments and translocation through the central NPC channel. Models of the precise mechanism for this FG-dependent Kap movement are reviewed extensively elsewhere (Guttler and Gorlich, 2011; Strambio-De-Castillia et al., 2010; Terry and Wente, 2009). Importantly, directional release of the import cargo in the nucleus is mediated by binding of the small GTPase Ran to the Kap (Moore and Blobel, 1993; Stewart, 2007).

For integral INM proteins, a convergence of efforts has uncovered key molecular targeting requirements. Integral INM proteins are composed of lumenal, transmembrane and cytosolic domains, all of which must be moved from the rough ER/ONM through the pore membrane of the NPCs. Early reports proposed both active and passive transport mechanisms for integral INM proteins (Ohba et al., 2004; Soullam and Worman, 1995). The most comprehensive study to date measured NE dynamics for 15 distinct integral INM proteins using fluorescence-recovery after-photobleaching (FRAP) and photoactivation assays (Zuleger et al.). These mobility-based assays reveal a full range of integral INM protein dynamics supporting distinct mechanisms of integral INM localization. For one class, the integral INM protein dynamics agree with a lateral diffusion-retention mechanism (Figure A.2C), whereas other integral INM proteins

require active transport mechanisms with differential requirements for ATP, Ran GTPase activity (Figure A.2B), and NPC components (Figure A.1B). The ATP-requirement for integral INM protein transport remains less defined with speculations of ER licensing steps and/or ATP-dependent restructuring of the NPC (Braunagel et al., 2007; Ohba et al., 2004). We focus here on recent studies with mechanistic insights for several integral INM protein trafficking pathways.

Ran-GTP dependent integral INM protein transport:

As noted above, Kaps specifically recognize NLSs to mediate import of soluble cargo. Curiously, the majority of integral INM proteins analyzed to date have putative NLSs. In *S. cerevisiae*, NLSs in scHeh1 and scHeh2 facilitate INM localization through scKap60-Kap95 (King et al., 2006) (Figure A.2B). These studies suggest a specific function for scKap60-Kap95 and a distinct pathway for integral INM protein transit (Figure A.2B-I), as other scKap-NLSs pairs did not mediate INM localization of scHeh2 (King et al., 2006). Similarly, mSUN2 contains a NLS that plays a role in import and specifically interacts with the scKap60/Kap95 orthologues, mImp-α/Imp-β (Turgay et al.). Interestingly, the most recent studies of scHeh1 and scHeh2 identified an intrinsically disordered (ID) linker domain between the transmembrane and NLS domains (Meinema et al., 2011). As shown in Figure 2B-II, these long ID linker domains enable the cytosolic NLS domains that are bound to scKap60-Kap95 to span from the pore membrane region to the FG Nups in the central NPC channel (Meinema et al.). Other INM integral membrane proteins contain similar ID regions, suggesting a shared mechanism exists (Meinema et al.). As with soluble protein import, following NPC

130

translocation, directional release of the integral membrane protein at the INM is facilitated by Ran-GTP binding to the Kap (Figure A.2A,B) (Moore and Blobel, 1993; Stewart, 2006).

Diffusion-retention for integral INM protein localization:

An early model for INM trafficking invoked passive diffusion of proteins through the pore membrane and INM retention by binding to nucleoplasmic proteins (Smith and Blobel, 1993; Soullam and Worman, 1995). Substantial support for this mechanism comes from analyses of integral INM proteins that associate with the lamins (Wu et al., 2002; Zuleger et al., 2011). The scMps3, a SUN-domain containing protein, provides additional evidence for selective localization of INM proteins that lack intrinsic active transport mechanisms (Gardner et al.). It is reported that interactions of scMps3 with the histone variant, scH2A.Z, mediate INM targeting. Thus, a soluble nuclear protein with an NLS can effectively piggyback an integral INM protein from the ONM to the INM. It will be important to see if this simple, yet surprising, trafficking mechanism is utilized across species.

Multiple mechanisms within single integral INM proteins:

Single integral INM proteins can require multiple mechanisms for localization, as revealed by studies of SUN family members, mSUN2 and mUNC-84. For mSUN2, targeting requires three distinct domains (Turgay et al.). Two of these domains, the NLS and SUN domain, are sufficient for INM trafficking when transferred to heterologous proteins (Turgay et al.). However, simple single deletion of each domain indicates that

neither alone is necessary (Turgay et al.). Interestingly, the remaining mSUN2 targeting

domain is necessary but not sufficient, and functions in retrograde transport of integral

INM proteins from the Golgi to the ER-NE network (Turgay et al.). This Golgi retrieval

signal is common to many integral INM proteins and could represent the undefined ATP-

dependent INM trafficking class (Braunagel et al., 2007). mUNC-84 also requires

multiple signals for INM trafficking: a NLS, a NE localization signal, and the

transmembrane domain (Tapley et al.). Together, these studies highlight the expanding

diversity of mechanisms for INM transport.

Section III: Links between NPC structure and INM trafficking

Many molecular aspects of integral INM transit remain to be further

characterized. The central FG-Nups likely bind scKap60/Kap95 for integral INM proteins

with long ID linker domains. In support of this, deletion of FG-domains from the Nup57,

Nup100, and Nup145N FG-Nups results in less efficient trafficking of an scHeh1-derived

reporter to the INM (Meinema et al., 2011) (Figure A.2B-I). Additional evidence also

indicates roles for structural NPC regions flanking the NE. The Pom and inner ring Nups

(scPom152, scNup170, scNup188, mNup188 and mNup35) are selectively required in

integral INM protein trafficking (Deng and Hochstrasser, 2006; King et al., 2006;

Theerthagiri et al.; Zuleger et al., 2011) (Figure A.1B). These membrane proximal NPC

subcomplexes are proposed to serve structural roles in forming the peripheral channels

between the pore membrane and the NPC (Figure A.1A) (Antonin et al., 2011; Lusk et

al., 2007). However, it is not clear whether these Pom/Nups are required strictly for their

structural roles or if they also facilitate transport independent of the FG-Nups. Early work

on INM trafficking proposed a size restriction for the cytosolic regions of integral INM proteins with experimentally determined limits of <60-70kDa (Ohba et al., 2004; Soullam and Worman, 1995; Zuleger et al.). This size restriction is potentially linked to the physical restrictions of the proposed peripheral NPC channels. However, with the recent discovery of the role for ID domains, reporters with cytosolic domains as large as 174kDa have been shown to traffic to the INM (Meinema et al., 2011). Continued characterization of endogenous integral INM proteins will be critical in resolving the physiological constraints on this trafficking pathway.

One recent study examined the effects of depleting Nups in the inner ring NPC structure from *Xenopus* nuclear assembly and import assays (Theerthagiri et al., 2010). The absence of mNup188-Nup93 has no apparent effect on the NPC permeability barrier; however, it results in a two-fold increase in import rate for integral INM protein reporters (Theerthagiri et al., 2010). This change in INM trafficking correlates directly with a three-fold increase in the size of the nuclei, whereas NPC assembly and permeability remains unaffected. Intriguingly, nuclei co-depleted of mNup205-Nup93 are similar in size to control nuclei (Theerthagiri et al., 2010). Together, this suggests that mNup188 is a major effector of integral INM protein trafficking in *Xenopus* and potentially in other metazoans. In contrast, in *S. cerevisiae*, removal of an inner ring Nup (scNup188, scNup170) does not accelerate, but rather inhibits transport of the INM proteins scHeh1/scHeh2 and scDoa10 (Deng and Hochstrasser, 2006; King et al., 2006). Moreover, the cells lacking either scNup170 or scNup188 do not result in significant changes in nuclear size or NE expansion (Aitchison et al., 1995; Nehrbass et al., 1996). This species-specific effect on INM trafficking could reflect differences in NPC

component redundancy wherein the *S. cerevisiae* genome harbors paralogues of multiple Nups. Indeed, in the absence of both scNup170 and scNup157 (the scNup170 paralog), NE projections and invaginations of membrane sheets are observed (Makio et al., 2009). The difference could also be due to the distinct experimental approaches, with the yeast experiments only capable of assaying viable genetic deletion mutants versus the *Xenopus* experiment assaying *in vitro* biochemically depleted extracts. Finally, the different physiological consequences on nuclear size and shape could be linked to species-specific differences in INM functions and proteins. For example, *S. cerevisiae* lacks nuclear lamins and INM lamin-associated proteins (Taddei et al., 2004). Overall, structural disturbances of NPC, notably within the inner ring Nup subcomplex, lead to significant alterations in integral INM protein trafficking.

Section IV: Proper INM trafficking requirements in nuclear physiology

As a whole, the cohort of INM proteins act in a number of diverse nuclear functions, many of which have been recently summarized (Egecioglu and Brickner, 2011; Hiraoka and Dernburg, 2009; Mejat and Misteli, 2010; Mekhail and Moazed, 2010; Razafsky and Hodzic, 2009; Santos-Rosa et al., 2005; Towbin et al., 2009; Webster et al., 2010). These roles include transcriptional activation and silencing, chromatin organization, genomic stability and repair, DNA replication, cell division, nuclear positioning, and linkers between cytoskeleton and nucleoskeleton complexes. As such, one would predict that perturbations in INM trafficking have pleiotropic cellular effects.

In addition to the mutually dependent links between the NPC assembly and INM trafficking, there are also inherent connections between NPCs and proper NE lipid

homeostasis and between the NE and chromatin organization. There are well-established roles for INM proteins in lipid homeostasis (Hodge et al., 2010; Santos-Rosa et al., 2005; Scarcelli et al., 2007; Schneiter et al., 1996; Siniossoglou et al., 1998), with altered expression and localization leading affects on nuclear shape and NE integrity. In *S. cerevisiae*, two NE-ER integral membrane proteins, scApq12 and scBrr6, aid in NE membrane homeostasis and fluidity. Cells lacking functional scApq12 and scBrr6 accumulate NE sheets, show disturbances in lipid composition, and are defective in nucleocytoplasmic transport (Hodge et al., 2010). Another INM regulator of lipid biosynthesis is the phosphatidate phosphatase scPah1 (Santos-Rosa et al., 2005). Interestingly, scPah1 INM localization requires the scSpo7/Nem1 activator complex and is mediated through a phosphorylation-regulated amphipathic helix in scPah1 (Karanasios et al.). *S. cerevisiae* cells with mutations in *sc-pah1* or *sc-spo7/nem1* have gross NE expansion (Santos-Rosa et al., 2005). Additionally, nuclear localization of the metazoan orthologue of scPah1, mLipin1, leads to significant impacts on lipid biosynthesis and nuclear shape. When mLipin is localized to the INM, lipid biosynthetic target genes are repressed and the nucleus coincidentally increases in nuclear eccentricity (ratio of horizontal-vertical axes) (Peterson et al.). Therefore, the INM composition includes several protein regulators of lipid biosynthesis and contributes greatly to maintaining NE morphology.

Genetics screens for mutants with NE structural defects (conducted by monitoring the localization of Nups) have identified requirements for nuclear transport (Ran/Kap), RNA metabolism, chromatin structure, secretion, protein degradation, glycosylphosphatidyl inositol (GPI) anchoring, and lipid biosynthesis (Ryan et al., 2003;

Ryan and Wente, 2002b; Ryan et al., 2007; Teixeira et al., 2002; Titus et al., 2010). Some of these mutants might directly compromise localization or expression of INM proteins that regulate lipid biosynthetis (e.g. scApq12, scBrr6, and scPah1) and therefore result in the observed NE mutant phenotypes. For example, loss of function mutants in genes encoding components of the scRSC chromatin-remodeling complex show gross NE structural defects (Titus et al., 2010). These NE defects are rescued by the addition of a membrane fluidizing agent, benzyl alcohol, and upon inhibition of transcription (Titus et al., 2010). Thus, in these RSC mutants, altered transcription of lipid biosynthetic genes or, alternatively, changes in NPC and/or INM protein contacts with chromatin might contribute to the NE phenotype. It has also been shown that *sc-spo7* mutants combined with Golgi trafficking mutants have even more severe defects (Webster et al.). Links between Golgi trafficking and NE expansion suggest that the Golgi/ER network might regulate trafficking to the NE. Further evidence for this connection is the requirement of a Golgi retrieval sequence for mSUN2 INM localization (Turgay et al., 2010). Within these contexts, it is clear that delicate balance of both localization and activity of INM proteins is key in maintaining appropriate nuclear shape, size and function.

Section V: A potential NPC-independent trafficking pathway for the NE

With the analysis of novel INM proteins, new insights into NE trafficking mechanisms have been gained. For soluble protein transport and RNA export, multiple insights have also come from studies of viral life cycles and nucleocytoplasmic dynamics (Cullen, 2003). Interestingly, recent studies of Herpes Simplex Virus (HSV) trafficking suggest that the virus has pirated cellular factors linked to endogenous INM trafficking to

enable its proliferation. Although the NPC channel allows passage of cargo up to ~39nm

in size (Pante and Kann, 2002), the HSV capsid diameter is ~125nm (Zhou et al., 2000).

Thus, HSV gains nuclear access through docking and uncoating at the NPC cytoplasmic

face (Pasdeloup et al., 2009). In contrast, mature capsids exit the nucleus through a

different, non-NPC, mechanism (Johnson and Baines, 2011). The mature capsids are

enveloped into a vesicle from the nuclear face of the INM, and are observed in vesicles in

the NE lumen. The capsids in the vesicles are then de-enveloped through membrane

fusion with the ONM, resulting in release into the cytoplasm. This process is termed

nuclear egress (Johnson and Baines) and requires that HSV capsids initially interface

directly with the INM. To do this, the virus exploits endogenous protein kinase-C (PKC)

and encodes viral Cdc2-like kinases, which together phosphorylate lamins (Hamirally et

al., 2009; Lee et al., 2006). This leads to local disruption of the lamin network at the INM

and allows the capsids to interact with an INM-localized nuclear envelopment complex

composed of viral proteins pUL31 and pUL34 (Yang and Baines, 2011). These two viral

proteins are targeted to the INM, requiring an INM-targeting domain of pUL34 (Roller et

al.). Therefore, understanding the INM localization mechanism for pUL34 will

potentially identify host INM trafficking targets for HSV therapies.

Remarkably, HSV capsid primary envelopment at the INM results in the

appearance of striking membrane vesicles in the NE lumen (Johnson and Baines, 2011).

Such a vesicular trafficking pathway through the NE lumen has not been reported for

endogenous cellular proteins. In this light, it is intriguing to re-examine known *S.

cerevisiae* mutants with defects in NE homeostasis. Indeed, an acetyl coenzyme A

carboxylase mutant, *sc-acc1-7-1,* with altered fatty acid biosynthesis shows aberrant NE

phenotypes (Schneiter et al., 1996). These include accumulation of large NE lumenal

vesicles, expanded NE lumenal space, and cytoplasmic vesicles adjacent to the NE and

NPC (Schneiter et al., 1996). Additionally, mouse models with mutant and knockout

versions of m-torsinA and mLAP1, provide further insight into a potential vesicular

trafficking pathway between the INM and ONM (Kim et al., 2010). The m-torsinA

protein is an AAA+ protein with predicted ATPase activity and resides in the ER-NE

lumen where it is membrane-associated and interacts with the lumenal domain of the

integral INM protein LAP1 (Goodchild and Dauer, 2005). Mice lacking either m-torsinA

or mLAP1 exhibit NE-lumenal vesicles similar to the *sc-acc1-1* mutant. The m-torsinA

knockout mice show neuronal selective phenotypes, whereas LAP1 knockouts show NE-

lumenal vesicles across many different cell types (Kim et al., 2010).

From these observations of NE vesicles in HSV pathogenesis and in yeast and

metazoans mutants, we speculate that an endogenous vesicular trafficking pathway

between the INM to the ONM might exist (Figure A.2D). The vesicles in NE lumen of

the m-torsinA knockouts and the *sc-acc1-7-1* mutant could contain cellular cargo and

vesicular trafficking machinery of such a pathway. This pathway would be independent

of the NPC-dependent pathways shown in Figure 2A-C. Further, the m-torsins and

mLAP1 might cooperate together to mediate NPC-independent vesicular trafficking

between the ONM and INM. In support of this hypothesis, overexpression of m-torsinA

inhibits HSV production and further results in disrupted localization of integral INM

localized pUL34 viral protein from NE to cytoplasmic vesicles (Maric et al., 2011). The

disturbance in pUL34 localization might stem from defective m-torsinA-dependent

trafficking pathway through the NE. Interestingly, the AAA+ protein family includes the

138

NSF ATPase involved in membrane fusion events of the secretory pathway (Hanson and Whiteheart, 2005). Thus, this suggests that the torsin protein family may be the missing piece of the puzzle in understanding the ATP-dependent INM trafficking pathway. Torsin orthologs have not been reported in yeast, though to date the ATP-dependent INM transport has only been described in metazoan systems. Future studies in metazoans and yeast will be important to further resolve this putative INM and ONM vesicular trafficking pathway.

Conclusion

There remain many significant questions to be answered and uncharted NE territory to explore. Importantly, understanding how perturbations in INM trafficking and NE composition result in human diseases are only beginning to be resolved. The reports to date of direct pathophysiology implications for altered NE protein function indicate this is an area ripe for discovery. For example, several recent reviews have documented the clear evidence for devastating human inherited diseases linked to genes encoding lamins and lamin-associated INM proteins (Fridkin et al., 2009; Wilkie and Schirmer, 2006; Worman, 2012). Proteomic characterization of the NE proteome across multiple different cell types (Korfali et al., 2010; Schirmer et al., 2003; Wilkie et al., 2011), paired with continued studies of INM protein targeting and INM protein functions will be needed to contribute to a deeper understanding of the tissue-specific nature of INM disease alleles (Fridkin et al., 2009; Wilkie and Schirmer, 2006; Worman, 2012). Expanded analysis of the INM trafficking mechanisms and INM protein function in model systems (Bank and Gruenbaum, 2011) will further allow a convergence of

temporal and spatial requirements for NE-associated proteins from the single cell level to the context of multicellular organism development, cell differentiation, and tissue morphogenesis.

NUCLEAR "GPS" COORDINATES FOR INTERCHROMOSOMAL CLUSTERING

Regulation of gene expression in response to environmental and developmental cues requires both genetic and epigenetic factors. Brickner *et al.* (2012) now reveal that cis-encoded DNA elements, the Put3 transcription factor and nuclear pore complexes mediate nuclear global positioning of genes. This interchromosomal clustering has important impacts on optimal expression.

As a cell differentiates and undergoes distinguishing gross morphological changes, much more is happening than meets the eye. The organization of DNA within nucleus also changes dramatically. Functionally, nuclear "global" positioning of a particular gene in a cell lineage during development is thought to reflect whether the gene is primed for activation or repression (Schoenfelder et al., 2010). Pinpointing the molecular determinants required will likely benefit therapies for laminopathies, cancers, and other diseases with aberrant nuclear architectures (Misteli, 2010).

Classic studies first revealing that chromosomes were confined to select nuclear regions (Zorn et al., 1979) fueled an interest in whether the information for such precise arrangements was encoded within the DNA itself. It is now clear that additional complexity is layered through epigenetic modifications and cell/tissue-specific protein

---

expression. A frequently observed nuclear arrangement, termed interchromosomal

clustering, suggests that spatial positioning of genes together reflects shared modes of transcriptional regulation (Schoenfelder et al., 2010; Xu and Cook, 2008). Overall, the elaborate mechanisms for establishing such higher order chromatin organization are only beginning to unfold. Excitingly, using the yeast *S. cerevisiae* model, a recent paper reveals both DNA and protein determinants by which genes from different chromosomes are co-clustered to the same region at the nuclear periphery (Brickner et al., 2012).

The yeast *S. cerevisiae* nucleus is a robust model for studying nuclear organization having three distinct subdomains: the nucleoplasm, the nuclear periphery and the nucleolus (Figure B.1A). In a more detailed view (reviewed in (Zimmer and Fabre, 2011), the nuclear periphery can be further broken down into distinct repressive and active zones for gene expression. While centromere and telomere anchoring sites represent repressive DNA or silent regions of the genome, the intervening spaces are occupied with nuclear pore complexes (NPCs) and provide a permissive environment for active gene expression (Figure B.1A). There are several examples wherein inducible genes are positioned in the nucleoplasm when inactive and then are localized to the nuclear periphery coincident with specific environmental conditions for transcriptional activation (reviewed in (Zimmer and Fabre, 2011). This peripheral positioning in *S. cerevisiae* allows for the execution of proper expression patterns in response to changes in nutrient availability and temperature, and for programmed cell morphological changes during the yeast-mating pathway.

The Brickner group previously identified *S. cerevisiae* DNA 'zip codes' that are both necessary and sufficient for positioning of genes within respect to the nuclear
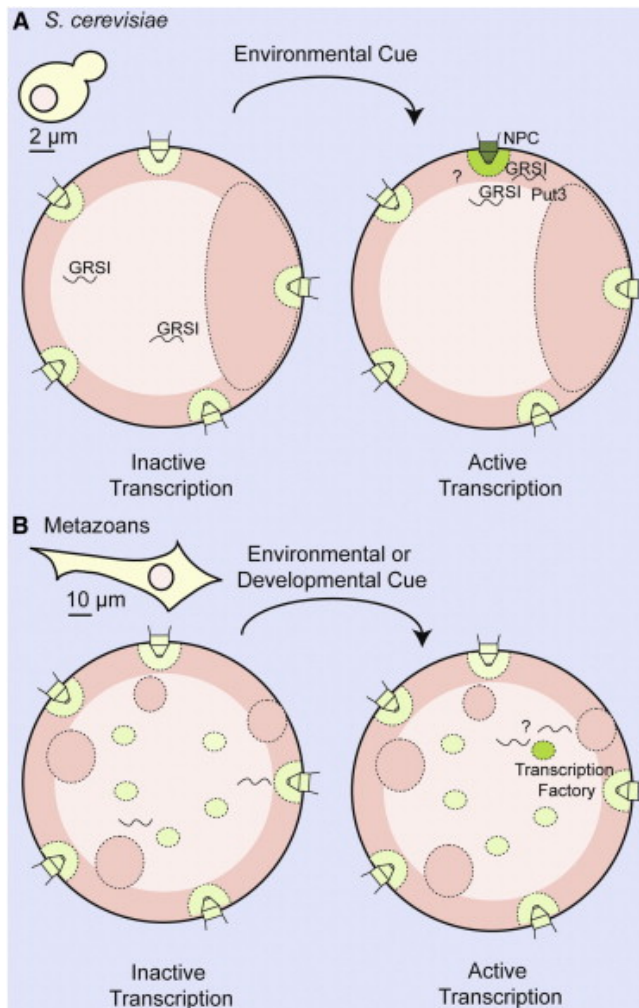
Figure B.1. Interchromosomal clustering to subnuclear regions in *S. cerevisiae* and metazoans. A. In *S. cerevisiae*, the nucleus is composed of a nuclear periphery (red), a nucleolus (red outlined in dashed line) and the nucleoplasm (light red). The nuclear pore complex (NPC) and surrounding local environment is predicted to provide a subdomain permissive for gene expression (light green outlined in dashed line). In this issue of *Developmental Cell*, Brickner et al. (2012) discover that changes in the environment trigger genes with similar GRS elements to cluster together at the nuclear periphery (green outlined in dashed line). The localization mechanism requires the transcription factor Put3 and the nuclear pore complex (NPC) component Nup2. B. Metazoan nuclei have multiple nuclear bodies for specific nuclear functions (reviewed in (Mao et al., 2011b). The nuclear periphery (red) is composed of a heterochromatin and a nuclear lamina meshwork (red) alternating with heterochromatic exclusion zones and NPCs (light green outlined in dashed line). Nuclei can have from 1-4 nucleoli (red outlined in dashed line). In metazoans, nuclear rearrangements occur in response environmental and developmental cues, wherein genes colocalize to specialized transcription factories (green outlined in dashed line). The molecular determinants in each system remain to be fully elucidated (as indicated by ? symbol). Note: drawing is not scaled. *S. cerevisiae* and metazoan cells with approximate nuclear diameters are indicated.

143

periphery (Light et al., 2010). These zip codes are cis-encoded DNA elements found within promoter regions of inducible genes. With two well-defined zip codes, termed gene recruitment sequences (GRSI and GRSII), the *INO1* gene locus becomes enriched at the nuclear periphery under activating conditions of inositol starvation. Interactions with specific components of the NPC are also necessary for this GRS-mediated peripheral localization and optimal *INO1* transcriptional induction (Light et al., 2010).

To further investigate the mechanism for *INO1* gene positioning, these new studies began by using clever genetic tools and comparisons to other GRS-containing genes (Brickner et al., 2012). Strikingly, *INO1* and *TSA2* both contain GRSI and cluster to an overlapping region in the nuclear periphery. However, *INO1* and *HSP104* that contain distinct GRSI and GRSIII elements do not. Thus, shared GRS sequences mediate interchromosomal clustering being both necessary and sufficient. Furthermore, they find that peripheral targeting via NPCs is a critical step prior to interchromosomal clustering.

Can these well-described principles of subnuclear organization in *S. cerevisiae* be applied to metazoans? Given the unique aspects of metazoan nuclear architecture (Figure 1B) (Mao et al., 2011), caution is certainly needed in proposing conserved cross-species mechanisms. However, unraveling the machinery for positioning genes to the periphery in *S. cerevisiae* will uncover potential mechanisms for positioning genes to active sites of transcription (i.e. transcription factories) in metazoan nuclei (Shoenfelder et al., 2010; Xu and Cook, 2008). One might predict that metazoan transcription factories are not random assemblies of active genes, but rather result from unique associations of genes with common DNA zip codes. Further, in response to developmental and environmental cues,

144

DNA zip codes might help define a metazoan subnuclear organization that supports a tailored or robust transcriptional program.

Brickner et al. (2012) further extend their work to tackle a more difficult task of identifying trans-protein determinants with GRSI-binding affinity. They speculate that if a protein factor has binding affinity for the GRSI sequence, then it could directly contribute to peripheral targeting and interchromosomal clustering. Their DNA affinity purification scheme, followed by mass spectrometry identified several candidate GRSI binding proteins. Follow up genetic experiments honed in on Put3, a member of the Zn_2-Cys_6 zinc finger transcription factor family. Interestingly, Put3 is involved in regulating the transcription of genes with UAS_{PUT} elements. As the UAS_{PUT} is unrelated to the GRSI sequence, this suggests potential dual functions for Put3 at promoters. Their *in vivo* studies confirm Put3 is necessary for GRSI-mediated peripheral targeting and interchromosomal clustering. Functionally, Put3 is also required for NPC-interactions and optimal expression of the *INO1* gene. Overall, these are important steps in defining the precise protein machinery at work.

Taken together with studies by others, an overall paradigm is emerging for gene positioning machinery (or a nuclear global positioning system ('GPS')). Two critical observations are that both NPC components and specialized transcription factors are necessary for the positioning of distinct DNA zip codes to restricted *S. cerevisiae* nuclear subdomains. This corresponds directly with studies of Klf1 in erythroid cells (Schoenfelder et al., 2010). The transcription factor, Klf1, plays a similar role to Put3 and influences the localization of coregulated genes to the distinct transcription factories. Interestingly, during development in *C. elegans*, tissue-specific promoters localize to the

nucleoplasm coincident with transcriptional activation (Meister et al., 2010). In light of the recent findings, it will be important to determine whether tissue-specific promoters contain DNA zip codes and are clustered to subdomains for gene expression regulation by shared factors. Evidence in metazoans also points to potential conserved roles for the NPC proteins in interchromosomal clustering. This includes proper expression in response to environmental cues in *Drosophila* and during development in differentiating myoblasts (Capelson et al., 2010; D'Angelo et al., 2012).

The environmentally cued gene expression pathways in *S. cerevisiae* will be excellent systems to pair single-cell based microscopy approaches and population-based genome-wide association analysis, namely the 3C derivatives (Hakim and Misteli, 2012). These strategies and others can begin to answer remaining questions in the field. Do different environmental responses require distinct interchromosomal clustering events? In this manner, each response might involve distinct transcription factors. It is also unclear whether gene localization to nuclear subdomains is established through active localization machinery or through a passive mechanism of retention. Do NPCs provide a local environment that is permissive for gene expression or a nuclear "GPS" coordinate for interchromosomal clustering? If so, Put3 might be part of a tethering scaffold between NPC components and GRSI-containing genes. Given that the localization occurs in response to environmental cues, it is tempting to speculate that Put3 dual functions are modulated through signaling-dependent changes. Ongoing studies will further discern how the non-randomness of gene clustering is linked to functional specificity. Ultimately, testing these principles in additional developmental systems and disease models will expand our understandings of context specific genome architectures.

Table C.1. Plasmids

Plasmid	Encoded gene	Source
pSW3478	pRS316:*POM152*	Unpublished
pSW3616	pRS424:*pom34ΔC*	Unpublished
pSW3617	pRS424:*pom34ΔN*	Unpublished
pSW3628	pYEX-BS:*NUP53-mCherry*	Unpublished
pSW3632	pRS306:*CTT1-3'UTR:LacO128*	Chapter 3
pSW3633	pRS306:*STL1-3'UTR:LacO128*	Chapter 3
pSW3972	pRS306:*HXT1-3'UTR:LacI128*	Unpublished
pSW3717	*tdTomato:HYGB* for C-term tagging endogenous	Unpublished
pSW3767	pRS415:*mCherry* for C-term tagging plasmid	Unpublished
pSW3768	*SPINACH:spHIS5* for 3'UTR tagging endogenous	Unpublished
pSW3837	pRS316:*GPD:NUP1-3xHA*	Unpublished
pSW3838	pRS316*:GPD:nup1-8-3xHA*	Unpublished
pSW3839	pRS316:*GPD:nup1-15-3xHA*	Unpublished
pSW3840	pRS316:*GPD:nup1-21-3xHA*	Unpublished
pSW3846	pRS316:*GPD:NUP1-GFP*	Unpublished
pSW3849	pRS316:*GPD:CCR4-GFP*	Unpublished
pSW3850	pRS426:*GAL:SSK2ΔN-HA*	Chapter 3
pSW3883	pGEX-5-3*:GST-HOT1*	Chapter 3
pSW3884	pRS415:*HOT1-GFP*	Unpublished
pSW3885	pRS415:*hot1-A-GFP*	Unpublished
pSW3886	pRS415:*hot11-D-GFP*	Unpublished
pSW3887	pRS415:*hot1-AA-GFP*	Unpublished
pSW3888	pRS415:*hot11-DD-GFP*	Unpublished
pSW3889	pRS415:*hot1-3A-GFP*	Chapter 3
pSW3890	pRS415:*hot1-3D-GFP*	Unpublished
pSW3899	pRS416:HOT1-GFP	Unpublished
pSW3917	pGEX-5-3:*GST-hot1-3A*	Chapter 3
pSW3928	pRS306:*HIS3:mCherry-LacI*	Unpublished
pSW3929	pRS415:*HIS3:mCherry-LacI*	Unpublished
pSW3948	pRS425:*HIS3:mCherry-LacI*	Chapter 3

REFERENCES

Ahmed, S., Brickner, D.G., Light, W.H., Cajigas, I., McDonough, M., Froyshteter, A.B., Volpe, T., and Brickner, J.H. (2010). DNA zip codes control an ancient mechanism for gene targeting to the nuclear periphery. Nat Cell Biol *12*, 111-118.

Aitchison, J.D., Rout, M.P., Marelli, M., Blobel, G., and Wozniak, R.W. (1995). Two novel related yeast nucleoporins Nup170p and Nup157p: complementation with the vertebrate homologue Nup155p and functional interactions with the yeast nuclear pore-membrane protein Pom152p. J Cell Biol *131*, 1133-1148.

Alber, F., Dokudovskaya, S., Veenhoff, L.M., Zhang, W., Kipper, J., Devos, D., Suprapto, A., Karni-Schmidt, O., Williams, R., Chait, B.T.*, et al.* (2007). The molecular architecture of the nuclear pore complex. Nature *450*, 695-701.

Albert, B., Mathon, J., Shukla, A., Saad, H., Normand, C., Leger-Silvestre, I., Villa, D., Kamgoue, A., Mozziconacci, J., Wong, H.*, et al.* (2013). Systematic characterization of the conformation and dynamics of budding yeast chromosome XII. J Cell Biol *202*, 201-210.

Albuquerque, C.P., Smolka, M.B., Payne, S.H., Bafna, V., Eng, J., and Zhou, H. (2008). A multidimensional chromatography technology for in-depth phosphoproteome analysis. Mol Cell Proteomics *7*, 1389-1396.

Alepuz, P.M., de Nadal, E., Zapater, M., Ammerer, G., and Posas, F. (2003). Osmostress-induced transcription by Hot1 depends on a Hog1-mediated recruitment of the RNA Pol II. EMBO J *22*, 2433-2442.

Alepuz, P.M., Jovanovic, A., Reiser, V., and Ammerer, G. (2001). Stress-induced map kinase Hog1 is part of transcription activation complexes. Mol Cell *7*, 767-777.

Anderson, D.J., and Hetzer, M.W. (2008). Reshaping of the endoplasmic reticulum limits the rate for nuclear envelope formation. J Cell Biol *182*, 911-924.

Andrulis, E.D., Neiman, A.M., Zappulla, D.C., and Sternglanz, R. (1998). Perinuclear localization of chromatin facilitates transcriptional silencing. Nature *394*, 592-595.

Angus-Hill, M.L., Schlichter, A., Roberts, D., Erdjument-Bromage, H., Tempst, P., and Cairns, B.R. (2001). A Rsc3/Rsc30 zinc cluster dimer reveals novel roles for the chromatin remodeler RSC in gene expression and cell cycle control. Mol Cell *7*, 741-751.

Antonin, W., Franz, C., Haselmann, U., Antony, C., and Mattaj, I.W. (2005). The integral membrane nucleoporin pom121 functionally links nuclear pore complex assembly and nuclear envelope formation. Mol Cell *17*, 83-92.

Antonin, W., Ungricht, R., and Kutay, U. (2011). Traversing the NPC along the pore membrane: targeting of membrane proteins to the INM. Nucleus *2*, 87-91.

Badis, G., Chan, E.T., van Bakel, H., Pena-Castillo, L., Tillo, D., Tsui, K., Carlson, C.D., Gossett, A.J., Hasinoff, M.J., Warren, C.L., *et al.* (2008). A library of yeast transcription factor motifs reveals a widespread function for Rsc3 in targeting nucleosome exclusion at promoters. Mol Cell *32*, 878-887.

Baetz, K.K., Krogan, N.J., Emili, A., Greenblatt, J., and Hieter, P. (2004). The ctf13-30/CTF13 genomic haploinsufficiency modifier screen identifies the yeast chromatin remodeling complex RSC, which is required for the establishment of sister chromatid cohesion. Mol Cell Biol *24*, 1232-1244.

Bank, E.M., and Gruenbaum, Y. (2011). Caenorhabditis elegans as a model system for studying the nuclear lamina and laminopathic diseases. Nucleus *2*, 350-357.

Bassett, A.R., Tibbit, C., Ponting, C.P., and Liu, J.L. (2013). Highly Efficient Targeted Mutagenesis of Drosophila with the CRISPR/Cas9 System. Cell Rep *4*, 220-228.

Baur, T., Ramadan, K., Schlundt, A., Kartenbeck, J., and Meyer, H.H. (2007). NSF- and SNARE-mediated membrane fusion is required for nuclear envelope formation and completion of nuclear pore complex assembly in Xenopus laevis egg extracts. J Cell Sci *120*, 2895-2903.

Bayliss, R., Littlewood, T., Strawn, L.A., Wente, S.R., and Stewart, M. (2002). GLFG and FxFG nucleoporins bind to overlapping sites on importin-beta. J Biol Chem *277*, 50597-50606.

Beck, M., Forster, F., Ecke, M., Plitzko, J.M., Melchior, F., Gerisch, G., Baumeister, W., and Medalia, O. (2004). Nuclear pore complex structure and dynamics revealed by cryoelectron tomography. Science *306*, 1387-1390.

Berger, A.B., Cabal, G.G., Fabre, E., Duong, T., Buc, H., Nehrbass, U., Olivo-Marin, J.C., Gadal, O., and Zimmer, C. (2008). High-resolution statistical mapping reveals gene territories in live yeast. Nat Methods *5*, 1031-1037.

Biamonti, G., and Vourc'h, C. (2010). Nuclear stress bodies. Cold Spring Harb Perspect Biol *2*, a000695.

Bidwai, A.P., Reed, J.C., and Glover, C.V. (1995). Cloning and disruption of CKB1, the gene encoding the 38-kDa beta subunit of Saccharomyces cerevisiae casein kinase II (CKII). Deletion of CKII regulatory subunits elicits a salt-sensitive phenotype. J Biol Chem *270*, 10395-10404.

Bogerd, A.M., Hoffman, J.A., Amberg, D.C., Fink, G.R., and Davis, L.I. (1994). nup1 mutants exhibit pleiotropic defects in nuclear pore complex function. J Cell Biol *127*, 319-332.

Bolger, T.A., Folkmann, A.W., Tran, E.J., and Wente, S.R. (2008). The mRNA export factor Gle1 and inositol hexakisphosphate regulate distinct stages of translation. Cell *134*, 624-633.

Braunagel, S.C., Williamson, S.T., Ding, Q., Wu, X., and Summers, M.D. (2007). Early sorting of inner nuclear membrane proteins is conserved. Proc Natl Acad Sci U S A *104*, 9307-9312.

Brianna Caddle, L., Grant, J.L., Szatkiewicz, J., van Hase, J., Shirley, B.J., Bewersdorf, J., Cremer, C., Arneodo, A., Khalil, A., and Mills, K.D. (2007). Chromosome neighborhood composition determines translocation outcomes after exposure to high-dose radiation in primary cells. Chromosome Res *15*, 1061-1073.

Brickner, D.G., Ahmed, S., Meldi, L., Thompson, A., Light, W., Young, M., Hickman, T.L., Chu, F., Fabre, E., and Brickner, J.H. (2012). Transcription factor binding to a DNA zip code controls interchromosomal clustering at the nuclear periphery. Dev Cell *22*, 1234-1246.

Brickner, D.G., and Brickner, J.H. (2010). Cdk phosphorylation of a nucleoporin controls localization of active genes through the cell cycle. Mol Biol Cell *21*, 3421-3432.

Brickner, D.G., Cajigas, I., Fondufe-Mittendorf, Y., Ahmed, S., Lee, P.C., Widom, J., and Brickner, J.H. (2007). H2A.Z-mediated localization of genes at the nuclear periphery confers epigenetic memory of previous transcriptional state. PLoS Biol *5*, e81.

Brickner, D.G., Light, W., and Brickner, J.H. (2010). Quantitative localization of chromosomal loci by immunofluorescence. Methods Enzymol *470*, 569-580.

Brickner, J.H., and Walter, P. (2004). Gene recruitment of the activated INO1 locus to the nuclear membrane. PLoS Biol *2*, e342.

Brohawn, S.G., Leksa, N.C., Spear, E.D., Rajashankar, K.R., and Schwartz, T.U. (2008). Structural evidence for common ancestry of the nuclear pore complex and vesicle coats. Science *322*, 1369-1373.

Brohawn, S.G., Partridge, J.R., Whittle, J.R., and Schwartz, T.U. (2009). The nuclear pore complex has entered the atomic age. Structure *17*, 1156-1168.

Brown, C.R., and Silver, P.A. (2007). Transcriptional regulation at the nuclear pore complex. Curr Opin Genet Dev *17*, 100-106.

Bucci, M., and Wente, S.R. (1998). A novel fluorescence-based genetic strategy identifies mutants of *Saccharomyces cerevisiae* defective for nuclear pore complex assembly. Mol Biol Cell *9*, 2439-2461.

Bumgarner, S.L., Dowell, R.D., Grisafi, P., Gifford, D.K., and Fink, G.R. (2009). Toggle involving cis-interfering noncoding RNAs controls variegated gene expression in yeast. Proc Natl Acad Sci U S A *106*, 18321-18326.

Bumgarner, S.L., Neuert, G., Voight, B.F., Symbor-Nagrabska, A., Grisafi, P., van Oudenaarden, A., and Fink, G.R. (2012). Single-cell analysis reveals that noncoding RNAs contribute to clonal heterogeneity by modulating transcription factor recruitment. Mol Cell *45*, 470-482.

Burns, L.T., and Wente, S.R. (2012a). Nuclear GPS for interchromosomal clustering. Dev Cell *22*, 1119-1120.

Burns, L.T., and Wente, S.R. (2012b). Trafficking to uncharted territory of the nuclear envelope. Curr Opin Cell Biol *24*, 341-349.

Butin-Israeli, V., Adam, S.A., Goldman, A.E., and Goldman, R.D. (2012). Nuclear lamin functions and disease. Trends Genet *28*, 464-471.

Bystricky, K., Laroche, T., van Houwe, G., Blaszczyk, M., and Gasser, S.M. (2005). Chromosome looping in yeast: telomere pairing and coordinated movement reflect anchoring efficiency and territorial organization. J Cell Biol *168*, 375-387.

Cabal, G.G., Genovesio, A., Rodriguez-Navarro, S., Zimmer, C., Gadal, O., Lesne, A., Buc, H., Feuerbach-Fournier, F., Olivo-Marin, J.C., Hurt, E.C., *et al.* (2006). SAGA interacting factors confine sub-diffusion of transcribed genes to the nuclear envelope. Nature *441*, 770-773.

Cairns, B.R., Lorch, Y., Li, Y., Zhang, M., Lacomis, L., Erdjument-Bromage, H., Tempst, P., Du, J., Laurent, B., and Kornberg, R.D. (1996). RSC, an essential, abundant chromatin-remodeling complex. Cell *87*, 1249-1260.

Campbell, J.L., Lorenz, A., Witkin, K.L., Hays, T., Loidl, J., and Cohen-Fix, O. (2006). Yeast nuclear envelope subdomains with distinct abilities to resist membrane expansion. Mol Biol Cell *17*, 1768-1778.

Capaldi, A.P., Kaplan, T., Liu, Y., Habib, N., Regev, A., Friedman, N., and O'Shea, E.K. (2008). Structure and function of a transcriptional network activated by the MAPK Hog1. Nat Genet *40*, 1300-1306.

Capelson, M., and Hetzer, M.W. (2009). The role of nuclear pores in gene regulation, development and disease. EMBO Rep *10*, 697-705.

Capelson, M., Liang, Y., Schulte, R., Mair, W., Wagner, U., and Hetzer, M.W. (2010). Chromatin-bound nuclear pore components regulate gene expression in higher eukaryotes. Cell *140*, 372-383.

Carmody, S.R., Tran, E.J., Apponi, L.H., Corbett, A.H., and Wente, S.R. (2010). The mitogen-activated protein kinase Slt2 regulates nuclear retention of non-heat shock mRNAs during heat shock-induced stress. Mol Cell Biol *30*, 5168-5179.

Casolari, J.M., Brown, C.R., Komili, S., West, J., Hieronymus, H., and Silver, P.A. (2004). Genome-wide localization of the nuclear transport machinery couples transcriptional status and nuclear organization. Cell *117*, 427-439.

Chai, B., Hsu, J.M., Du, J., and Laurent, B.C. (2002). Yeast RSC function is required for organization of the cellular cytoskeleton via an alternative PKC1 pathway. Genetics *161*, 575-584.

Chai, B., Huang, J., Cairns, B.R., and Laurent, B.C. (2005). Distinct roles for the RSC and Swi/Snf ATP-dependent chromatin remodelers in DNA double-strand break repair. Genes Dev *19*, 1656-1661.

Chow, K.H., Factor, R.E., and Ullman, K.S. (2012). The nuclear envelope environment and its cancer connections. Nat Rev Cancer *12*, 196-209.

Cisse, II, Izeddin, I., Causse, S.Z., Boudarene, L., Senecal, A., Muresan, L., Dugast-Darzacq, C., Hajj, B., Dahan, M., and Darzacq, X. (2013). Real-Time Dynamics of RNA Polymerase II Clustering in Live Human Cells. Science.

Clapier, C.R., and Cairns, B.R. (2009). The biology of chromatin remodeling complexes. Annu Rev Biochem *78*, 273-304.

Colley, C.M., and Metcalfe, J.C. (1972). The localisation of small molecules in lipid bilayers. FEBS Lett *24*, 241-246.

Cook, A., Bono, F., Jinek, M., and Conti, E. (2007). Structural biology of nucleocytoplasmic transport. Annu Rev Biochem *76*, 647-671.

Cook, K.E., and O'Shea, E.K. (2012). Hog1 controls global reallocation of RNA Pol II upon osmotic shock in *Saccharomyces cerevisiae*. G3 (Bethesda) *2*, 1129-1136.

Cremer, T., and Cremer, M. (2010). Chromosome territories. Cold Spring Harb Perspect Biol *2*, a003889.

Cremer, T., Lichter, P., Borden, J., Ward, D.C., and Manuelidis, L. (1988). Detection of chromosome aberrations in metaphase and interphase tumor cells by in situ hybridization using chromosome-specific library probes. Hum Genet *80*, 235-246.

Cronshaw, J.M., Krutchinsky, A.N., Zhang, W., Chait, B.T., and Matunis, M.J. (2002). Proteomic analysis of the mammalian nuclear pore complex. J Cell Biol *158*, 915-927.

Cullen, B.R. (2003). Nuclear mRNA export: insights from virology. Trends Biochem Sci *28*, 419-424.

D'Angelo, M.A., Anderson, D.J., Richard, E., and Hetzer, M.W. (2006). Nuclear pores form de novo from both sides of the nuclear envelope. Science *312*, 440-443.

D'Angelo, M.A., Gomez-Cavazos, J.S., Mei, A., Lackner, D.H., and Hetzer, M.W. (2012). A change in nuclear pore complex composition regulates cell differentiation. Dev Cell *22*, 446-458.

Damelin, M., Simon, I., Moy, T.I., Wilson, B., Komili, S., Tempst, P., Roth, F.P., Young, R.A., Cairns, B.R., and Silver, P.A. (2002). The genome-wide localization of Rsc9, a component of the RSC chromatin-remodeling complex, changes in response to stress. Mol Cell *9*, 563-573.

Dawson, T.R., Lazarus, M.D., Hetzer, M.W., and Wente, S.R. (2009). ER membrane-bending proteins are necessary for de novo nuclear pore formation. J Cell Biol *184*, 659-675.

de Bruyn Kops, A., and Guthrie, C. (2001). An essential nuclear envelope integral membrane protein, Brr6p, required for nuclear transport. EMBO J *20*, 4183-4193.

De Craene, J.O., Coleman, J., Estrada de Martin, P., Pypaert, M., Anderson, S., Yates, J.R., 3rd, Ferro-Novick, S., and Novick, P. (2006). Rtn1p is involved in structuring the cortical endoplasmic reticulum. Mol Biol Cell *17*, 3009-3020.

de Nadal, E., Ammerer, G., and Posas, F. (2011). Controlling gene expression in response to stress. Nat Rev Genet *12*, 833-845.

de Nadal, E., Calero, F., Ramos, J., and Arino, J. (1999). Biochemical and genetic analyses of the role of yeast casein kinase 2 in salt tolerance. J Bacteriol *181*, 6456-6462.

de Nadal, E., and Posas, F. (2010). Multilayered control of gene expression by stress-activated protein kinases. EMBO J *29*, 4-13.

Debler, E.W., Ma, Y., Seo, H.S., Hsia, K.C., Noriega, T.R., Blobel, G., and Hoelz, A. (2008). A fence-like coat for the nuclear pore membrane. Mol Cell *32*, 815-826.

Dechat, T., Adam, S.A., Taimen, P., Shimi, T., and Goldman, R.D. (2010). Nuclear lamins. Cold Spring Harb Perspect Biol *2*, a000547.

Dekker, J., Rippe, K., Dekker, M., and Kleckner, N. (2002). Capturing chromosome conformation. Science *295*, 1306-1311.

Denegri, M., Moralli, D., Rocchi, M., Biggiogera, M., Raimondi, E., Cobianchi, F., De Carli, L., Riva, S., and Biamonti, G. (2002). Human chromosomes 9, 12, and 15 contain the nucleation sites of stress-induced nuclear bodies. Mol Biol Cell *13*, 2069-2079.

Deng, M., and Hochstrasser, M. (2006). Spatially regulated ubiquitin ligation by an ER/nuclear membrane ligase. Nature *443*, 827-831.

Devos, D., Dokudovskaya, S., Williams, R., Alber, F., Eswar, N., Chait, B.T., Rout, M.P., and Sali, A. (2006). Simple fold composition and modular architecture of the nuclear pore complex. Proc Natl Acad Sci U S A *103*, 2172-2177.

DiCarlo, J.E., Norville, J.E., Mali, P., Rios, X., Aach, J., and Church, G.M. (2013). Genome engineering in *Saccharomyces cerevisiae* using CRISPR-Cas systems. Nucleic Acids Res *41*, 4336-4343.

Dieppois, G., Iglesias, N., and Stutz, F. (2006). Cotranscriptional recruitment to the mRNA export receptor Mex67p contributes to nuclear pore anchoring of activated genes. Mol Cell Biol *26*, 7858-7870.

Dilworth, D.J., Tackett, A.J., Rogers, R.S., Yi, E.C., Christmas, R.H., Smith, J.J., Siegel, A.F., Chait, B.T., Wozniak, R.W., and Aitchison, J.D. (2005). The mobile nucleoporin Nup2p and chromatin-bound Prp20p function in endogenous NPC-mediated transcriptional control. J Cell Biol *171*, 955-965.

Ding, R., West, R.R., Morphew, D.M., Oakley, B.R., and McIntosh, J.R. (1997). The spindle pole body of Schizosaccharomyces pombe enters and leaves the nuclear envelope as the cell cycle proceeds. Mol Biol Cell *8*, 1461-1479.

Dixon, J.R., Selvaraj, S., Yue, F., Kim, A., Li, Y., Shen, Y., Hu, M., Liu, J.S., and Ren, B. (2012). Topological domains in mammalian genomes identified by analysis of chromatin interactions. Nature *485*, 376-380.

Doucet, C.M., and Hetzer, M.W. (2010). Nuclear pore biogenesis into an intact nuclear envelope. Chromosoma *119*, 469-477.

Doye, V., Wepf, R., and Hurt, E.C. (1994). A novel nuclear pore protein Nup133p with distinct roles in poly(A)+ RNA transport and nuclear pore distribution. EMBO J *13*, 6062-6075.

Drin, G., Casella, J.F., Gautier, R., Boehmer, T., Schwartz, T.U., and Antonny, B. (2007). A general amphipathic alpha-helical motif for sensing membrane curvature. Nat Struct Mol Biol *14*, 138-146.

Du, J., Nasir, I., Benton, B.K., Kladde, M.P., and Laurent, B.C. (1998). Sth1p, a *Saccharomyces cerevisiae* Snf2p/Swi2p homolog, is an essential ATPase in RSC and

differs from Snf/Swi in its interactions with histones and chromatin-associated proteins. Genetics *150*, 987-1005.

Duan, Z., Andronescu, M., Schutz, K., McIlwain, S., Kim, Y.J., Lee, C., Shendure, J., Fields, S., Blau, C.A., and Noble, W.S. (2010). A three-dimensional model of the yeast genome. Nature *465*, 363-367.

Dundr, M., and Misteli, T. (2010). Biogenesis of nuclear bodies. Cold Spring Harb Perspect Biol *2*, a000711.

Dunham, I., Kundaje, A., Aldred, S.F., Collins, P.J., Davis, C.A., Doyle, F., Epstein, C.B., Frietze, S., Harrow, J., Kaul, R.*, et al.* (2012). An integrated encyclopedia of DNA elements in the human genome. Nature *489*, 57-74.

Dykhuizen, E.C., Hargreaves, D.C., Miller, E.L., Cui, K., Korshunov, A., Kool, M., Pfister, S., Cho, Y.J., Zhao, K., and Crabtree, G.R. (2013). BAF complexes facilitate decatenation of DNA by topoisomerase IIalpha. Nature *497*, 624-627.

Edelman, L.B., and Fraser, P. (2012). Transcription factories: genetic programming in three dimensions. Curr Opin Genet Dev *22*, 110-114.

Egecioglu, D., and Brickner, J.H. (2011). Gene positioning and expression. Curr Opin Cell Biol *23*, 338-345.

Engreitz, J.M., Pandya-Jones, A., McDonel, P., Shishkin, A., Sirokman, K., Surka, C., Kadri, S., Xing, J., Goren, A., Lander, E.S.*, et al.* (2013). The Xist lncRNA Exploits Three-Dimensional Genome Architecture to Spread Across the X Chromosome. Science.

Eymery, A., Souchier, C., Vourc'h, C., and Jolly, C. (2010). Heat shock factor 1 binds to and transcribes satellite II and III sequences at several pericentromeric regions in heat-shocked cells. Exp Cell Res *316*, 1845-1855.

Fahrenkrog, B., and Aebi, U. (2003). The nuclear pore complex: nucleocytoplasmic transport and beyond. Nat Rev Mol Cell Biol *4*, 757-766.

Fernandez-Martinez, J., and Rout, M.P. (2009). Nuclear pore complex biogenesis. Curr Opin Cell Biol *21*, 603-612.

Flemming, D., Sarges, P., Stelter, P., Hellwig, A., Bottcher, B., and Hurt, E. (2009). Two structurally distinct domains of the nucleoporin Nup170 cooperate to tether a subset of nucleoporins to nuclear pores. J Cell Biol *185*, 387-395.

Franz, C., Walczak, R., Yavuz, S., Santarella, R., Gentzel, M., Askjaer, P., Galy, V., Hetzer, M., Mattaj, I.W., and Antonin, W. (2007). MEL-28/ELYS is required for the

recruitment of nucleoporins to chromatin and postmitotic nuclear pore complex assembly. EMBO Rep *8*, 165-172.

Frenkiel-Krispin, D., Maco, B., Aebi, U., and Medalia, O. (2010). Structural analysis of a metazoan nuclear pore complex reveals a fused concentric ring architecture. J Mol Biol *395*, 578-586.

Fridkin, A., Penkner, A., Jantsch, V., and Gruenbaum, Y. (2009). SUN-domain and KASH-domain proteins during development, meiosis and disease. Cell Mol Life Sci *66*, 1518-1533.

Gardner, J.M., Smoyer, C.J., Stensrud, E.S., Alexander, R., Gogol, M., Wiegraebe, W., and Jaspersen, S.L. (2011). Targeting of the SUN protein Mps3 to the inner nuclear membrane by the histone variant H2A.Z. J Cell Biol *193*, 489-507.

Gerstein, M.B., Lu, Z.J., Van Nostrand, E.L., Cheng, C., Arshinoff, B.I., Liu, T., Yip, K.Y., Robilotto, R., Rechtsteiner, A., Ikegami, K.*, et al.* (2010). Integrative analysis of the Caenorhabditis elegans genome by the modENCODE project. Science *330*, 1775-1787.

Geyer, P.K., Vitalini, M.W., and Wallrath, L.L. (2011). Nuclear organization: taking a position on gene expression. Curr Opin Cell Biol *23*, 354-359.

Ghamari, A., van de Corput, M.P., Thongjuea, S., van Cappellen, W.A., van Ijcken, W., van Haren, J., Soler, E., Eick, D., Lenhard, B., and Grosveld, F.G. (2013). In vivo live imaging of RNA polymerase II transcription factories in primary cells. Genes Dev *27*, 767-777.

Gilbert, L.A., Larson, M.H., Morsut, L., Liu, Z., Brar, G.A., Torres, S.E., Stern-Ginossar, N., Brandman, O., Whitehead, E.H., Doudna, J.A.*, et al.* (2013). CRISPR-Mediated Modular RNA-Guided Regulation of Transcription in Eukaryotes. Cell *154*, 442-451.

Gillespie, P.J., Khoudoli, G.A., Stewart, G., Swedlow, J.R., and Blow, J.J. (2007). ELYS/MEL-28 chromatin association coordinates nuclear pore complex assembly and replication licensing. Curr Biol *17*, 1657-1662.

Goffeau, A., Barrell, B.G., Bussey, H., Davis, R.W., Dujon, B., Feldmann, H., Galibert, F., Hoheisel, J.D., Jacq, C., Johnston, M.*, et al.* (1996). Life with 6000 genes. Science *274*, 546, 563-547.

Goodchild, R.E., and Dauer, W.T. (2005). The AAA+ protein torsinA interacts with a conserved domain present in LAP1 and a novel ER protein. J Cell Biol *168*, 855-862.

Gordon, L.M., Dipple, I., Sauerheber, R.D., Esgate, J.A., and Houslay, M.D. (1980). The selective effects of charged local anaesthetics on the glucagon- and fluoride-

stimulated adenylate cyclase activity of rat-liver plasma membranes. J Supramol Struct *14*, 21-32.

Gruenbaum, Y., Margalit, A., Goldman, R.D., Shumaker, D.K., and Wilson, K.L. (2005). The nuclear lamina comes of age. Nat Rev Mol Cell Biol *6*, 21-31.

Guelen, L., Pagie, L., Brasset, E., Meuleman, W., Faza, M.B., Talhout, W., Eussen, B.H., de Klein, A., Wessels, L., de Laat, W.*, et al.* (2008). Domain organization of human chromosomes revealed by mapping of nuclear lamina interactions. Nature *453*, 948-951.

Guttler, T., and Gorlich, D. (2011). Ran-dependent nuclear export mediators: a structural perspective. EMBO J *30*, 3457-3474.

Haim-Vilmovsky, L., and Gerst, J.E. (2009). m-TAG: a PCR-based genomic integration method to visualize the localization of specific endogenous mRNAs in vivo in yeast. Nat Protoc *4*, 1274-1284.

Hakim, O., and Misteli, T. (2012). SnapShot: Chromosome confirmation capture. Cell *148*, 1068 e1061-1062.

Hamirally, S., Kamil, J.P., Ndassa-Colday, Y.M., Lin, A.J., Jahng, W.J., Baek, M.C., Noton, S., Silva, L.A., Simpson-Holley, M., Knipe, D.M.*, et al.* (2009). Viral mimicry of Cdc2/cyclin-dependent kinase 1 mediates disruption of nuclear lamina during human cytomegalovirus nuclear egress. PLoS Pathog *5*, e1000275.

Hanson, P.I., and Whiteheart, S.W. (2005). AAA+ proteins: have engine, will work. Nat Rev Mol Cell Biol *6*, 519-529.

Harel, A., Orjalo, A.V., Vincent, T., Lachish-Zalait, A., Vasu, S., Shah, S., Zimmerman, E., Elbaum, M., and Forbes, D.J. (2003). Removal of a single pore subcomplex results in vertebrate nuclei devoid of nuclear pores. Mol Cell *11*, 853-864.

Hartley, P.D., and Madhani, H.D. (2009). Mechanisms that specify promoter nucleosome location and identity. Cell *137*, 445-458.

Hawryluk-Gara, L.A., Platani, M., Santarella, R., Wozniak, R.W., and Mattaj, I.W. (2008). Nup53 is required for nuclear envelope and nuclear pore complex assembly. Mol Biol Cell *19*, 1753-1762.

Heath, C.V., Copeland, C.S., Amberg, D.C., Del Priore, V., Snyder, M., and Cole, C.N. (1995). Nuclear pore complex clustering and nuclear accumulation of poly(A)+ RNA associated with mutation of the *Saccharomyces cerevisiae* RAT2/NUP120 gene. J Cell Biol *131*, 1677-1697.

Hediger, F., Neumann, F.R., Van Houwe, G., Dubrana, K., and Gasser, S.M. (2002). Live imaging of telomeres: yKu and Sir proteins define redundant telomere-anchoring pathways in yeast. Curr Biol *12*, 2076-2089.

Hetzer, M.W. (2010). The nuclear envelope. Cold Spring Harb Perspect Biol *2*, a000539.

Hetzer, M.W., Walther, T.C., and Mattaj, I.W. (2005). Pushing the envelope: structure, function, and dynamics of the nuclear periphery. Annu Rev Cell Dev Biol *21*, 347-380.

Hiraoka, Y., and Dernburg, A.F. (2009). The SUN rises on meiotic chromosome dynamics. Dev Cell *17*, 598-605.

Hodge, C.A., Choudhary, V., Wolyniak, M.J., Scarcelli, J.J., Schneiter, R., and Cole, C.N. (2010). Integral membrane proteins Brr6 and Apq12 link assembly of the nuclear pore complex to lipid homeostasis in the endoplasmic reticulum. J Cell Sci *123*, 141-151.

Hoelz, A., Debler, E.W., and Blobel, G. (2011). The structure of the nuclear pore complex. Annu Rev Biochem *80*, 613-643.

Hou, C., Li, L., Qin, Z.S., and Corces, V.G. (2012). Gene density, transcription, and insulators contribute to the partition of the Drosophila genome into physical domains. Mol Cell *48*, 471-484.

Hsia, K.C., Stavropoulos, P., Blobel, G., and Hoelz, A. (2007). Architecture of a coat for the nuclear pore membrane. Cell *131*, 1313-1326.

Hsu, J.M., Huang, J., Meluh, P.B., and Laurent, B.C. (2003). The yeast RSC chromatin-remodeling complex is required for kinetochore function in chromosome segregation. Mol Cell Biol *23*, 3202-3215.

Hu, J., Shibata, Y., Voss, C., Shemesh, T., Li, Z., Coughlin, M., Kozlov, M.M., Rapoport, T.A., and Prinz, W.A. (2008). Membrane proteins of the endoplasmic reticulum induce high-curvature tubules. Science *319*, 1247-1250.

Huang, J., Hsu, J.M., and Laurent, B.C. (2004). The RSC nucleosome-remodeling complex is required for Cohesin's association with chromosome arms. Mol Cell *13*, 739-750.

Huh, W.K., Falvo, J.V., Gerke, L.C., Carroll, A.S., Howson, R.W., Weissman, J.S., and O'Shea, E.K. (2003). Global analysis of protein localization in budding yeast. Nature *425*, 686-691.

Hwang, W.Y., Fu, Y., Reyon, D., Maeder, M.L., Tsai, S.Q., Sander, J.D., Peterson, R.T., Yeh, J.R., and Joung, J.K. (2013). Efficient genome editing in zebrafish using a CRISPR-Cas system. Nat Biotechnol *31*, 227-229.

Iborra, F.J., Pombo, A., Jackson, D.A., and Cook, P.R. (1996). Active RNA polymerases are localized within discrete transcription "factories' in human nuclei. J Cell Sci *109 (Pt 6)*, 1427-1436.

Iouk, T., Kerscher, O., Scott, R.J., Basrai, M.A., and Wozniak, R.W. (2002). The yeast nuclear pore complex functionally interacts with components of the spindle assembly checkpoint. J Cell Biol *159*, 807-819.

Iovine, M.K., Watkins, J.L., and Wente, S.R. (1995). The GLFG repetitive region of the nucleoporin Nup116p interacts with Kap95p, an essential yeast nuclear import factor. J Cell Biol *131*, 1699-1713.

Irarrazabal, C.E., Liu, J.C., Burg, M.B., and Ferraris, J.D. (2004). ATM, a DNA damage-inducible kinase, contributes to activation by high NaCl of the transcription factor TonEBP/OREBP. Proc Natl Acad Sci U S A *101*, 8809-8814.

Ishii, K., Arib, G., Lin, C., Van Houwe, G., and Laemmli, U.K. (2002). Chromatin boundaries in budding yeast: the nuclear pore connection. Cell *109*, 551-562.

Jackson, D.A., Hassan, A.B., Errington, R.J., and Cook, P.R. (1993). Visualization of focal sites of transcription within human nuclei. EMBO J *12*, 1059-1065.

Jaspersen, S.L., and Winey, M. (2004). The budding yeast spindle pole body: structure, duplication, and function. Annu Rev Cell Dev Biol *20*, 1-28.

Jeon, Y., Sarma, K., and Lee, J.T. (2012). New and Xisting regulatory mechanisms of X chromosome inactivation. Curr Opin Genet Dev *22*, 62-71.

Jin, Q.W., Fuchs, J., and Loidl, J. (2000). Centromere clustering is a major determinant of yeast interphase nuclear organization. J Cell Sci *113 (Pt 11)*, 1903-1912.

Johnson, D.C., and Baines, J.D. (2011). Herpesviruses remodel host membranes for virus egress. Nat Rev Microbiol *9*, 382-394.

Kadoch, C., Hargreaves, D.C., Hodges, C., Elias, L., Ho, L., Ranish, J., and Crabtree, G.R. (2013). Proteomic and bioinformatic analysis of mammalian SWI/SNF complexes identifies extensive roles in human malignancy. Nat Genet *45*, 592-601.

Kagey, M.H., Newman, J.J., Bilodeau, S., Zhan, Y., Orlando, D.A., van Berkum, N.L., Ebmeier, C.C., Goossens, J., Rahl, P.B., Levine, S.S.*, et al.* (2010). Mediator and cohesin connect gene expression and chromatin architecture. Nature *467*, 430-435.

Kaiser, T.E., Intine, R.V., and Dundr, M. (2008). De novo formation of a subnuclear body. Science *322*, 1713-1717.

Kalverda, B., Pickersgill, H., Shloma, V.V., and Fornerod, M. (2010). Nucleoporins directly stimulate expression of developmental and cell-cycle genes inside the nucleoplasm. Cell *140*, 360-371.

Karanasios, E., Han, G.S., Xu, Z., Carman, G.M., and Siniossoglou, S. (2010). A phosphorylation-regulated amphipathic helix controls the membrane translocation and function of the yeast phosphatidate phosphatase. Proc Natl Acad Sci U S A *107*, 17539-17544.

Kasten, M., Szerlong, H., Erdjument-Bromage, H., Tempst, P., Werner, M., and Cairns, B.R. (2004). Tandem bromodomains in the chromatin remodeler RSC recognize acetylated histone H3 Lys14. EMBO J *23*, 1348-1359.

Kerscher, O., Hieter, P., Winey, M., and Basrai, M.A. (2001). Novel role for a *Saccharomyces cerevisiae* nucleoporin, Nup170p, in chromosome segregation. Genetics *157*, 1543-1553.

Khadaroo, B., Teixeira, M.T., Luciano, P., Eckert-Boulet, N., Germann, S.M., Simon, M.N., Gallina, I., Abdallah, P., Gilson, E., Geli, V.*, et al.* (2009). The DNA damage response at eroded telomeres and tethering to the nuclear pore complex. Nat Cell Biol *11*, 980-987.

Kharchenko, P.V., Alekseyenko, A.A., Schwartz, Y.B., Minoda, A., Riddle, N.C., Ernst, J., Sabo, P.J., Larschan, E., Gorchakov, A.A., Gu, T.*, et al.* (2011). Comprehensive analysis of the chromatin landscape in Drosophila melanogaster. Nature *471*, 480-485.

Kim, C.E., Perez, A., Perkins, G., Ellisman, M.H., and Dauer, W.T. (2010). A molecular mechanism underlying the neural-specific defect in torsinA mutant mice. Proc Natl Acad Sci U S A *107*, 9861-9866.

Kind, J., Pagie, L., Ortabozkoyun, H., Boyle, S., de Vries, S.S., Janssen, H., Amendola, M., Nolen, L.D., Bickmore, W.A., and van Steensel, B. (2013). Single-cell dynamics of genome-nuclear lamina interactions. Cell *153*, 178-192.

King, M.C., Lusk, C.P., and Blobel, G. (2006). Karyopherin-mediated import of integral inner nuclear membrane proteins. Nature *442*, 1003-1007.

Kleinewietfeld, M., Manzel, A., Titze, J., Kvakan, H., Yosef, N., Linker, R.A., Muller, D.N., and Hafler, D.A. (2013). Sodium chloride drives autoimmune disease by the induction of pathogenic TH17 cells. Nature *496*, 518-522.

Korfali, N., Wilkie, G.S., Swanson, S.K., Srsen, V., Batrakou, D.G., Fairley, E.A., Malik, P., Zuleger, N., Goncharevich, A., de Las Heras, J.*, et al.* (2010). The leukocyte nuclear envelope proteome varies with cell activation and contains novel transmembrane proteins that affect genome architecture. Mol Cell Proteomics *9*, 2571-2585.

Kosova, B., Pante, N., Rollenhagen, C., and Hurt, E. (1999). Nup192p is a conserved nucleoporin with a preferential location at the inner site of the nuclear membrane. J Biol Chem *274*, 22646-22651.

Koyama, H., Itoh, M., Miyahara, K., and Tsuchiya, E. (2002). Abundance of the RSC nucleosome-remodeling complex is important for the cells to tolerate DNA damage in *Saccharomyces cerevisiae*. FEBS Lett *531*, 215-221.

Kubben, N., Adriaens, M., Meuleman, W., Voncken, J.W., van Steensel, B., and Misteli, T. (2012). Mapping of lamin A- and progerin-interacting genome regions. Chromosoma *121*, 447-464.

Kuroda, M., Tanabe, H., Yoshida, K., Oikawa, K., Saito, A., Kiyuna, T., Mizusawa, H., and Mukai, K. (2004). Alteration of chromosome positioning during adipocyte differentiation. J Cell Sci *117*, 5897-5903.

Larson, D.R., Zenklusen, D., Wu, B., Chao, J.A., and Singer, R.H. (2011). Real-time observation of transcription initiation and elongation on an endogenous yeast gene. Science *332*, 475-478.

Laser, H., Bongards, C., Schuller, J., Heck, S., Johnsson, N., and Lehming, N. (2000). A new screen for protein interactions reveals that the *Saccharomyces cerevisiae* high mobility group proteins Nhp6A/B are involved in the regulation of the GAL1 promoter. Proc Natl Acad Sci U S A *97*, 13732-13737.

Lee, B.J., Cansizoglu, A.E., Suel, K.E., Louis, T.H., Zhang, Z., and Chook, Y.M. (2006). Rules for nuclear localization sequence recognition by karyopherin beta 2. Cell *126*, 543-558.

Lee, S.J., Matsuura, Y., Liu, S.M., and Stewart, M. (2005). Structural basis for nuclear import complex dissociation by RanGTP. Nature *435*, 693-696.

Liang, B., Qiu, J., Ratnakumar, K., and Laurent, B.C. (2007). RSC functions as an early double-strand-break sensor in the cell's response to DNA damage. Curr Biol *17*, 1432-1437.

Liang, Y., Franks, T.M., Marchetto, M.C., Gage, F.H., and Hetzer, M.W. (2013). Dynamic association of NUP98 with the human genome. PLoS Genet *9*, e1003308.

Lieberman-Aiden, E., van Berkum, N.L., Williams, L., Imakaev, M., Ragoczy, T., Telling, A., Amit, I., Lajoie, B.R., Sabo, P.J., Dorschner, M.O*., et al.* (2009). Comprehensive mapping of long-range interactions reveals folding principles of the human genome. Science *326*, 289-293.

Light, W.H., Brickner, D.G., Brand, V.R., and Brickner, J.H. (2010). Interaction of a DNA zip code with the nuclear pore complex promotes H2A.Z incorporation and INO1 transcriptional memory. Mol Cell *40*, 112-125.

Liu, H.L., De Souza, C.P., Osmani, A.H., and Osmani, S.A. (2009). The three fungal transmembrane nuclear pore complex proteins of Aspergillus nidulans are dispensable in the presence of an intact An-Nup84-120 complex. Mol Biol Cell *20*, 616-630.

Liu, S.M., and Stewart, M. (2005). Structural basis for the high-affinity binding of nucleoporin Nup1p to the *Saccharomyces cerevisiae* importin-beta homologue, Kap95p. J Mol Biol *349*, 515-525.

Loven, J., Hoke, H.A., Lin, C.Y., Lau, A., Orlando, D.A., Vakoc, C.R., Bradner, J.E., Lee, T.I., and Young, R.A. (2013). Selective inhibition of tumor oncogenes by disruption of super-enhancers. Cell *153*, 320-334.

Lusk, C.P., Blobel, G., and King, M.C. (2007). Highway to the inner nuclear membrane: rules for the road. Nat Rev Mol Cell Biol *8*, 414-420.

Madrid, A.S., Mancuso, J., Cande, W.Z., and Weis, K. (2006). The role of the integral membrane nucleoporins Ndc1p and Pom152p in nuclear pore complex assembly and function. J Cell Biol *173*, 361-371.

Makio, T., Stanton, L.H., Lin, C.C., Goldfarb, D.S., Weis, K., and Wozniak, R.W. (2009). The nucleoporins Nup170p and Nup157p are essential for nuclear pore complex assembly. J Cell Biol *185*, 459-473.

Mali, P., Yang, L., Esvelt, K.M., Aach, J., Guell, M., DiCarlo, J.E., Norville, J.E., and Church, G.M. (2013). RNA-guided human genome engineering via Cas9. Science *339*, 823-826.

Mansfeld, J., Guttinger, S., Hawryluk-Gara, L.A., Pante, N., Mall, M., Galy, V., Haselmann, U., Muhlhausser, P., Wozniak, R.W., Mattaj, I.W.*, et al.* (2006). The conserved transmembrane nucleoporin NDC1 is required for nuclear pore complex assembly in vertebrate cells. Mol Cell *22*, 93-103.

Mao, Y.S., Sunwoo, H., Zhang, B., and Spector, D.L. (2011a). Direct visualization of the co-transcriptional assembly of a nuclear body by noncoding RNAs. Nat Cell Biol *13*, 95-101.

Mao, Y.S., Zhang, B., and Spector, D.L. (2011b). Biogenesis and function of nuclear bodies. Trends Genet *27*, 295-306.

Marelli, M., Lusk, C.P., Chan, H., Aitchison, J.D., and Wozniak, R.W. (2001). A link between the synthesis of nucleoporins and the biogenesis of the nuclear envelope. J Cell Biol *153*, 709-724.

Maric, M., Shao, J., Ryan, R.J., Wong, C.S., Gonzalez-Alegre, P., and Roller, R.J. (2011). A functional role for TorsinA in herpes simplex virus 1 nuclear egress. J Virol *85*, 9667-9679.

Martens, J.A., Laprade, L., and Winston, F. (2004). Intergenic transcription is required to repress the *Saccharomyces cerevisiae* SER3 gene. Nature *429*, 571-574.

Martens, J.A., and Winston, F. (2003). Recent advances in understanding chromatin remodeling by Swi/Snf complexes. Curr Opin Genet Dev *13*, 136-142.

Mas, G., de Nadal, E., Dechant, R., Rodriguez de la Concepcion, M.L., Logie, C., Jimeno-Gonzalez, S., Chavez, S., Ammerer, G., and Posas, F. (2009). Recruitment of a chromatin remodelling complex by the Hog1 MAP kinase to stress genes. EMBO J *28*, 326-336.

Mattout, A., Pike, B.L., Towbin, B.D., Bank, E.M., Gonzalez-Sandoval, A., Stadler, M.B., Meister, P., Gruenbaum, Y., and Gasser, S.M. (2011). An EDMD mutation in C. elegans lamin blocks muscle-specific gene relocation and compromises muscle integrity. Curr Biol *21*, 1603-1614.

Maul, G.G., Price, J.W., and Lieberman, M.W. (1971). Formation and distribution of nuclear pore complexes in interphase. J Cell Biol *51*, 405-418.

McCord, R.P., Nazario-Toole, A., Zhang, H., Chines, P.S., Zhan, Y., Erdos, M.R., Collins, F.S., Dekker, J., and Cao, K. (2013). Correlated alterations in genome organization, histone methylation, and DNA-lamin A/C interactions in Hutchinson-Gilford progeria syndrome. Genome Res *23*, 260-269.

McCullagh, E., Seshan, A., El-Samad, H., and Madhani, H.D. (2010). Coordinate control of gene expression noise and interchromosomal interactions in a MAP kinase pathway. Nat Cell Biol *12*, 954-962.

Meggio, F., and Pinna, L.A. (2003). One-thousand-and-one substrates of protein kinase CK2? FASEB J *17*, 349-368.

Meinema, A.C., Laba, J.K., Hapsari, R.A., Otten, R., Mulder, F.A., Kralt, A., van den Bogaart, G., Lusk, C.P., Poolman, B., and Veenhoff, L.M. (2011). Long unfolded linkers facilitate membrane protein import through the nuclear pore complex. Science *333*, 90-93.

Meister, P., Towbin, B.D., Pike, B.L., Ponti, A., and Gasser, S.M. (2010). The spatial dynamics of tissue-specific promoters during C. elegans development. Genes Dev *24*, 766-782.

Mejat, A., and Misteli, T. (2010). LINC complexes in health and disease. Nucleus *1*, 40-52.

Mekhail, K., and Moazed, D. (2010). The nuclear envelope in genome organization, expression and stability. Nat Rev Mol Cell Biol *11*, 317-328.

Mekhail, K., Seebacher, J., Gygi, S.P., and Moazed, D. (2008). Role for perinuclear chromosome tethering in maintenance of genome stability. Nature *456*, 667-670.

Menon, B.B., Sarma, N.J., Pasula, S., Deminoff, S.J., Willis, K.A., Barbara, K.E., Andrews, B., and Santangelo, G.M. (2005). Reverse recruitment: the Nup84 nuclear pore subcomplex mediates Rap1/Gcr1/Gcr2 transcriptional activation. Proc Natl Acad Sci U S A *102*, 5749-5754.

Meuleman, W., Peric-Hupkes, D., Kind, J., Beaudry, J.B., Pagie, L., Kellis, M., Reinders, M., Wessels, L., and van Steensel, B. (2013). Constitutive nuclear lamina-genome interactions are highly conserved and associated with A/T-rich sequence. Genome Res *23*, 270-280.

Miao, M., Ryan, K.J., and Wente, S.R. (2006). The integral membrane protein Pom34p functionally links nucleoporin subcomplexes. Genetics *172*, 1441-1457.

Misteli, T. (2013). The cell biology of genomes: bringing the double helix to life. Cell *152*, 1209-1212.

Misteli, T., and Soutoglou, E. (2009). The emerging role of nuclear architecture in DNA repair and genome maintenance. Nat Rev Mol Cell Biol *10*, 243-254.

Mitchell, J.A., and Fraser, P. (2008). Transcription factories are nuclear subcompartments that remain in the absence of transcription. Genes Dev *22*, 20-25.

Mitchell, J.M., Mansfeld, J., Capitanio, J., Kutay, U., and Wozniak, R.W. (2010). Pom121 links two essential subcomplexes of the nuclear pore complex core to the membrane. J Cell Biol *191*, 505-521.

Miyao, T., Barnett, J.D., and Woychik, N.A. (2001). Deletion of the RNA polymerase subunit RPB4 acts as a global, not stress-specific, shut-off switch for RNA polymerase II transcription at high temperatures. J Biol Chem *276*, 46408-46413.

Mnaimneh, S., Davierwala, A.P., Haynes, J., Moffat, J., Peng, W.T., Zhang, W., Yang, X., Pootoolal, J., Chua, G., Lopez, A., *et al.* (2004). Exploration of essential gene functions via titratable promoter alleles. Cell *118*, 31-44.

Mojica, F.J., Diez-Villasenor, C., Garcia-Martinez, J., and Almendros, C. (2009). Short motif sequences determine the targets of the prokaryotic CRISPR defence system. Microbiology *155*, 733-740.

Moore, M.S., and Blobel, G. (1993). The GTP-binding protein Ran/TC4 is required for protein import into the nucleus. Nature *365*, 661-663.

Mosammaparast, N., and Pemberton, L.F. (2004). Karyopherins: from nuclear-transport mediators to nuclear-function regulators. Trends Cell Biol *14*, 547-556.

Nadal-Ribelles, M., Conde, N., Flores, O., Gonzalez-Vallinas, J., Eyras, E., Orozco, M., de Nadal, E., and Posas, F. (2012). Hog1 bypasses stress-mediated down-regulation of transcription by RNA polymerase II redistribution and chromatin remodeling. Genome Biol *13*, R106.

Nagai, S., Dubrana, K., Tsai-Pflugfelder, M., Davidson, M.B., Roberts, T.M., Brown, G.W., Varela, E., Hediger, F., Gasser, S.M., and Krogan, N.J. (2008). Functional targeting of DNA damage to a nuclear pore-associated SUMO-dependent ubiquitin ligase. Science *322*, 597-602.

Nanduri, J., Mitra, S., Andrei, C., Liu, Y., Yu, Y., Hitomi, M., and Tartakoff, A.M. (1999). An unexpected link between the secretory path and the organization of the nucleus. J Biol Chem *274*, 33785-33789.

Nanduri, J., and Tartakoff, A.M. (2001). The arrest of secretion response in yeast: signaling from the secretory path to the nucleus via Wsc proteins and Pkc1p. Mol Cell *8*, 281-289.

Nehrbass, U., Rout, M.P., Maguire, S., Blobel, G., and Wozniak, R.W. (1996). The yeast nucleoporin Nup188p interacts genetically and physically with the core structures of the nuclear pore complex. J Cell Biol *133*, 1153-1162.

Neil, H., Malabat, C., d'Aubenton-Carafa, Y., Xu, Z., Steinmetz, L.M., and Jacquier, A. (2009). Widespread bidirectional promoters are the major source of cryptic transcripts in yeast. Nature *457*, 1038-1042.

Nemeth, A., Conesa, A., Santoyo-Lopez, J., Medina, I., Montaner, D., Peterfia, B., Solovei, I., Cremer, T., Dopazo, J., and Langst, G. (2010). Initial genomics of the human nucleolus. PLoS Genet *6*, e1000889.

Neuert, G., Munsky, B., Tan, R.Z., Teytelman, L., Khammash, M., and van Oudenaarden, A. (2013). Systematic identification of signal-activated stochastic gene regulation. Science *339*, 584-587.

Ng, H.H., Robert, F., Young, R.A., and Struhl, K. (2002). Genome-wide location and regulated recruitment of the RSC nucleosome-remodeling complex. Genes Dev *16*, 806-819.

Nora, E.P., Lajoie, B.R., Schulz, E.G., Giorgetti, L., Okamoto, I., Servant, N., Piolot, T., van Berkum, N.L., Meisig, J., Sedat, J.*, et al.* (2012). Spatial partitioning of the regulatory landscape of the X-inactivation centre. Nature *485*, 381-385.

O'Rourke, S.M., Herskowitz, I., and O'Shea, E.K. (2002). Yeast go the whole HOG for the hyperosmotic response. Trends Genet *18*, 405-412.

Ohba, T., Schirmer, E.C., Nishimoto, T., and Gerace, L. (2004). Energy- and temperature-dependent transport of integral proteins to the inner nuclear membrane via the nuclear pore. J Cell Biol *167*, 1051-1062.

Onischenko, E., Stanton, L.H., Madrid, A.S., Kieselbach, T., and Weis, K. (2009). Role of the Ndc1 interaction network in yeast nuclear pore complex assembly and maintenance. J Cell Biol *185*, 475-491.

Osborne, C.S., Chakalova, L., Brown, K.E., Carter, D., Horton, A., Debrand, E., Goyenechea, B., Mitchell, J.A., Lopes, S., Reik, W.*, et al.* (2004). Active genes dynamically colocalize to shared sites of ongoing transcription. Nat Genet *36*, 1065-1071.

Pagano, M.A., Sarno, S., Poletto, G., Cozza, G., Pinna, L.A., and Meggio, F. (2005). Autophosphorylation at the regulatory beta subunit reflects the supramolecular organization of protein kinase CK2. Mol Cell Biochem *274*, 23-29.

Palancade, B., Liu, X., Garcia-Rubio, M., Aguilera, A., Zhao, X., and Doye, V. (2007). Nucleoporins prevent DNA damage accumulation by modulating Ulp1-dependent sumoylation processes. Mol Biol Cell *18*, 2912-2923.

Pante, N., and Kann, M. (2002). Nuclear pore complex is able to transport macromolecules with diameters of about 39 nm. Mol Biol Cell *13*, 425-434.

Parada, L.A., McQueen, P.G., and Misteli, T. (2004). Tissue-specific spatial organization of genomes. Genome Biol *5*, R44.

Parada, L.A., McQueen, P.G., Munson, P.J., and Misteli, T. (2002). Conservation of relative chromosome positioning in normal and cancer cells. Curr Biol *12*, 1692-1697.

Parada, L.A., Roix, J.J., and Misteli, T. (2003). An uncertainty principle in chromosome positioning. Trends Cell Biol *13*, 393-396.

Parnell, T.J., Huff, J.T., and Cairns, B.R. (2008). RSC regulates nucleosome positioning at Pol II genes and density at Pol III genes. EMBO J *27*, 100-110.

Pasdeloup, D., Blondel, D., Isidro, A.L., and Rixon, F.J. (2009). Herpesvirus capsid association with the nuclear pore complex and viral DNA release involve the nucleoporin CAN/Nup214 and the capsid protein pUL25. J Virol *83*, 6610-6623.

Pelet, S., Rudolf, F., Nadal-Ribelles, M., de Nadal, E., Posas, F., and Peter, M. (2011). Transient activation of the HOG MAPK pathway regulates bimodal gene expression. Science *332*, 732-735.

Pemberton, L.F., and Paschal, B.M. (2005). Mechanisms of receptor-mediated nuclear import and nuclear export. Traffic *6*, 187-198.

Peric-Hupkes, D., Meuleman, W., Pagie, L., Bruggeman, S.W., Solovei, I., Brugman, W., Graf, S., Flicek, P., Kerkhoven, R.M., van Lohuizen, M.*, et al.* (2010). Molecular maps of the reorganization of genome-nuclear lamina interactions during differentiation. Mol Cell *38*, 603-613.

Peterson, T.R., Sengupta, S.S., Harris, T.E., Carmack, A.E., Kang, S.A., Balderas, E., Guertin, D.A., Madden, K.L., Carpenter, A.E., Finck, B.N.*, et al.* (2011). mTOR complex 1 regulates lipin 1 localization to control the SREBP pathway. Cell *146*, 408-420.

Pickersgill, H., Kalverda, B., de Wit, E., Talhout, W., Fornerod, M., and van Steensel, B. (2006). Characterization of the Drosophila melanogaster genome at the nuclear lamina. Nat Genet *38*, 1005-1014.

Radu, A., Moore, M.S., and Blobel, G. (1995). The peptide repeat domain of nucleoporin Nup98 functions as a docking site in transport across the nuclear pore complex. Cell *81*, 215-222.

Ragoczy, T., Bender, M.A., Telling, A., Byron, R., and Groudine, M. (2006). The locus control region is required for association of the murine beta-globin locus with engaged transcription factories during erythroid maturation. Genes Dev *20*, 1447-1457.

Rasala, B.A., Orjalo, A.V., Shen, Z., Briggs, S., and Forbes, D.J. (2006). ELYS is a dual nucleoporin/kinetochore protein required for nuclear pore assembly and proper cell division. Proc Natl Acad Sci U S A *103*, 17801-17806.

Rasala, B.A., Ramos, C., Harel, A., and Forbes, D.J. (2008). Capture of AT-rich chromatin by ELYS recruits POM121 and NDC1 to initiate nuclear pore assembly. Mol Biol Cell *19*, 3982-3996.

Razafsky, D., and Hodzic, D. (2009). Bringing KASH under the SUN: the many faces of nucleo-cytoskeletal connections. J Cell Biol *186*, 461-472.

Reichelt, R., Holzenburg, A., Buhle, E.L., Jr., Jarnik, M., Engel, A., and Aebi, U. (1990). Correlation between structure and mass distribution of the nuclear pore complex and of distinct pore complex components. J Cell Biol *110*, 883-894.

Rep, M., Krantz, M., Thevelein, J.M., and Hohmann, S. (2000). The transcriptional response of *Saccharomyces cerevisiae* to osmotic shock. Hot1p and Msn2p/Msn4p are required for the induction of subsets of high osmolarity glycerol pathway-dependent genes. J Biol Chem *275*, 8290-8300.

Rodriguez-Navarro, S., Fischer, T., Luo, M.J., Antunez, O., Brettschneider, S., Lechner, J., Perez-Ortin, J.E., Reed, R., and Hurt, E. (2004). Sus1, a functional component of the SAGA histone acetylase complex and the nuclear pore-associated mRNA export machinery. Cell *116*, 75-86.

Roller, R.J., Haugo, A.C., and Kopping, N.J. (2011). Intragenic and extragenic suppression of a mutation in herpes simplex virus 1 UL34 that affects both nuclear envelope targeting and membrane budding. J Virol *85*, 11615-11625.

Rout, M.P., Aitchison, J.D., Suprapto, A., Hjertaas, K., Zhao, Y., and Chait, B.T. (2000). The yeast nuclear pore complex: composition, architecture, and transport mechanism. J Cell Biol *148*, 635-651.

Rout, M.P., and Blobel, G. (1993). Isolation of the yeast nuclear pore complex. J Cell Biol *123*, 771-783.

Roy, S., Ernst, J., Kharchenko, P.V., Kheradpour, P., Negre, N., Eaton, M.L., Landolin, J.M., Bristow, C.A., Ma, L., Lin, M.F.*, et al.* (2010). Identification of functional elements and regulatory circuits by Drosophila modENCODE. Science *330*, 1787-1797.

Ryan, K.J., McCaffery, J.M., and Wente, S.R. (2003). The Ran GTPase cycle is required for yeast nuclear pore complex assembly. J Cell Biol *160*, 1041-1053.

Ryan, K.J., and Wente, S.R. (2002a). Isolation and characterization of new *Saccharomyces cerevisiae* mutants perturbed in nuclear pore complex assembly. BMC Genet *3*, 17.

Ryan, K.J., and Wente, S.R. (2002b). Isolation and characterization of new *Saccharomyces cerevisiae* mutants perturbed in nuclear pore complex assembly. BMC Genet *3*, 17.

Ryan, K.J., Zhou, Y., and Wente, S.R. (2007). The karyopherin Kap95 regulates nuclear pore complex assembly into intact nuclear envelopes in vivo. Mol Biol Cell *18*, 886-898.

Saha, A., Wittmeyer, J., and Cairns, B.R. (2002). Chromatin remodeling by RSC involves ATP-dependent DNA translocation. Genes Dev *16*, 2120-2134.

Saha, A., Wittmeyer, J., and Cairns, B.R. (2006). Chromatin remodelling: the industrial revolution of DNA around histones. Nat Rev Mol Cell Biol *7*, 437-447.
Saito, H., and Posas, F. (2012). Response to hyperosmotic stress. Genetics *192*, 289-318.

Sambrook, J., Fritsch, E.F., and Maniatis, T. (1989a). Molecular cloning : a laboratory manual, 2nd edn (Cold Spring Harbor, N.Y.: Cold Spring Harbor Laboratory).

Sambrook, J., Maniatis, T., and Fritsch, E.F. (1989b). Molecular cloning : a laboratory manual, 2nd edn (Cold Spring Harbor, N.Y.: Cold Spring Harbor Laboratory Press).

Santos-Rosa, H., Leung, J., Grimsey, N., Peak-Chew, S., and Siniossoglou, S. (2005). The yeast lipin Smp2 couples phospholipid biosynthesis to nuclear membrane growth. EMBO J *24*, 1931-1941.

Sawa, C., Nedea, E., Krogan, N., Wada, T., Handa, H., Greenblatt, J., and Buratowski, S. (2004). Bromodomain factor 1 (Bdf1) is phosphorylated by protein kinase CK2. Mol Cell Biol *24*, 4734-4742.

Scarcelli, J.J., Hodge, C.A., and Cole, C.N. (2007). The yeast integral membrane protein Apq12 potentially links membrane dynamics to assembly of nuclear pore complexes. J Cell Biol *178*, 799-812.

Schirmer, E.C., Florens, L., Guan, T., Yates, J.R., 3rd, and Gerace, L. (2003). Nuclear membrane proteins with potential disease links found by subtractive proteomics. Science *301*, 1380-1382.

Schirmer, E.C., Florens, L., Guan, T., Yates, J.R., 3rd, and Gerace, L. (2005). Identification of novel integral membrane proteins of the nuclear envelope with potential disease links using subtractive proteomics. Novartis Found Symp *264*, 63-76; discussion 76-80, 227-230.

Schmid, M., Arib, G., Laemmli, C., Nishikawa, J., Durussel, T., and Laemmli, U.K. (2006). Nup-PI: the nucleopore-promoter interaction of genes in yeast. Mol Cell *21*, 379-391.

Schneiter, R., Hitomi, M., Ivessa, A.S., Fasch, E.V., Kohlwein, S.D., and Tartakoff, A.M. (1996). A yeast acetyl coenzyme A carboxylase mutant links very-long-chain fatty acid synthesis to the structure and function of the nuclear membrane-pore complex. Mol Cell Biol *16*, 7161-7172.

Schober, H., Ferreira, H., Kalck, V., Gehlen, L.R., and Gasser, S.M. (2009). Yeast telomerase and the SUN domain protein Mps3 anchor telomeres and repress subtelomeric recombination. Genes Dev *23*, 928-938.

Schoborg, T., Rickels, R., Barrios, J., and Labrador, M. (2013). Chromatin insulator bodies are nuclear structures that form in response to osmotic stress and cell death. J Cell Biol *202*, 261-276.

Schoenfelder, S., Sexton, T., Chakalova, L., Cope, N.F., Horton, A., Andrews, S., Kurukuti, S., Mitchell, J.A., Umlauf, D., Dimitrova, D.S., *et al.* (2010). Preferential associations between co-regulated genes reveal a transcriptional interactome in erythroid cells. Nat Genet *42*, 53-61.

Seeber, A., Hauer, M., and Gasser, S.M. (2013). Nucleosome remodelers in double-strand break repair. Curr Opin Genet Dev *23*, 174-184.

Sexton, T., Yaffe, E., Kenigsberg, E., Bantignies, F., Leblanc, B., Hoichman, M., Parrinello, H., Tanay, A., and Cavalli, G. (2012). Three-dimensional folding and functional organization principles of the Drosophila genome. Cell *148*, 458-472.

Shain, A.H., and Pollack, J.R. (2013). The spectrum of SWI/SNF mutations, ubiquitous in human cancers. PLoS One *8*, e55119.

Shaulov, L., Gruber, R., Cohen, I., and Harel, A. (2011). A dominant-negative form of POM121 binds chromatin and disrupts the two separate modes of nuclear pore assembly. J Cell Sci *124*, 3822-3834.

Sherman, F., Fink, G.R., Hicks, J.B., and Cold Spring Harbor Laboratory. (1986). Laboratory course manual for methods in yeast genetics (New York, N.Y.: Cold Spring Harbor Laboratory).

Shevtsov, S.P., and Dundr, M. (2011). Nucleation of nuclear bodies by RNA. Nat Cell Biol *13*, 167-173.

Shim, E.Y., Hong, S.J., Oum, J.H., Yanez, Y., Zhang, Y., and Lee, S.E. (2007). RSC mobilizes nucleosomes to improve accessibility of repair machinery to the damaged chromatin. Mol Cell Biol *27*, 1602-1613.

Shim, E.Y., Ma, J.L., Oum, J.H., Yanez, Y., and Lee, S.E. (2005). The yeast chromatin remodeler RSC complex facilitates end joining repair of DNA double-strand breaks. Mol Cell Biol *25*, 3934-3944.

Sikorski, R.S., and Hieter, P. (1989). A system of shuttle vectors and yeast host strains designed for efficient manipulation of DNA in *Saccharomyces cerevisiae*. Genetics *122*, 19-27.

Siniossoglou, S. (2009). Lipins, lipids and nuclear envelope structure. Traffic *10*, 1181-1187.

Siniossoglou, S., Santos-Rosa, H., Rappsilber, J., Mann, M., and Hurt, E. (1998). A novel complex of membrane proteins required for formation of a spherical nucleus. EMBO J *17*, 6449-6464.

Siniossoglou, S., Wimmer, C., Rieger, M., Doye, V., Tekotte, H., Weise, C., Emig, S., Segref, A., and Hurt, E.C. (1996). A novel complex of nucleoporins, which includes Sec13p and a Sec13p homolog, is essential for normal nuclear pores. Cell *84*, 265-275.

Sirri, V., Urcuqui-Inchima, S., Roussel, P., and Hernandez-Verdun, D. (2008). Nucleolus: the fascinating nuclear body. Histochem Cell Biol *129*, 13-31.
Smith, S., and Blobel, G. (1993). The first membrane spanning region of the lamin B receptor is sufficient for sorting to the inner nuclear membrane. J Cell Biol *120*, 631-637.

Soufi, B., Kelstrup, C.D., Stoehr, G., Frohlich, F., Walther, T.C., and Olsen, J.V. (2009). Global analysis of the yeast osmotic stress response by quantitative proteomics. Mol Biosyst *5*, 1337-1346.

Soullam, B., and Worman, H.J. (1995). Signals and structural features involved in integral membrane protein targeting to the inner nuclear membrane. J Cell Biol *130*, 15-27.

Soutourina, J., Bordas-Le Floch, V., Gendrel, G., Flores, A., Ducrot, C., Dumay-Odelot, H., Soularue, P., Navarro, F., Cairns, B.R., Lefebvre, O.*, et al.* (2006). Rsc4 connects the chromatin remodeler RSC to RNA polymerases. Mol Cell Biol *26*, 4920-4933.

Stavru, F., Hulsmann, B.B., Spang, A., Hartmann, E., Cordes, V.C., and Gorlich, D. (2006). NDC1: a crucial membrane-integral nucleoporin of metazoan nuclear pore complexes. J Cell Biol *173*, 509-519.

Stewart, M. (2006). Structural basis for the nuclear protein import cycle. Biochem Soc Trans *34*, 701-704.

Stewart, M. (2007). Molecular mechanism of the nuclear protein import cycle. Nat Rev Mol Cell Biol *8*, 195-208.

Strambio-De-Castillia, C., Niepel, M., and Rout, M.P. (2010). The nuclear pore complex: bridging nuclear transport and gene regulation. Nat Rev Mol Cell Biol *11*, 490-501.

Taddei, A., Hediger, F., Neumann, F.R., and Gasser, S.M. (2004). The function of nuclear architecture: a genetic approach. Annu Rev Genet *38*, 305-345.

Taddei, A., Van Houwe, G., Hediger, F., Kalck, V., Cubizolles, F., Schober, H., and Gasser, S.M. (2006). Nuclear pore association confers optimal expression levels for an inducible yeast gene. Nature *441*, 774-778.

Takizawa, T., Gudla, P.R., Guo, L., Lockett, S., and Misteli, T. (2008). Allele-specific nuclear positioning of the monoallelically expressed astrocyte marker GFAP. Genes Dev *22*, 489-498.

Talamas, J.A., and Hetzer, M.W. (2011). POM121 and Sun1 play a role in early steps of interphase NPC assembly. J Cell Biol *194*, 27-37.

Tan-Wong, S.M., Zaugg, J.B., Camblong, J., Xu, Z., Zhang, D.W., Mischo, H.E., Ansari, A.Z., Luscombe, N.M., Steinmetz, L.M., and Proudfoot, N.J. (2012). Gene loops enhance transcriptional directionality. Science *338*, 671-675.

Tapley, E.C., Ly, N., and Starr, D.A. (2011). Multiple mechanisms actively target the SUN protein UNC-84 to the inner nuclear membrane. Mol Biol Cell *22*, 1739-1752.

Tcheperegine, S.E., Marelli, M., and Wozniak, R.W. (1999). Topology and functional domains of the yeast pore membrane protein Pom152p. J Biol Chem *274*, 5252-5258.

Teixeira, M.T., Dujon, B., and Fabre, E. (2002). Genome-wide nuclear morphology screen identifies novel genes involved in nuclear architecture and gene-silencing in *Saccharomyces cerevisiae*. J Mol Biol *321*, 551-561.

Tenney, K.A., and Glover, C.V. (1999). Transcriptional regulation of the *S. cerevisiae* ENA1 gene by casein kinase II. Mol Cell Biochem *191*, 161-167.

Terry, L.J., and Wente, S.R. (2009). Flexible gates: dynamic topologies and functions for FG nucleoporins in nucleocytoplasmic transport. Eukaryot Cell *8*, 1814-1827.

Tetenbaum-Novatt, J., and Rout, M.P. (2010). The mechanism of nucleocytoplasmic transport through the nuclear pore complex. Cold Spring Harb Symp Quant Biol *75*, 567-584.

Theerthagiri, G., Eisenhardt, N., Schwarz, H., and Antonin, W. (2010). The nucleoporin Nup188 controls passage of membrane proteins across the nuclear pore complex. J Cell Biol *189*, 1129-1142.

Therizols, P., Duong, T., Dujon, B., Zimmer, C., and Fabre, E. (2010). Chromosome arm length and nuclear constraints determine the dynamic relationship of yeast subtelomeres. Proc Natl Acad Sci U S A *107*, 2025-2030.

Therizols, P., Fairhead, C., Cabal, G.G., Genovesio, A., Olivo-Marin, J.C., Dujon, B., and Fabre, E. (2006). Telomere tethering at the nuclear periphery is essential for

efficient DNA double strand break repair in subtelomeric region. J Cell Biol *172*, 189-199.

Thompson, M., Haeusler, R.A., Good, P.D., and Engelke, D.R. (2003). Nucleolar clustering of dispersed tRNA genes. Science *302*, 1399-1401.

Thomson, I., Gilchrist, S., Bickmore, W.A., and Chubb, J.R. (2004). The radial positioning of chromatin is not inherited through mitosis but is established de novo in early G1. Curr Biol *14*, 166-172.

Titus, L.C., Dawson, T.R., Rexer, D.J., Ryan, K.J., and Wente, S.R. (2010). Members of the RSC chromatin-remodeling complex are required for maintaining proper nuclear envelope structure and pore complex localization. Mol Biol Cell *21*, 1072-1087.

Tjong, H., Gong, K., Chen, L., and Alber, F. (2012). Physical tethering and volume exclusion determine higher-order genome organization in budding yeast. Genome Res *22*, 1295-1305.

Tolstorukov, M.Y., Sansam, C.G., Lu, P., Koellhoffer, E.C., Helming, K.C., Alver, B.H., Tillman, E.J., Evans, J.A., Wilson, B.G., Park, P.J.*, et al.* (2013). Swi/Snf chromatin remodeling/tumor suppressor complex establishes nucleosome occupancy at target promoters. Proc Natl Acad Sci U S A *110*, 10165-10170.

Towbin, B.D., Meister, P., and Gasser, S.M. (2009). The nuclear envelope--a scaffold for silencing? Curr Opin Genet Dev *19*, 180-186.

Tran, E.J., and Wente, S.R. (2006). Dynamic nuclear pore complexes: life on the edge. Cell *125*, 1041-1053.

Tsuchiya, E., Hosotani, T., and Miyakawa, T. (1998). A mutation in NPS1/STH1, an essential gene encoding a component of a novel chromatin-remodeling complex RSC, alters the chromatin structure of *Saccharomyces cerevisiae* centromeres. Nucleic Acids Res *26*, 3286-3292.

Turgay, Y., Ungricht, R., Rothballer, A., Kiss, A., Csucs, G., Horvath, P., and Kutay, U. (2010). A classical NLS and the SUN domain contribute to the targeting of SUN2 to the inner nuclear membrane. EMBO J *29*, 2262-2275.

Upton, T., Wiltshire, S., Francesconi, S., and Eisenberg, S. (1995). ABF1 Ser-720 is a predominant phosphorylation site for casein kinase II of *Saccharomyces cerevisiae*. J Biol Chem *270*, 16153-16159.

Valero, E., De Bonis, S., Filhol, O., Wade, R.H., Langowski, J., Chambaz, E.M., and Cochet, C. (1995). Quaternary structure of casein kinase 2. Characterization of

multiple oligomeric states and relation with its catalytic activity. J Biol Chem *270*, 8345-8352.

Valgardsdottir, R., Chiodi, I., Giordano, M., Rossi, A., Bazzini, S., Ghigna, C., Riva, S., and Biamonti, G. (2008). Transcription of Satellite III non-coding RNAs is a general stress response in human cells. Nucleic Acids Res *36*, 423-434.

Van de Vosse, D.W., Wan, Y., Wozniak, R.W., and Aitchison, J.D. (2011). Role of the nuclear envelope in genome organization and gene expression. Wiley Interdiscip Rev Syst Biol Med *3*, 147-166.

van Koningsbruggen, S., Gierlinski, M., Schofield, P., Martin, D., Barton, G.J., Ariyurek, Y., den Dunnen, J.T., and Lamond, A.I. (2010). High-resolution whole-genome sequencing reveals that specific chromatin domains from most human chromosomes associate with nucleoli. Mol Biol Cell *21*, 3735-3748.

van Werven, F.J., Neuert, G., Hendrick, N., Lardenois, A., Buratowski, S., van Oudenaarden, A., Primig, M., and Amon, A. (2012). Transcription of two long noncoding RNAs mediates mating-type control of gametogenesis in budding yeast. Cell *150*, 1170-1181.

Vaquerizas, J.M., Suyama, R., Kind, J., Miura, K., Luscombe, N.M., and Akhtar, A. (2010). Nuclear pore proteins nup153 and megator define transcriptionally active regions in the Drosophila genome. PLoS Genet *6*, e1000846.

Vidal, S.E., Pincus, D., Stewart-Ornstein, J., and El-Samad, H. (2013). Formation of subnuclear foci is a unique spatial behavior of mating MAPKs during hyperosmotic stress. Cell Rep *3*, 328-334.

Voeltz, G.K., Prinz, W.A., Shibata, Y., Rist, J.M., and Rapoport, T.A. (2006). A class of membrane proteins shaping the tubular endoplasmic reticulum. Cell *124*, 573-586.

Vogelmann, J., Valeri, A., Guillou, E., Cuvier, O., and Nollmann, M. (2011). Roles of chromatin insulator proteins in higher-order chromatin organization and transcription regulation. Nucleus *2*, 358-369.

Walther, T.C., Alves, A., Pickersgill, H., Loiodice, I., Hetzer, M., Galy, V., Hulsmann, B.B., Kocher, T., Wilm, M., Allen, T.*, et al.* (2003). The conserved Nup107-160 complex is critical for nuclear pore complex assembly. Cell *113*, 195-206.

Wang, H., Yang, H., Shivalila, C.S., Dawlaty, M.M., Cheng, A.W., Zhang, F., and Jaenisch, R. (2013). One-step generation of mice carrying mutations in multiple genes by CRISPR/Cas-mediated genome engineering. Cell *153*, 910-918.

Wansink, D.G., Schul, W., van der Kraan, I., van Steensel, B., van Driel, R., and de Jong, L. (1993). Fluorescent labeling of nascent RNA reveals transcription by RNA polymerase II in domains scattered throughout the nucleus. J Cell Biol *122*, 283-293.

Webster, M.T., McCaffery, J.M., and Cohen-Fix, O. (2010). Vesicle trafficking maintains nuclear shape in *Saccharomyces cerevisiae* during membrane proliferation. J Cell Biol *191*, 1079-1088.

Wente, S.R., and Blobel, G. (1993). A temperature-sensitive NUP116 null mutant forms a nuclear envelope seal over the yeast nuclear pore complex thereby blocking nucleocytoplasmic traffic. J Cell Biol *123*, 275-284.

Wente, S.R., and Blobel, G. (1994). NUP145 encodes a novel yeast glycine-leucine-phenylalanine-glycine (GLFG) nucleoporin required for nuclear envelope structure. J Cell Biol *125*, 955-969.

West, A.G., Gaszner, M., and Felsenfeld, G. (2002). Insulators: many functions, many mechanisms. Genes Dev *16*, 271-288.

Wilkie, G.S., Korfali, N., Swanson, S.K., Malik, P., Srsen, V., Batrakou, D.G., de las Heras, J., Zuleger, N., Kerr, A.R., Florens, L*., et al.* (2011). Several novel nuclear envelope transmembrane proteins identified in skeletal muscle have cytoskeletal associations. Mol Cell Proteomics *10*, M110 003129.

Wilkie, G.S., and Schirmer, E.C. (2006). Guilt by association: the nuclear envelope proteome and disease. Mol Cell Proteomics *5*, 1865-1875.

Williams, R.R., Azuara, V., Perry, P., Sauer, S., Dvorkina, M., Jorgensen, H., Roix, J., McQueen, P., Misteli, T., Merkenschlager, M*., et al.* (2006). Neural induction promotes large-scale chromatin reorganisation of the Mash1 locus. J Cell Sci *119*, 132-140.

Wilson, B., Erdjument-Bromage, H., Tempst, P., and Cairns, B.R. (2006). The RSC chromatin remodeling complex bears an essential fungal-specific protein module with broad functional roles. Genetics *172*, 795-809.

Wilson, K.L., and Foisner, R. (2010). Lamin-binding Proteins. Cold Spring Harb Perspect Biol *2*, a000554.

Winey, M., Yarar, D., Giddings, T.H., Jr., and Mastronarde, D.N. (1997). Nuclear pore complex number and distribution throughout the *Saccharomyces cerevisiae* cell cycle by three-dimensional reconstruction from electron micrographs of nuclear envelopes. Mol Biol Cell *8*, 2119-2132.

Worman, H.J. (2012). Nuclear lamins and laminopathies. J Pathol *226*, 316-325.

Worman, H.J., Ostlund, C., and Wang, Y. (2010). Diseases of the nuclear envelope. Cold Spring Harb Perspect Biol *2*, a000760.

Woychik, N.A., and Young, R.A. (1989). RNA polymerase II subunit RPB4 is essential for high- and low-temperature yeast cell growth. Mol Cell Biol *9*, 2854-2859.

Wu, C., Yosef, N., Thalhamer, T., Zhu, C., Xiao, S., Kishi, Y., Regev, A., and Kuchroo, V.K. (2013). Induction of pathogenic TH17 cells by inducible salt-sensing kinase SGK1. Nature *496*, 513-517.

Wu, J., Delneri, D., and O'Keefe, R.T. (2012). Non-coding RNAs in *Saccharomyces cerevisiae*: what is the function? Biochem Soc Trans *40*, 907-911.

Wu, W., Lin, F., and Worman, H.J. (2002). Intracellular trafficking of MAN1, an integral protein of the nuclear envelope inner membrane. J Cell Sci *115*, 1361-1371.

Wutz, A. (2011). Gene silencing in X-chromosome inactivation: advances in understanding facultative heterochromatin formation. Nat Rev Genet *12*, 542-553.

Xu, Z., Wei, W., Gagneur, J., Perocchi, F., Clauder-Munster, S., Camblong, J., Guffanti, E., Stutz, F., Huber, W., and Steinmetz, L.M. (2009). Bidirectional promoters generate pervasive transcription in yeast. Nature *457*, 1033-1037.

Yang, C.H., Lambie, E.J., Hardin, J., Craft, J., and Snyder, M. (1989). Higher order structure is present in the yeast nucleus: autoantibody probes demonstrate that the nucleolus lies opposite the spindle pole body. Chromosoma *98*, 123-128.

Yang, K., and Baines, J.D. (2011). Selection of HSV capsids for envelopment involves interaction between capsid surface components pUL31, pUL17, and pUL25. Proc Natl Acad Sci U S A *108*, 14276-14281.

Yao, J., Fetter, R.D., Hu, P., Betzig, E., and Tjian, R. (2011). Subnuclear segregation of genes and core promoter factors in myogenesis. Genes Dev *25*, 569-580.

Yavuz, S., Santarella-Mellwig, R., Koch, B., Jaedicke, A., Mattaj, I.W., and Antonin, W. (2010). NLS-mediated NPC functions of the nucleoporin Pom121. FEBS Lett *584*, 3292-3298.

Yewdell, W.T., Colombi, P., Makhnevych, T., and Lusk, C.P. (2011). Lumenal interactions in nuclear pore complex assembly and stability. Mol Biol Cell *22*, 1375-1388.

Zentner, G.E., and Henikoff, S. (2013). Regulation of nucleosome dynamics by histone modifications. Nat Struct Mol Biol *20*, 259-266.

Zhang, Y., McCord, R.P., Ho, Y.J., Lajoie, B.R., Hildebrand, D.G., Simon, A.C., Becker, M.S., Alt, F.W., and Dekker, J. (2012). Spatial organization of the mouse genome and its role in recurrent chromosomal translocations. Cell *148*, 908-921.

Zhou, Z.H., Dougherty, M., Jakana, J., He, J., Rixon, F.J., and Chiu, W. (2000). Seeing the herpesvirus capsid at 8.5 A. Science *288*, 877-880.

Zimmer, C., and Fabre, E. (2011). Principles of chromosomal organization: lessons from yeast. J Cell Biol *192*, 723-733.

Zorn, C., Cremer, C., Cremer, T., and Zimmer, J. (1979). Unscheduled DNA synthesis after partial UV irradiation of the cell nucleus. Distribution in interphase and metaphase. Exp Cell Res *124*, 111-119.

Zuleger, N., Kelly, D.A., Richardson, A.C., Kerr, A.R., Goldberg, M.W., Goryachev, A.B., and Schirmer, E.C. (2011). System analysis shows distinct mechanisms and common principles of nuclear envelope protein dynamics. J Cell Biol *193*, 109-123.

Zullo, J.M., Demarco, I.A., Pique-Regi, R., Gaffney, D.J., Epstein, C.B., Spooner, C.J., Luperchio, T.R., Bernstein, B.E., Pritchard, J.K., Reddy, K.L.*, et al.* (2012). DNA sequence-dependent compartmentalization and silencing of chromatin at the nuclear lamina. Cell *149*, 1474-1487.